ASSESSING AQUIFER VULNERABILITY TO LANDFILL POLLUTION USING DRASTIC METHOD IN GAUTENG, SOUTH AFRICA

WITS
UNIVERSITY

A Research Report submitted to the Faculty of Science, University of the Witwatersrand, Johannesburg, in partial fulfilment of the requirements for the degree of Master of Science in Hydrogeology

By

IDAH MPHAPHULI (880363)

SUPERVISOR: PROF TAMIRU ABIYE

School of Geosciences, University of the Witwatersrand, P.O. Box Wits 2050, Braamfontein, Johannesburg

28 August 2023

DECLARATION

I declare that this research project is my own unaided work. It is being submitted for the Degree of Master of Science at the University of the Witwatersrand, Johannesburg. It has not been submitted before for any degree or examination at any other University.

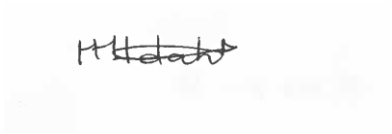

(Signature of candidate)

28 August 2023

ABSTRACT

This study integrated the DRASTIC method and field investigations into mapping the degree of vulnerability of aquifers to landfill pollution in the Gauteng Province, which is one of the most populated provinces in South Africa. In order to investigate the aquifer vulnerability of Gauteng's heterogeneous and complex geology, the DRASTIC method was used to generate intrinsic and specific vulnerability maps. Three vulnerability classes were generated from the DRASTIC index, namely, low vulnerability, moderate vulnerability and high vulnerability, which covered 46%, 37% and 17% of the study area, respectively. The highly-vulnerable areas were associated with the karst aquifer of Malmani dolomite, permeable vadose zone, high hydraulic conductivity and loamy sand/sandy loam soil type, whilst moderately-vulnerable areas were associated with fractured/weathered aquifers, high recharge and low topography. The intrinsic vulnerability was validated using average NO_3+NO_2-N (nitrate + nitrite as nitrogen) and the results of water samples from field investigations conducted in Marie Louise and Robinson landfill sites. Elevated NO_3+NO_2-N concentration (9.85-16.03 mg/l) was observed in the highly-vulnerable areas. Water samples were collected, in order to analyse the water chemistry, stable isotopes and radioactive isotopes (tritium). Gibbs and Piper diagrams were used to evaluate the main mechanism controlling the groundwater chemistry and the dominant major ions that influence it. Pollution by leachate was detected in the Marie Louise landfill site, where the groundwater showed high tritium and ammonia concentration. The main hydrochemical facies detected in Marie Louise were Mg-SO_4, Ca-SO_4, Na-SO_4 and Na-Cl. The hydrochemical facies detected in Robinson were Na-SO_4, Ca-HCO_3, Na-Cl and Ca-Cl. The DRASTIC method was shown to be effective in assessing groundwater vulnerability on a regional scale, provided that there is adequate input data.

ACKNOWLEDGEMENTS

Firstly, I would like to thank GOD for providing me with the strength and resilience to keep going.

I would like to thank my supervisor, Professor Tamiru Abiye for his support, patience, guidance, and for imparting me with all the knowledge necessary for the completion of this research project. Being part of the MSc hydrogeology program at Wits was absolutely rewarding.

I would like to thank my funders, the South African National Space Agency (SANSA), and the Environmental Resources Management (ERM) for their financial support. Without them, this research would have not been possible.

I would like to thank the managers at Robinson and Marie Louise landfill sites for their patience and assistance during my sampling campaign in the two landfill sites.

I would like to thank the Department of Water and Sanitation (DWS), the Council for Geosciences (CGS), and the South African Weather Services (SAWS) for all the data provided upon request.

I am immensely grateful to my friends, Chantel Nthabiseng Chiloane for all the proofreading and Refiloe Mercy Khotha for all the assistance during my sampling trips.

To my brother-in-law, Rendani Mutavhatsindi, thank you for all the trips to the landfill sites and for the endless support you have shown me. I am also grateful to Ndivhuwo and his team for all the sampling assistance.

To my siblings, Beauty, Jeaneth (Mbavhalelo), and Kutama Mphaphuli, thank you for your unwavering support, love, and care during this journey.

To my Mother, my pillar of strength, I am immensely grateful for your patience and care during my academic journey.

.

TABLE OF CONTENTS

LIST OF FIGURES

LIST OF TABLES

ABBREVIATIONS

Units	
mg/l	Milligrams per litre
mS/m	MilliSiemens per metre
TU	Tritium Unit
‰	Per Mil
°C	Degree Celsius
ppm	Parts per million
Universal	
DI	Drastic Index
DWS	Department of Water and Sanitation
EC	Electrical Conductivity
Mbgl	Meters below ground level
GMWL	Global Meteoric Water Line
JLMWL	Johannesburg Local Meteoric Water Line
SAWS	South African Weather Services
TDS	Total Dissolved Solids
^{3}H	Tritium/Hydrogen-3 (Isotope of hydrogen)
$\delta^{18}O$	Oxygen Isotope value (‰)
$\delta^{2}H$	Hydrogen Isotope value (‰)

CHAPTER 1: INTRODUCTION

1.1 Background

Groundwater is a valuable resource that is significant in supplying water in countries where the surface water is inadequate. In most parts of the world, groundwater is the main source of fresh water, which is extensively used for domestic, industrial and agricultural purposes. It can be replenished and has advantages over surface water, because of its relative purity, low evaporation loss and widespread distribution (Senthilkumar and Elango, 2013). The occurrence of groundwater in southern Africa is controlled by the wide range of geological structures and climatic variations that influence the region's hydrogeological settings (Braune and Xu, 2008). For the vast majority of rural residents and communities of small towns, the contribution of groundwater is extremely important, especially in a country like South Africa, which is situated in a semi-arid region that relies on groundwater for its social and economic development. Big cities, such as Johannesburg and Pretoria, obtain their water primarily from surface water (Vaal dam), due to their high consumption (Abiye, 2011). However, the water availability patterns and their variability and distribution are changing, due to the effects of global climate change and, as a result, most countries are turning to groundwater for various purposes (Swain *et al.*, 2022).

In an economy where cities are expanding, over-use is not the only problem affecting the groundwater, but it is also the deterioration of groundwater that is caused by landfill leachate. Africa is reported to be one of the continents in the world with the highest number of dumpsites and un-engineered landfills, which affects the health of many people (Vaccari *et al.,* 2019). Simultaneously, approximately two billion people do not have access to waste collection services, whilst three billion have no controlled waste disposal system (CIWM and WasteAid UK, 2018). As a result, solid waste disposal has become a concerning contributor to the degradation of groundwater quality, especially in South Africa, particularly in the Gauteng Province, where the population is growing rapidly. Waste management is a major problem because it is rapidly generated, most especially in urban areas that are highly industrialised (Mepaiyeda *et al.,* 2019). In addition, poor waste management services, particularly in informal settlements, have resulted in many unsuitable illegal dumping sites. Moreover, the increased population growth and urbanisation have exacerbated the proliferation of illegal dumping sites (Rasmeni *et al.,* 2019),

which has created a substantial problem for the quality of groundwater, because of landfill leachate pollution.

It is essential to understand the vulnerability of groundwater resources to pollution from solid waste disposal in the Gauteng Province, where open dumps and non-engineered landfills are common. This can be achieved by studying and understanding the geology and hydrogeological characteristics of the aquifer system so that aquifers prone to contamination can be distinguished from those that are less vulnerable to contamination. A detailed study was conducted to better understand the hydrogeochemical characteristics of the underlying aquifer and its potential for preventing landfill pollution. Tritium, stable isotope and water chemistry analyses were conducted to understand the extent of pollution and to examine the water quality in two landfill sites located in the Central Rand Group rocks. This study will help to understand the degree of vulnerability of the complex geology of the Gauteng Province. By doing so, areas that are highly prone to pollution can be distinguished from those that are less vulnerable, which will enable the highly-vulnerable areas to be the focal point when monitoring and remediating. The results obtained from this study will help land managers and developers to implement strict groundwater measures and protocols for those economic activities located in highly-vulnerable areas, in order to conserve and protect the quality of the groundwater.

1.2 Aim

This study aims to assess areas where the groundwater is highly vulnerable to pollution from landfill leachate in the Gauteng Province, South Africa.

1.3 Objectives

The objectives of this study are as follows:

- to demonstrate the degree of the aquifers' susceptibility to landfill leachate contamination by assessing the hydrogeochemical characteristics of the aquifers in Gauteng;
- to determine an aquifer vulnerability map of the Gauteng Province, which indicates areas with low, moderate and high vulnerability to pollution; and
- to investigate groundwater pollution by assessing the water quality of the Robinson and Marie Louise aquifers.

CHAPTER 2: LITERATURE REVIEW

2.1 Groundwater

Groundwater serves as a source of water for animals, plants and humans, with over two billion people relying on it globally (Hoyos *et al.*, 2016). Apart from these uses, groundwater plays a fundamental role in supplying economic activities and augmenting water resources during drought seasons when surface water resources are inadequate. According to the International Association of Hydrogeologists (2020), one-third of the global population relies on groundwater for domestic use. Groundwater pollution is a slow process that is not vividly apparent, and once it is contaminated, it is difficult to remediate because of the complexity of aquifer systems. Although geogenic origin has, to some degree, contributed to the contamination of groundwater when natural mineral deposits dissolve (Basu *et al.*, 2014; Pandey et al., 2016; Subba Rao *et al.*, 2020; He *et al.*, 2020), economic development has led to a global rise in the population, industrial development and urbanisation, and it has also contributed significantly to the deterioration of the quality and quantity of groundwater (Peiyue *et al*., 2021).

Recently, groundwater deterioration is mostly caused by pollution from anthropogenic activities introduced into the subsurface through spreading or leakage, the burying of waste substances below the sub-surface (landfills) or the injection of chemicals underground (Lehr *et al*., 1976). The contamination introduced into the subsurface can thereafter infiltrate the soil and the vadose zone, and mix with the groundwater, provided that the volume of the contaminant is high. If it is not high, the soil or vadose zone can retain the contaminants. The effects of attenuation increase with the time and distance that the contaminants travel before they reach the groundwater (Aller *et al*., 1987). A material with a small surface area will experience less sorption potential than a material with a high surface area (Aller *et al*., 1987). The attenuation of contaminants increases when the material through which the contaminants are travelling has high reactivity with the material (Aller *et al*., 1987; Gogu and Dassargues, 2000). When contaminants reach the groundwater, they can move in the direction and velocity of the groundwater flow, or they can either float above the water table or sink to the bottom (Aller *et al*., 1987).

In the early establishment of landfills, various methods were applied to limit their impact on the groundwater resources; for example, improved designs, engineering/compaction and management (Reyes-López *et al*., 2008). Nonetheless, developing countries continue to have difficulties in managing solid waste because of their poor environmental policies and governance, the high cost of engineering and the absence of social and industrial organisation (Idowu *et al.*, 2019). In addition, most landfills are installed without having a systematic understanding of the hydrogeological characterisation of the aquifer (Reyes-López *et al*., 2008). This is evident in landfills situated in areas where groundwater is highly susceptible to pollution such as aquifers that are shallow or unconfined (Reyes-López *et al*., 2008). If contaminants can percolate through unconfined aquifers, the groundwater will be polluted, which will result in a degraded aquifer system, posing a potential health risk for water users (Reyes-López *et al*., 2008). The vulnerability of groundwater to contamination is determined by the properties of the aquifer, such as the slope gradient, the recharge rate and quantity and the groundwater depth, amongst other factors. It is highly expected that contamination in unconsolidated and shallow aquifers will easily seep into the groundwater system, as unconsolidated sediments are highly permeable (Reyes-López *et al*., 2008).

When selecting a suitable waste management site, factors such as human settlements, topography, geology and hydrology are considered (SoER, 2003). Waste is further classified into two categories, namely, general waste, which is less detrimental to the environment, and hazardous waste, which is detrimental to the environment. General waste contains Municipal Solid Waste (MSW), which encompasses a minor fraction of garden waste, ash and commercial waste (DWAF, 1998; Morris, 2001). Leachate may be theoretically contained by using a liner in the landfill sites; however, there is the possibility of leakage. Therefore, it is essential to monitor the water quality and the vulnerability of the aquifer, as the possibility of groundwater contamination is inevitable once the leachate has penetrated the aquifer system.

Leachate is generated when water percolates into waste piles. This builds up and creates toxic moisture that seeps into the groundwater system, which subsequently contaminates the aquifer system (Blight, 2011). Landfills in a wet climate, with a high quantity of waste and a high-water content, are likely to produce a lot of leachates, compared to landfills in dry climate setting. Therefore, the leachate characteristics are determined by the climate in the area, the waste

composition and the age of the waste (DEA, 2018). The probability of landfill leachate contacting the groundwater is inevitable because of the complexity of the groundwater system. Once the leachate has diffused below the sub-surface, it follows the movement of the groundwater, and it, therefore, becomes difficult to control. The probability of groundwater contamination depends on the pollutant load that has been deposited on the subsurface and the geological/lithological characteristics of the aquifer system.

2.2 Groundwater Vulnerability Assessment

A groundwater vulnerability assessment is based on the concept that the state of vulnerability is not uniform in all areas of the land. Some areas may be more vulnerable than others, due to their heterogeneity and their aquifer characteristics (Gogu and Dassargues, 2000; Babiker *et al.*, 2005). Groundwater vulnerability maps often come in two variables: they are either intrinsic or specific (Witkowski *et al.*, 2004). The intrinsic vulnerability of an aquifer is known as the natural susceptibility of that aquifer to contamination based on its physical properties, namely, geological, hydrogeological, and hydrological characteristics. In contrast, specific vulnerability is the vulnerability of an aquifer based on specific contamination that may pose a risk to the aquifer system, considering the hydrogeological, geological and hydrological characteristics of that area and the state of the contaminant (Gogu and Dassargues, 2000).

The natural attenuation processes in the vadose, or unsaturated zone frequently determine the degree of groundwater contamination (Gogu and Dassargues, 2000). Physical, natural and chemical processes that occur in the unsaturated zone can alter the physicochemical nature of the pollution, which may thereafter transform the contamination or alter the intensity of pollution to the groundwater, particularly in unsaturated zones where the concentration of contamination may be affected when compared to the saturated zone (Aller *et al.*, 1987). Chemical processes are complex and may function independently, or in conjunction with other processes, to offer different attenuation processes. Such chemical reactions depend on the aquifer characteristics, the soil media and the properties of pollutants. Therefore, the attenuation process can be moderately or completely bypassed, subject to the geological and infiltration conditions of the aquifer (Gogu and Dassargues, 2000).

2.3 Groundwater Vulnerability Methods

Different methods have been used to evaluate groundwater vulnerability. In order to determine the vulnerability of groundwater to pollution, most countries have utilised the process-based, statistical, overlay and index methods (Shirazi *et al.*, 2012), of which the overlay and index methods are the most widely used. A few of the most familiar overlay and index methods are the DRASTIC (Aller *et al.*, 1987), SINTACS (Civita, 1993), GOD (Foster, 1987) and AVI (van Stempvoort *et al.*, 1993) methods, which are addressed in-depth below:

2.3.1 The GOD method

The GOD method, which was developed by Foster (1987), is a rating system method that uses a simple concept for the quick analysis of groundwater vulnerability. It considers three main parameters that form the acronym GOD, namely: Groundwater occurrence, Overlying lithology, and groundwater Depth. The overlying lithology is only used to calculate the vulnerability index in unsaturated aquifers. The three main parameters range between 0-1, with a high vulnerability being represented by 1, and a low vulnerability being represented by 0.

GOD is calculated using Equation 2.1 below (Foster, 1987):

$$\textbf{GOD vulnerability index} = \textbf{Gr} \times \textbf{Or} \times \textbf{Dr} \qquad (2.1)$$

- Groundwater occurrence
- Overlying lithology
- Depth to groundwater

2.3.2 The AVI method

The AVI method, developed by van Stempvoort *et al.* (1993), uses only two parameters for assessing the degree of groundwater vulnerability, namely, the thickness of each sedimentary layer above the uppermost aquifer and the estimated hydraulic conductivity of the sedimentary layers.

The hydraulic resistance can be estimated based on the two parameters, using Equation 2.2 below (van Stempvoort *et al.*,1993):

$$\boldsymbol{C = \sum \frac{d_i}{K_i}} \qquad (2.2)$$

Where:

C = hydraulic resistance that determines the vertical flow resistance of an aquifer.

d_i = thickness of the sedimentary layers above the uppermost, saturated aquifer surface

K_i = Hydraulic conductivity of the sedimentary layers

Various limitations exist when applying AVI in a groundwater vulnerability assessment, for example:

- other parameters that are significant in the assessment of vulnerability are neglected;
- AVI only considers shallow aquifers;
- different aquifers are deemed to have an equal value, and
- the lateral continuity and discontinuity of an aquifer is not thoroughly considered.

2.3.3 The SINTACS method

SINTACS was developed by Civita (1994) and is a point count system method that is derived from the DRASTIC method. Just as in the DRASTIC method, SINTACS uses seven parameters, with a relatively flexible rating and weighing approach, compared to that of DRASTIC. Each parameter used in a groundwater vulnerability assessment has a weight that is multiplied by the ratings given to the parameters for every interval to produce the final numerical score, which measures the degree of vulnerability. The seven parameters used in groundwater vulnerability form the acronym used for the SINTACS method. These parameters are static level (S), net recharge (I), vadose zone (N), soil type (T), aquifer type (A), hydraulic conductivity (C), and topography (S).

The vulnerability index of SINTACS can be calculated, using Equation 2.3 below (Civita, 1994):

$$\boldsymbol{I_v = \sum P_{1.7} \times W_{1.n}} \qquad (2.3)$$

Where:

I_v = vulnerability index

$P_{(1.7)}$ = parameter ratings

$W_{(1.n)}$ = parameter weight

N = weight classification arrays number

2.4 Comparison studies

Various comparison studies have been conducted on different methods. Corniello *et al.* (1997) and Gogu *et al.* (1996) compared the DRASTIC, GOD, AVI and SINTACS methods and demonstrated that SINTACS produce high vulnerability in areas where there is surface and groundwater interaction. SINTACS favours land use parameters, since various weight classifications are used, whereas GOD provides uniform values in regions where the vulnerability rate has modest differences. Therefore, only highly-contrasted vulnerable areas can be employed with this technique (Gogu and Dassargues, 2000). The vulnerability map produced by using the AVI technique was comparable to those of the DRASTIC and SINTACS models, even with fewer parameters. The statistical analysis revealed a strong association between the DRASTIC, SINTACS and AVI methods. Another notable comparative analysis of the different approaches to assess groundwater vulnerability was carried out by Civita and de Regibus (1995). They studied a variety of hydrogeological settings in northern Italy, using the DRASTIC, SINTACS, GOD and Flemish methods in a region with different slope gradients. It was demonstrated that simple methods show comparable results to complex methods when different methods are applied using the same data in the same regions. It was concluded that GOD is ideal for assessing large land use areas, whilst DRASTIC and SINTACS are appropriate for detailed studies since they demonstrate high precision and adaptability (Gogu and Dassargues, 2000).

Dragoi and Popa (2007) compared the feasibility of the DRASTIC, AVI and GOD methods in assessing the intrinsic vulnerability of a shallow aquifer intersecting the Danube River. By comparing the three widely-used methods, they concluded that GOD is suitable for use in areas that require less data, in areas with less complex hydrogeological events and where there is no

human activities. Therefore, if one requires a quick assessment of the groundwater vulnerability to pollution, GOD is recommended (Dragoi and Popa, 2007); however, for a complex hydrogeological setting with various anthropogenic activities, a method with vast parameters is suggested, such as DRASTIC.

2.5 The DRASTIC Method

From the overlay and index methods, the DRASTIC method is the most preferred method for assessing groundwater vulnerability globally (Shirazi *et al.*, 2012). It is a numerical ranking method developed by the United States Environmental Protection Agency that uses seven parameters to monitor the susceptibility of groundwater to pollution (Aller *et al*., 1987). This method focuses on the depth of the water table, the recharge, aquifer properties, soil media, topography, the vadose zone and hydraulic conductivity. The seven parameters of the DRASTIC method are assigned ratings and a weight value based on the significance of each factor. A weight between 5 (the most significant factor) and 1 (the least significant) is allocated to each DRASTIC parameter. The difference in range determines the level of importance of each range, in accordance with the area's vulnerability; in contrast, the rating of factors is dependent on the user's knowledge. After the DRASTIC index is quantified by using the DRASTIC parameters, areas that are highly sensitive to pollution can be distinguished from those that are the least sensitive.

The DRASTIC method has the following seven parameters (Aller *et al.*, 1987):

2.5.1 Depth to water

Depth to water is the distance from the ground surface to the water level (Kwesi *et al.*, 2020). The distance that the water has to travel determines the time that the water will take to reach the water table. If the depth of the groundwater is shallow, the contaminant is likely to travel faster to the aquifer, which makes shallow unconfined aquifers highly susceptible to pollution. A deep groundwater depth allows attenuation to occur, as the travel time and distance are greater. Less permeable aquifer media will inhibit the movement of the water-carrying contaminant.

2.5.2 Recharge

The recharge of water into the aquifer is governed by the ability of precipitation to penetrate and percolate the unsaturated zones. If the unsaturated zone is permeable, the aquifer material allows recharge to occur, whereas non-dynamic aquifer systems that are impermeable, result in a delayed recharge. Regions that have a high recharge volume will serve as carriers of possible contamination. The quantity of recharge determines the dispersion and dilution of contaminants within the unsaturated zone. Leaching and the movement of contaminants depend on the quantity of water that has infiltrated the unsaturated zone (Kwesi *et al.,* 2020).

The recharge of groundwater in an area is generally regarded as being equivalent to the infiltration excess of the area (de Vries and Simmers, 2002). Even so, the total water that infiltrated may not reach the water table, as horizons with low conductivity may hinder the percolation of water to the aquifer, causing it to disperse as interflow to the neighbouring depressions. This water may runoff, or evaporate, and not join the regional groundwater system (de Vries and Simmers, 2002). The interaction between the climate, geology, morphology, soil quality and vegetation determines the recharge process. In semi-arid areas, near-surface conditions have a greater impact on groundwater recharge, compared to those in humid regions (de Vries and Simmers, 2002).

2.5.3 Aquifer media

An aquifer media is an unconsolidated or consolidated rock that is responsible for storing a specific quantity of water beneath the earth's surface (Jaseela *et al.,* 2016). The properties of the aquifer lithology govern the capability of an aquifer to store water. Confined aquifers are less susceptible to pollution, as they have impervious layers, whereas unconfined aquifers are more prone to pollution. Groundwater is stored in either open pore spaces, fractures or faults. The pollution potential of an aquifer depends on the degree of fractures and the grain size of that aquifer (Aller *et al.,* 1987). Limestone, dolomite, shale, siltstone, sandstone and conglomerate are important sedimentary rocks in groundwater hydrology, along with the granite and basalts of igneous rocks (Health, 1983).

2.5.4 Soil

Aller *et al.* (1987) defined soil as the uppermost weathered layer situated above the unsaturated zone/vadose zone. Soil provides the first defence against groundwater pollution. When contaminants are introduced onto the earth's surface by either spillage from industrial sites, pesticides from agriculture, or leachate from landfills, they can be retained or percolate into the groundwater, depending on the soil content. Various biological activities that occur in the uppermost weathered layers help to retain contaminants.

2.5.5 Topography

Topography refers to the slope gradient of an area. The difference in the slope gradient determines the chances of precipitation either running off as it reaches the earth's surface or infiltrating into the sub-surface. Runoff is favoured in areas with a steep topography (Jaseela *et al.*, 2016) where the rate of water movement is faster; reducing the resident time and minimising the chances of water infiltrating into the subsurface. Infiltration is normally favoured in flat areas where rainfall water is retained, and thereafter it infiltrates, as the resident time of rainwater in that area is expected to be longer than on steep slopes. Flat slopes are susceptible to aquifer pollution because contaminated water can easily infiltrate the sub-surface and unsaturated zones, whereas contaminated water on steep slopes is likely to run off.

2.5.6 Impact of the vadose zone

The vadose zone is the area below the land surface and above the water level. It can also be referred to as the unsaturated zone, where the voids and spaces are partially filled with water (Aller *et al.*, 1987). A vadose zone with high hydraulic conductivity, porosity and permeability will encourage the movement of contaminants into the aquifer, making the aquifer system highly vulnerable to pollution. The unsaturated zone exhibits different attenuation characteristics, depending on the type of vadose zone media. Various processes occur within the vadose zone, like biodegradation, neutralisation, mechanical filtration, chemical reaction, volatilisation and dispersion (Aller *et al.*, 1987; Moges and Dinka, 2021). At a shallow depth, less biodegradation and volatilisation occur.

The amount of material encountered, and the time available for attenuation, are both influenced by the media, which also determines the path length and routing (Hasiniaina *et al.*, 2010).

2.5.7 Hydraulic conductivity

Hydraulic conductivity determines the ease with which water will flow in an aquifer. The interconnection of voids and the number of void spaces determine the flow rate of contaminated water through the vadose zone to the aquifer (Tilahun and Merkel, 2009). Aquifers with a high hydraulic conductivity are prone to pollution, compared to those with a low hydraulic conductivity. The size and arrangement of the fractures and pores, as well as the different physical properties of the water, such as its density, gravitational field strength and kinematic viscosity, determine the hydraulic conductivity (Younger, 2009). Hydraulic conductivity varies between different rock types, and from place to place within the same rock. An aquifer is identified as a homogeneous aquifer if it is characterised by the same hydraulic conductivity, whilst a heterogeneous aquifer is identified as an aquifer that has a varying hydraulic conductivity (Health, 1983).

2.6 DRASTIC Method Principles

The DRASTIC method is centred on the following four assumptions: (a) the contaminants are introduced at the ground surface; (b) the contaminants are flushed into the groundwater by precipitation; (c) the contaminants have the mobility of water; and (d) the area evaluated using DRASTIC is 0.4 km^2 or larger (Aller *et al.,* 1987). Once the seven parameters have been weighted and given rankings according to their importance, a map overlaying the seven hydrogeological parameters is generated, in order to identify areas that are less vulnerable, moderately vulnerable and highly vulnerable to groundwater pollution. The identification of the vulnerable areas enables remediation practitioners to focus on areas that are most vulnerable to contamination, where management is more critical, which ensures that the limited resources are utilised sustainably and in the priority areas (Aller *et al.,* 1987).

The application of the DRASTIC method is not intended to substitute or negate field investigations (Aller *et al.,* 1987), neither does it in any way certify a site as being suitable for waste disposal site

or for the utilisation of land. For a site to be ideal for waste disposal, it does not solely depend on the prospective development of pollution in that area; however, other design measures are taken into consideration. The DRASTIC method is therefore utilised, together with other numerous design measures, in order to make a sound decision on the siting of an area where the groundwater is less susceptible to contamination, based on multiple hydrological and geological characterisations (Aller *et al.,* 1987). Hence, the accepted use would be to use it as a screening tool and focus DRASTIC on the area where the activity will be established. Nevertheless, a thorough and specific evaluation is required to determine the site's suitability for land use activities. DRASTIC is meant to assist in developing a baseline knowledge that will guide groundwater-related studies and management. Once a DRASTIC index has been computed, it is possible to identify areas that are more likely to be susceptible to groundwater contamination, in relation to one another. The higher the DRASTIC index, the greater the potential for groundwater pollution.

DRASTIC parameters are crucial for estimating the potential groundwater pollution, as groundwater occurs in heterogeneous geology, at different depths and geological formations. The DRASTIC method is convenient (Shirazi *et al.,* 2012) and it surmises that groundwater vulnerability can be assessed by studying the known factors that control the sensitivity of groundwater to contamination. It uses the Geographical Information System (GIS) approach, which is robust for spatial analyses and for interpreting, manipulating and incorporating geological, hydrogeological and geomorphological data. Although determining an aquifer's vulnerability to pollution is improved when many variables are considered (Evans and Myers, 1990), acquiring adequate data can be challenging (Napolitano and Fabbri, 1996).

2.7 The Application of the DRASTIC Method

2.7.1 The world

Wang *et al.* (2012) integrated three approaches when assessing the vulnerability of groundwater in the Beijing Plain, China. The first approach was to characterise six land activities (gas stations, oil depots, polluted rivers, agricultural areas, industrial areas and residential areas) that pose a potential contamination risk to the groundwater; thereafter, the intrinsic vulnerability was analysed by using the DRASTIC method. According to Wang *et al. (*2012), the northern and western regions with the highest groundwater storage had a high vulnerability rate, due to the shallow aquifer and soil type (sand and gravel) in the area. Areas with a low groundwater vulnerability had a deep groundwater depth and a less pollution-sensitive soil content. It was observed that the areas with a high risk of contamination are a result of their high intrinsic vulnerability and untreated landfills. The DRASTIC index had five vulnerability categories and it was validated by using the distribution of contamination within the study area and the field investigations.

Hosseini and Saremi (2018) compared the compatibility of the DRASTIC and GOD methods in assessing the groundwater vulnerability in the Malayer Plain aquifer in Iran. This Plain which consists of schist, slate, sandstone and granite, has a relatively low slope gradient and is highly impacted by nitrate from agriculture and leachate from landfills. According to Hosseini and Saremi (2008), DRASTIC showed better results when assessing groundwater vulnerability, whilst the simplicity of GOD was presumed to limit its potential to assess groundwater vulnerability in the Malayer Plain aquifer because it overlooked the impacts of land-use activities on groundwater vulnerability. Jeseela *et al.* (2016) used the DRASTIC method to evaluate groundwater vulnerability adjacent to a landfill site. The DRASTIC index ranged between 120 - 243 and was divided into three classes. High-vulnerability aquifers were observed in areas with a low topography, which favoured percolation over runoff. In contrast, the highly-vulnerable areas were attributed to the sandy and sandy loam soil types. The majority of the study had sand and gravel and a depth to water level of between 5-15 m. Chemical and bacterial results were used to validate the DRASTIC results, which confirmed that areas with high bacterial (E. coli) concentrations had a high groundwater vulnerability to landfill leachate.

Naqa (2004) used the DRASTIC method to assess the impact that the Russeifa landfill, in north-east Jordan, has on the groundwater of the Amman Wadi-Sir aquifer. The water level data collected from wells around the landfill were used to estimate the depth to groundwater, whilst recharge was estimated by using the precipitation rate, soil characteristics and land use. Furthermore, the impact of the vadose zone was estimated by using the rate of soil permeability and groundwater level. The area had a depth ranging between 30-40 m and 12.9 mm/year recharge. The study area had fractured limestone, a slope of 5%, and sandy loam soil. The DRASTIC index had an average of 101 -140 which, according to Naqa (2004), was a moderate vulnerability.

2.7.2 Africa

Oke (2020) evaluated the intrinsic vulnerability of a shallow aquifer in the Dahomey Basin. This shallow aquifer forms part of one of the most populated cities, Lagos, with land activities such as non-engineered landfill sites and industrial activities posing a risk to the shallow aquifer. The seven DRASTIC parameters were used, and a parameter sensitivity analysis was conducted to identify the relationship between the various DRASTIC parameters. High-vulnerability areas were associated with flat slopes and high recharge, whereas low-vulnerability areas were associated with steep slopes, a deep groundwater depth, a thick vadose zone and low recharge.

Kwesi *et al.* (2020) used the DRASTIC method to map the groundwater vulnerability in the Nsuaem Municipality in Tarkwa, for proper landfill site selection. This study employed seven DRASTIC parameters when estimating the DRASTIC index, which was divided into five classes: very low, low, moderate, high and very high. The areas with a very high and high vulnerability to pollution were situated in the northern and north-western region and comprised 30% of the area. The area with a low vulnerability to pollution was situated in the south of the study area. The DRASTIC method was commended for being a useful tool in the selection of a waste disposal area. However, the accuracy of this method depends on the data input and the parameter ratings. The validation of the DRASTIC method was not addressed in this study.

Tilahun and Merkel (2009) used the DRASTIC method to assess the groundwater vulnerability of the Dire Dawa Basin, which is situated in a semi-arid region in Ethiopia. The purpose of the study was to delineate the groundwater protection zones. The highly-vulnerable areas were located in a

region with a shallow groundwater depth, sandy loam soil, an alluvium vadose zone and high recharge rates. On the contrary, the low-vulnerable areas had low recharge, a deep groundwater depth and clay soil. Nitrate was used to validate the groundwater vulnerability map. It was noted that the area with a high vulnerability to pollution had a high nitrate concentration, which exceeded the nitrate concentration recommended by the World Health Organization (WHO).

The effectiveness of using the DRASTIC method for evaluating the degree of groundwater vulnerability has also been evaluated by Mato (2007), who mapped and delineated areas with a high groundwater vulnerability in the populous city of Dar Es Salaam, Tanzania, where there is a waste management challenge resulting from illegal dumping as a result of unplanned settlements due to population expansion. In this study, nitrate was used to validate the DRASTIC index. It can be observed from all these studies that areas with a high vulnerability were associated with a shallow groundwater depth, permeable soil, a steep slope, high recharge and a highly-permeable vadose zone.

2.8 South Africa

The DRASTIC method has been applied in several South African studies, by using similar parameters to those suggested by Aller *et al.* (1987), with slight modifications and additions. The most widely-known study is that of Lynch *et al.* (1994), who used the DRASTIC method to assess the vulnerability of groundwater to pollution and who produced a national groundwater vulnerability map of South Africa. The study used the six DRASTIC parameters recommended by Aller *et al.* (1987); however, it omitted hydraulic conductivity, as the data for this parameter were unavailable during the time of the study. In addition, several limitations were identified and documented that relate to the application of the DRASTIC method in the southern African context.

The following factors that are not considered by DRASTIC methods are ultimately a limitation:

- human activities that negatively impact the groundwater;
- hydro-structures, such as fractures and faults;
- the intensity and duration of precipitation;
- soil reactivity;
- specific contaminant mobility;
- the anisotropy and heterogeneity of the vadose zone, hydraulic conductivity and soil; and
- dilution.

Another study that aimed to improve the DRASTIC method for assessing groundwater vulnerability from aqueous-phase contaminants in the groundwater was conducted by Jovanovic *et al.* (2006), who modified the DRASTIC method by integrating hydrogeological factors (preferential flow and a multi-layer vadose zone) and contaminant properties (sorption and decay), which the DRASTIC method by Aller *et al.* (1987) ignores. The results enabled the production of insightful maps for assessing groundwater vulnerability in site-specific areas on a regional scale.

Besides these studies, Master of Science candidates from institutions across South Africa have also contributed to the application of the DRASTIC method in assessing groundwater vulnerability. An example is a study by Mohuba (2020), who used the DRASTIC method to assess the hydrogeological characteristics of a region in the Eastern Cape, where a Thyspunt nuclear plant was to be established. Since the DRASTIC method can only be utilised as a screening tool, various

field investigations were carried out that enabled the analysis of the hydrogeochemical characteristics of the area. This study also integrated stable isotopes and field investigations to validate the resultant DRASTIC index.

Mostert (2014) used the DRASTIC method to assess the groundwater vulnerability in South Africa and the impact that land use has on the Rustenburg Municipality. Due to the unavailability of hydraulic conductivity data, this parameter was excluded, and no attempts were made to estimate it. Press (2020) mapped the Upper Crocodile River to evaluate the aquifer's vulnerability to pollution by assessing the aquifer's intrinsic and specific vulnerability. Press (2020) used water strike instead of water level to remove confining pressure effects in confined or semi-confined aquifers. Various specific vulnerability maps were conducted for the multiple land uses which were validated using NO_3+NO_2-N (agriculture, urban and informal settlements) and sulphate (mining). Similar to the other studies, hydrogeological parameters were acquired from secondary sources. Dolomite was assigned a higher vulnerability rating because of the complex karst environment that makes this aquifer more vulnerable whilst the hydraulic conductivity values were obtained from the literature.

A study by Gintamo (2021) used the DRASTIC method to assess the impacts of land use and climate change variables on the groundwater of the Cape Flats aquifer. The hydrogeological parameters' weighting values were determined using the Analytical Hierarchy Process (AHP). Validation was conducted using physicochemical parameters such as chloride, sulphate, nitrate, and potassium. The specific DRASTIC index that ranged between 109-222 with four vulnerability classes was produced by integrating the DRASTIC method with land use activities. Furthermore, regions with very high and high vulnerability were characterised by shallow groundwater and a flat slope.

Musekiwa and Majola (2013) who produced a national groundwater map of South Africa used a modified DRASTIC method by assigning recharge a weight of 3 and not the suggested 4 by Aller *et al.* (1987). This was adapted from Robi *et al.* (2007) who recommended the reduction of the weight of recharge to ensure the assessment of aquifers that have social importance but have little productivity. Validation was done using NO_3+NO_2-N and electrical conductivity. In a study by Sakala *et al.* (2019), DRIST (modified DRASTIC) and Artificial Neural Networks (ANN) methods were used to evaluate pollution from Acid Mine Drainage (AMD) in the coalfield in Witbank.

Rainfall was used in this study as a representative of recharge, and validation was done using sulphate concentration. Sakala *et al.* (2019) focused solely on the specific vulnerability, adapting the statement by (Huan *et al*., 2012), who claimed that intrinsic vulnerability maps are not useful as the groundwater depth, recharge and soil are forever changing as the result of human activities occurring on land. A high correlation was observed between ANN and sulphate, with Sakala *et al.* (2019) relating the high correlation to ANN having more specificity to AMD pollution as the ANN training uses AMD indicators. Sakala *et al.* (2018) modified the mineral system approach by using the fuzzy expert system which used four factors, namely, energy sources, transportation pathways and traps, ligands sources, and pollutant sources to evaluate the groundwater vulnerability by AMD pollution of the Ermelo, Witbank and Highveld coalfield. This approach used average long-term rainfall as the source of the ligand, and slope as the source of energy for pollutants. In transportation pathways, hydrogeological parameters similar to those used in the DRASTIC method that affects groundwater vulnerability such as the soil, hydraulic conductivity, and vadose zone were considered. Preferential flow and drainage density were also considered. To validate the Fuzzy expert system approach, sulphate concentrations and pH values were used which correlated well with the model.

DRASTIC method has not been used to assess the groundwater vulnerability of aquifers beneath landfill sites in South Africa. This study aims to use Aller *et al.*'s (1987) DRASTIC method, in conjunction with fieldwork, to validate the method and to understand the risk that landfill leachates pose to the heterogeneous hydrogeochemical conditions of the most populated province in South Africa. The study attempts to use all seven hydrogeochemical parameters, with the assistance of literature, as they all play a significant role in the transportation of contaminants.

2.9 Motivation for using the DRASTIC Method

The advantage of using the DRASTIC method is that it can be applied across a large geographical area, and it requires a minimal amount of necessary data, which are easy to collect at a low cost (Aller *et al.*, 1987). The use of numerous parameters that are related to each other reduces the chance of overlooking certain crucial factors, which limits the impact of an accidental error in the calculation and which therefore increases the statistical correctness of the model (Rosen, 1994). Regardless of the lack of specific characteristic measurements that most specialist approaches would need, the DRASTIC method provides rather accurate results for large regions with a complicated geological structure (Kalinski *et al.*, 1994; McLay *et al.*, 2001).

Some researchers have proposed enhancing the DRASTIC model, with most of them suggesting that some variables be removed (Evans and Myers 1990; Rupert 1999). For example, Secunda *et al.* (1998), Rupert (1999) and McLay *et al.* (2001) proposed the addition of land use or irrigation variables, whilst Foster (1987) and Merchant (1994) suggested that DRASTIC be combined with other processes or models, such as a capture zone delineation or finite element flow and transport models. In this study, all the parameters will be used, as they play a vital role in the movement of contaminants.

CHAPTER 3: SITE DESCRIPTION

3.1 Location of the study area

The DRASTIC method was applied in the Gauteng Province (Figure 3.1), which is one of the most populated provinces in South Africa. Over one-third of South Africa's Gross Domestic Product (GDP) and one-tenth of Africa's GDP are produced in Gauteng (DEA, 2018). It is geographically the smallest province, with a total area of over 16 500 km^2. Even so, it is home to almost 20% (9.6 million) of the country's population (Dyson, 2009). According to the Gauteng Department of Housing (2006), 405 informal settlements were reported in the Province in 2006. These settlements are extremely crowded, with a living space of about 40 m^2 being shared by approximately 24 people (Beavon, 2004). Shacks have been built in informal settlements on vacant riverbank land, which makes these areas particularly susceptible to flash flooding. Gauteng leads the other provinces with respect to population density (786 persons/km^2) (DEA, 2018). As it stands, the economic activities in the Province add pressure on the management of waste (Muzenda, 2012). Gauteng has demonstrated a high growth in urbanisation (97%), which is inextricably linked to urban waste generation (DEA, 2018).

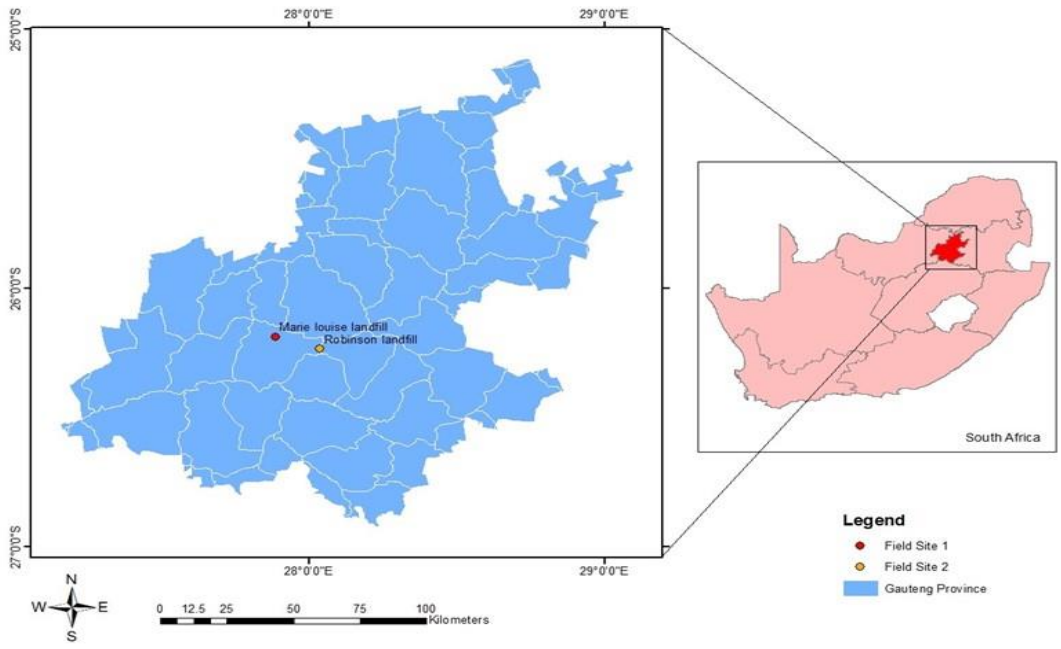

Figure 3-1: Study site and the location of the Marie Louise and Robinson landfills

3.2 Rainfall

The Gauteng Province is comprised of two climatic regions, namely, Central Bushveld and Moist Highveld Grassland. The Central Bushveld climate covers the far northern reaches of Gauteng, whilst the Moist Highveld Grassland covers the southern region (SAWS, 2021). Since these two regions in the Gauteng Province have different climates, due to their topographical differences, two stations were used to represent their average monthly rainfall. Rainfall and temperature data for this Province over a period of 22 years (2000-2021) were provided by the South African Weather Services (SAWS) and used to generate the average monthly rainfall, maximum and minimum temperature (Figure 3.2). The Pretoria UNISA weather station represents the northern region, which recorded the highest rainfall in January and December, with a monthly rainfall of 125.50 mm and 126.22 mm, respectively. March and November also recorded high rainfall of 89.77 mm and 89.75, respectively. The lowest rainfall was in May, June, July and August, with 7.72 mm, 6.51 mm, 1.92 mm and 4.27 mm, respectively. In terms of temperature, the month of January received maximum and minimum temperatures of 29.79°C and 16.49°C. The Johannesburg Botanical Garden weather station (JHB BOT TUINE) represents the southern region, where the highest monthly rainfall and temperature were recorded in January, February, and December, with a rainfall of 113 mm, 95.31 mm and 105.42 mm, respectively. As demonstrated by the two stations, the highest average monthly rainfall was in January and December (the wet season), while the lowest temperatures were between May and August (the dry seasons). The Province's climate is most significantly influenced by its topography, which is moderately elevated, with an average elevation of more than 1000 meters above sea level and elevations exceeding 1500 meters above sea level over large areas (SAWS, 2021). Nevertheless, Pretoria UNISA demonstrated a higher temperature than the JHB BOT TUINE, which had higher rainfall in February and November.

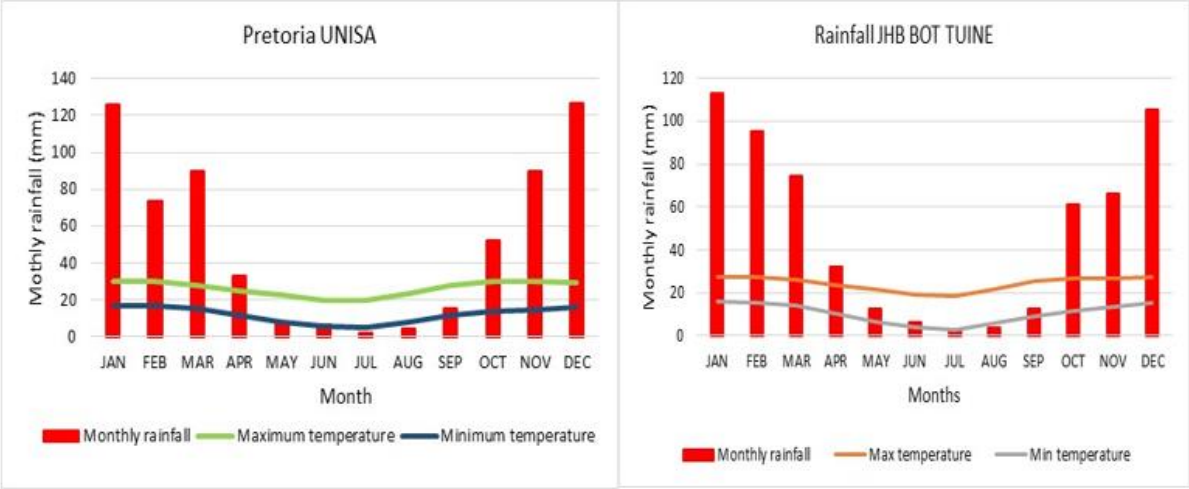

Figure 3-2: Mean monthly rainfall and temperature of the Pretoria UNISA station and the JHB BOT TUINE station (source: South African Weather Service)

Figure 3.3 depicts the annual rainfall for the 22-year period (2000-2021) at the Pretoria (PTA) UNISA and Johannesburg Botanical Garden weather stations. The highest rainfall data obtained from the Pretoria UNISA station was experienced in 2009, 2014 and 2021, with rainfall of 958 mm/y, 920 mm/y and 841 mm/y, respectively. The lowest rainfall was in 2000, 2015 and 2002, with 127 mm/y, 392 mm/y and 447 mm/y, respectively. At the Johannesburg Botanical Gardens station, the highest rainfall was experienced in 2017, 2010 and 2000, with rainfall of 923 mm/y, 906 mm/y and 820 mm/y, respectively. Conversely, the lowest rainfall was recorded in 2002 (195 mm/y) and 2021 (247 mm/y).

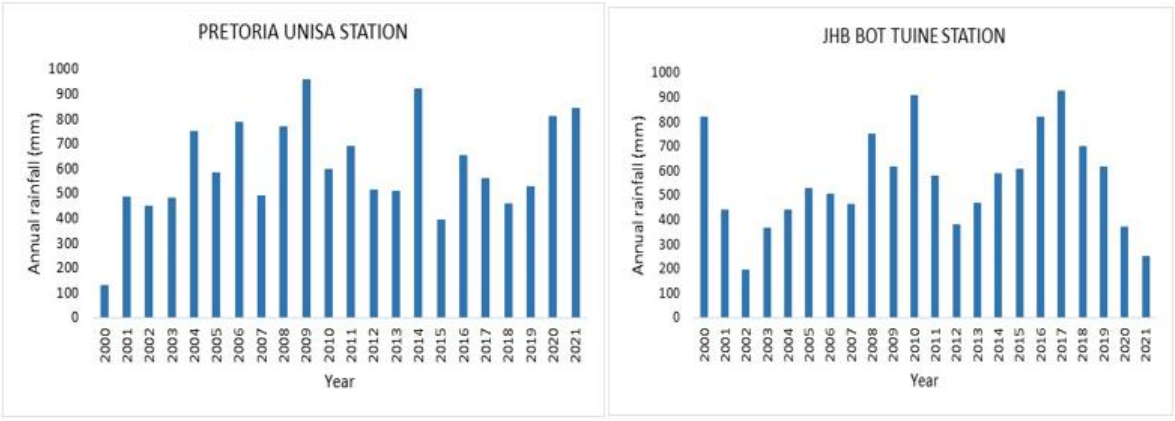

Figure 3-3: Annual rainfall at the Pretoria UNISA and JHB BOT TUINE stations (Source: South African weather service)

The PTA UNISA station recorded the highest average wind speed in June (2.16 m/s) and August (22.22 m/s) (Figure 3.4). The highest wind speed was experienced during the afternoon. In the morning, the wind speed was highest in the dry season and the lowest in the wet season, and it was directly the opposite in the evenings. The JHB BOT TUINE station showed the highest average wind speed in October (1.32 m/s) and November (1.32 m/s). The wind speed was lowest in the mornings and evenings of April, May and June. Overall, the PTA UNISA station recorded the highest wind speed in the 22 year record.

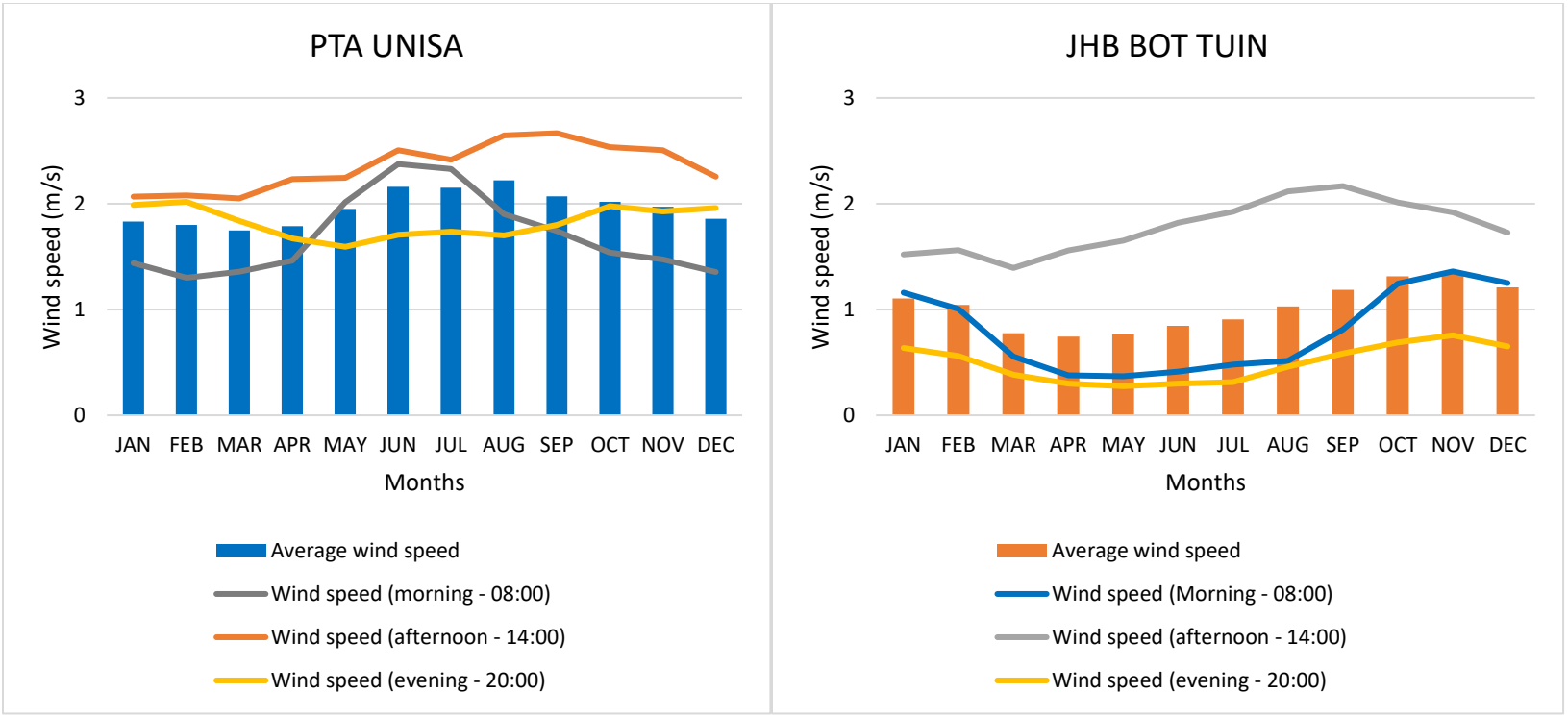

Figure 3-4: Wind speed of the Pretoria UNISA station and JHB BOT TUINE station (source: South African Weather Service, SAWS)

3.3 Regional Geology

The study area falls part of the Archean crystalline basement, the Dominion Group, the Witwatersrand Supergroup, the Ventersdorp Supergroup, the Transvaal Supergroup and the Karoo Supergroup. The Archean basement is represented by the Johannesburg dome that contains rocks such as the granitic gneiss, gabbro, serpentinite, and granodiorite that have undergone tectonic alteration, weathering, and erosion (McCarthy & Rubidge, 2005). The Witwatersrand Supergroup rocks, whose formation occurred between 2714 and 2074 Ma, unconformably overlie the Kaapvaal craton's Archean basement and conformably overlie the volcanic and sediments of the Dominion Group, which were deposited between 3086-3074 Ma (Robb and Meyer, 1995). According to Robb and Meyer (1995), the Witwatersrand Supergroup is 7000 m thick and consists of a succession of arenaceous and argillaceous rocks. The Witwatersrand Supergroup is divided into two groups, namely, the West Rand Group and the Central Rand Group. The West Rand Group deposition occurred between 2970 and 2914 Ma and is subdivided into three sub-groups, namely the Hospital Hill, Government and Jeppestown sub-groups, which are comprised of quartzite and shale, whereas the Central Rand Group, the formation of which took place between 2894 and 2714 Ma (Robb and Meyer, 1995), is subdivided into two sub-groups, namely the Johannesburg and Turffontein sub-groups, which consist of conglomerate, quartzite and shale (McCarthy, 2006).

The Witwatersrand Supergroup is overlain by the Venterdorp Supergroup, which was deposited between 2714 and 2665 Ma. The Ventersdorp Supergroup consists of three groups, namely the Kliprivierberg, Platberg and Pniel Groups, which are represented by basalts/andesites, quartzite, conglomerate and shale. The Ventersdorp Supergroup is overlain by the succession of underformed and unmetamorphosed volcanic, chemical and clastic sedimentary rocks of the Proterozoic Transvaal Supergroup (Eriksson and Clendenin, 1990). The Transvaal Supergroup is further divided into the Black Reef Formation, the Chuniespoort Group and the Pretoria Group. The iron formation and dolomite of the Chuniespoort Group that overlies the quartzite and shale of the Black Reef Formation are overlain by the interbedded basaltic-andesitic lavas, diamictites, carbonate, conglomerate and mudrock of the Pretoria group that have been exposed to low-grade metamorphism (Eriksson and Clendenin, 2006). Furthermore, the Transvaal Supergroup is overlain by the largest layered mafic intrusion in the world, the Bushveld Complex, which formed 2050 Ma ago when lava erupted onto the Transvaal Supergroup sediments. The Bushveld Complex

is made up of the Rustenburg Layered Suite (RLS), which is capped by the Rashoop Granophyre, Lebowa Granite, and the Rooiberg Volcanic Suite (Zeh *et al*., 2015).

The deposition of the Karoo Supergroup occurred during the Late Paleozoic and Early Mesozoic, with the deposition of the Karoo Supergroup sedimentation being dated in the Late Carboniferous around 300 Ma (Catuneanu *et al.,* 2005). After the occurrence of inversion tectonics along the super continent's southern margin that resulted in the Pangea convention, the deposition of Karoo sedimentation ceased after the break-up of the continent. The youngest deposition of the Karoo Supergroup differs from Triassic and Jurassic, due to the erosion that occurred during the post-Gondwana (Catuneanu *et al.,* 2005). The Karoo Supergroup is subdivided into five groups, namely the Dwyka, Ecca, Beaufort, Stormberg and Drakensburg Groups. The succession of sandstone, mudstone, siltstone and coal of the Ecca Group, which is overlain by the succession of sandstone and mudstone of the Beaufort Group, overlies the Dwyka Group. The Beaufort Group is overlain by the Stormberg Group, which is comprised of the Molteno, Elliot and Claren formations. Furthermore, the Stormberg Group is overlain by the succession of the Drakensberg Group.

The local geology of the study area where field campaigns took place comprises of the quartzite and conglomerate rocks of the Turffontein Subgroup, Central Rand Group of the Witwatersrand Supergroup (Figure 3.5). The conglomerate of the Central Rand Group consists of concentrated mineralization, with a complex paragenetic sequence developed by the assemblage of the detrital heavy metals. The source of the Central Rand rocks is abundant in granite and basalt, with small components of tonalite (Wronkiewicz and Condie, 1987). The conglomerate consists of a different combination of sand and pebble layers, which extends from the individual layers of dispersed pebbles to a thick conglomerate that is comprised of pyritic arenite (Robb and Meyer, 1995).

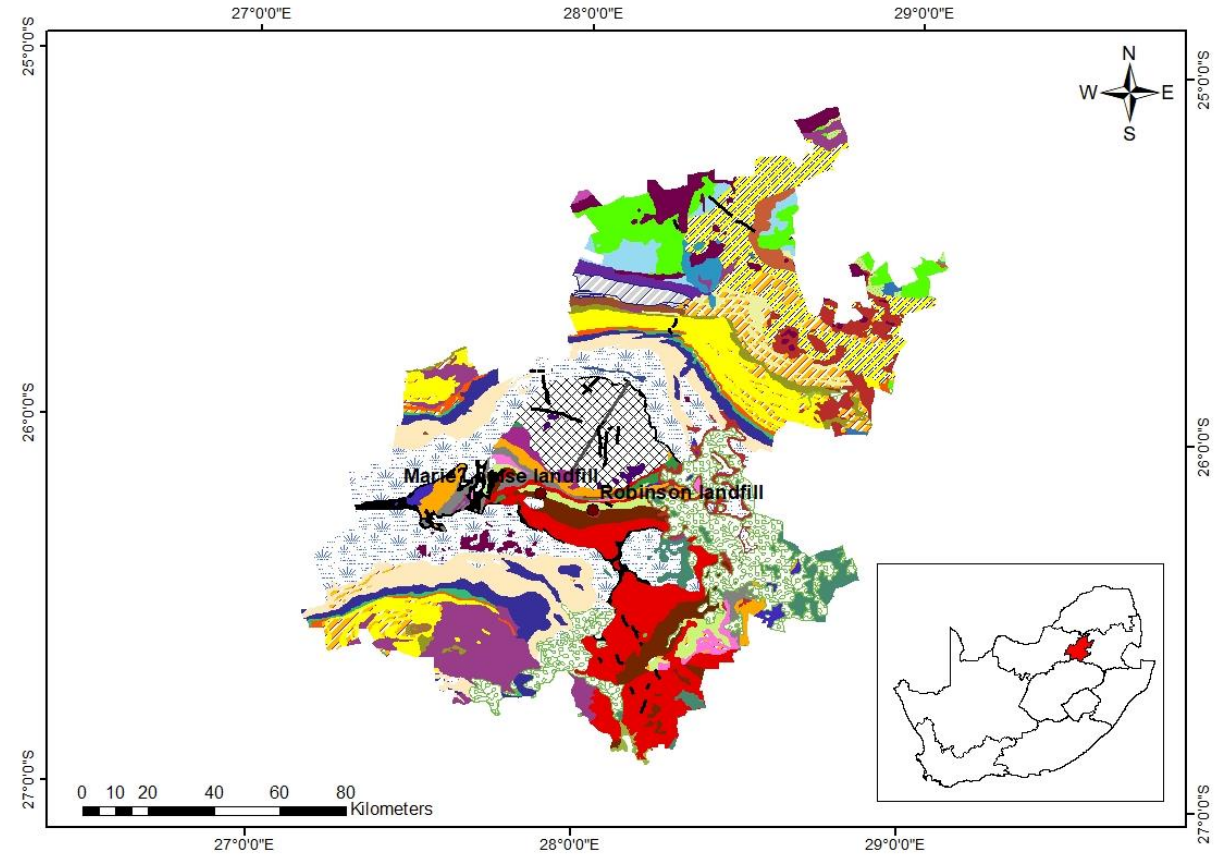

Legend

- Landfill sites
- Karoo dolerite dykes
- WATER
- ALLUVIUM, COLLUVIUM, ELUVIUM, GRAVEL
- KAROO DOLERITE SUITE
- LEHAU - mudstone, sandstone
- ECCA GROUP - shale
- ROODEPLAAT COMPLEX - trachyte
- DWYKA GROUP - diamictite
- VRYHEID FORMATION - sandstone, shale, coal
- NEBO GRANITE
- WILGE RIVER - sandstone, conglomerate
- DWARSFONTEIN SUITE
- VLAKFONTEIN SUBSUITE
- RASHOOP GRANOPHYRE - granite granophyre (Bushveld complex)
- BIERKRAAL SUBSUITE - Magnetitite (Bushveld complex)
- PYRAMID SUBSUITE - norite (Bushveld complex)
- GLENTIG, RUST DE WINTER AND LOSKOP FORMATIONS
- SCHIKFONTEIN COMPLEX
- SCHRIKKLOOF FORMATION - Porphyritic
- KWAGGASNEK FORMATION - porphyritic felsite, sandstone, quartzite
- DIABASE - tholeiite, melanorite
- RAYTON FORMATION - Quartzite, shale
- MAGALIESBERG FORMATION - quartzite
- SILVERTON FORMATION - Shale
- DASPOORT FORMATION - quartzite
- STRUBENKOP FORMATION - shale
- HEKPOORT - andesite
- TIMEBALL HILL - shale, quartzite
- MALMANI - dolomite
- BLACK REEF FORMATION - quartzite
- PLATBERG GROUP - conglomerate
- KLIPRIVIERSBERG GROUP - andesite, tuff
- TURFFONTEIN SUBGROUP - quartzite, conglomerate
- JOHANNESBURG SUBGROUP - quartzite, conglomerate
- JEPPESTOWN SUBGROUP - conglomerate
- GOVERNMENT SUBGROUP - quartzite
- HOSPITAL HILL SUBGROUP - shale
- Basement Migmatite
- MULDERSDRIF - dunite
- Archean Granite Gneiss

Figure 3-5: The geology of Gauteng Province (sourced from Council for Geosciences)

3.4 Hydrogeology

Features such as elongated ridges and wide plain areas that resulted from intrusion, sedimentation and erosion activities, influence the hydrological condition of rocks, as they control the recharge in the study area. In essence, these features control the circulation of the groundwater. Besides dolomite, which is known for its high productivity, all the other rocks that are classified as hard rocks have low groundwater productivity. Although four different types of aquifers, mainly karstic, fractured, intergranular, and intergranular and fractured aquifers, were identified by Barnard (1999; 2000), groundwater is said to occur in weathering profiles near the surface, shear zones and dykes, as well as the dissolution cavities in dolomites (Abiye, 2011). Furthermore, the study area is characterised by fractures, dykes and faults. Pockets of conduits in the dolomitic aquifer are a representation of groundwater occurrence, whereas perched aquifers are formed as a result of dykes, quartz veins and sills (Abiye, 2011). Dykes and faults are some of the important features in groundwater circulation and recharge regulation, whilst the Witwatersrand and the Transvaal Supergroups semi-circular deformation potentially participate in slowing down the circulation of groundwater (Abiye, 2011). The dykes in the Johannesburg crystalline rocks play a vital role in controlling groundwater movement. Shale has compressed fractures on the southern inclined beds, whereas granitic gneisses have wide fracture networks that may potentially regulate groundwater circulation (Abiye, 2011). The dykes in the Wilge River formation, and across the whole study area, control the movement of water. As depicted by the hydrogeological cross-section in Figure 3.6, Gauteng consists of three aquifers, mainly, karst, intergranular and fractured, and fractured aquifers. According to the Aquifer Classification Map of South Africa, karst aquifers have a borehole yield >5 L/s, whilst intergranular and fractured, and fractured aquifers have a borehole yield between 0.5 and 2.0 L/s. Intergranular and fractured are areas where alluvials/weathered zones cover the underlying fractured areas. The fractured regime is present in the rocks of the Witwatersrand Supergroup, the Bothaville formation of the Ventersdorp Supergroup, and the quartzite and sandstone of the Wilger River formation (Waterberg Group) (Barnard, 1999). The carbonate rocks of the Chuniespoort Group reflect the karst aquifer, which denotes cavities linked to fractures and jointing.

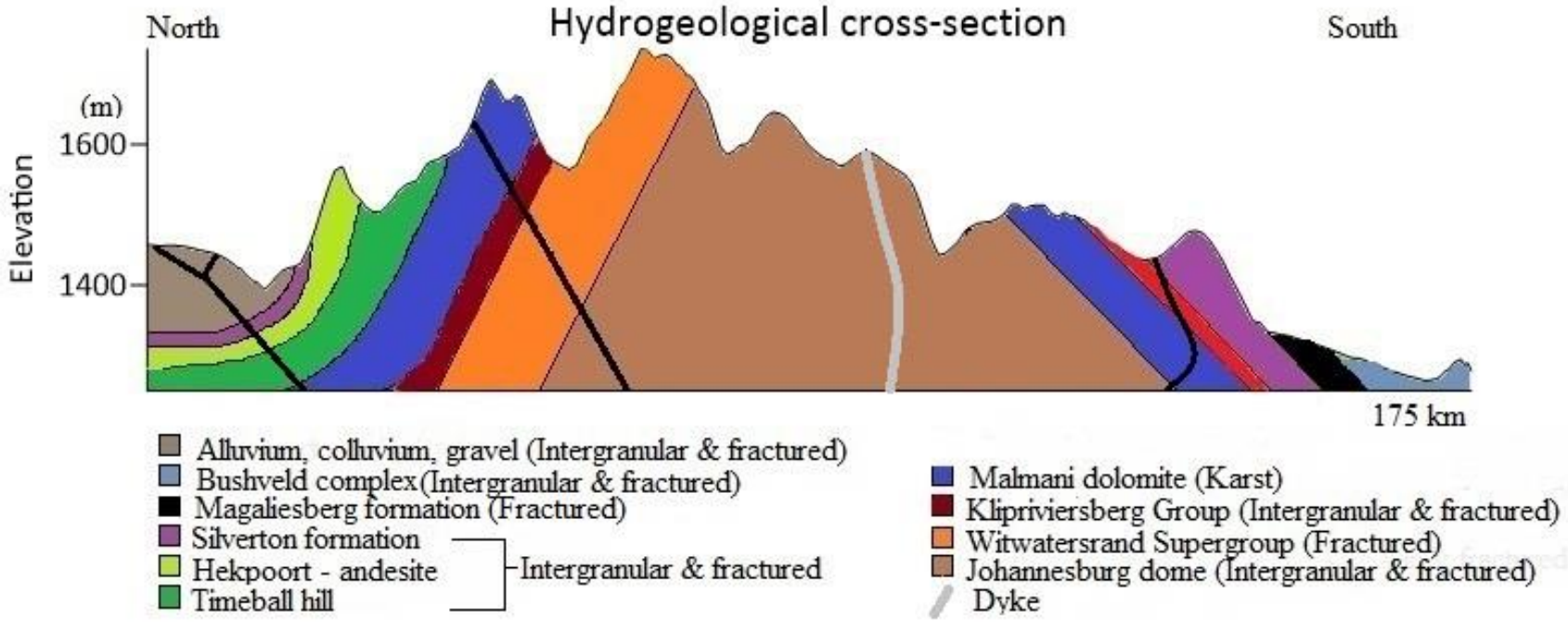

Figure 3-6: Hydrogeological cross-section of Gauteng showing karst, intergranular and fractured, and fractured aquifers (modified from Barnard, 1999)

Figure 3-7: Buried borehole (GMLS11) situated in a highly waste-polluted environment, and adjacent to the exposed undrained leachate.

CHAPTER 4: METHODOLOGY

4.1 Introduction

This chapter looks at the seven parameters of the DRASTIC method and how the DRASTIC index was estimated from the rating and weighing of the parameters. Field investigations conducted at the Marie Louise and Robinson landfill sites were used to validate the groundwater vulnerability map of Gauteng. Fieldwork was conducted during November and December 2021, and January 2022. Water and soil samples were collected during the site visit. Water samples were collected for tritium, chemistry and environmental isotope analyses, in order to better comprehend the aquifer dynamics and the water quality in the Robinson and Marie Louise landfill sites. The pH, temperature and electrical conductivity readings were taken from the groundwater, surface water and ponds. The sources of the DRASTIC parameters are presented in Table 4.1. The choice of ratings was adopted and modified from different literature (Lynch *et al*, 1994; Musekiwa and Majola, 2013; Mohuba, 2020; Press, 2020; and Moges and Dinka, 2021). Even so, overestimation and underestimation of the different hydrogeological parameters ratings was avoided.

Table 4.1: Sources of the DRASTIC parameters data

Drastic Parameters	**Data source**	**Form**
Depth to groundwater	Department of Water and Sanitation National Groundwater Archive (NGA)	Numerical
Net recharge	Department of Water and Sanitation	Digital
Aquifer media	Department of Water and Sanitation (1:500,000 hydrogeological map of South Africa by Barnard (1999))	Digital
Soil media	ISRIC world soil information	Digital

Topography	Earth Explorer (United States Geological Survey)	Digital
Impact of vadose zone	Council for Geosciences	Digital
Hydraulic conductivity	Literature (Health, 1983)	Numerical
Land use	Environmental Geographical Information System	Digital
NO_3+NO_2-N	Department of Water and Sanitation	Numerical

4.2 DRASTIC Method

The following procedures were followed when generating the D-parameter:

4.2.1 Depth to the water table

1. The shape file of Gauteng, extracted from the shape file of South Africa, was added to ArcMap 10.8.
2. An Excel spreadsheet with the depth to groundwater data and their localities (X and Y coordinates) acquired from the Department of Water and Sanitation was added to ArcMap 10.8.
3. The depth to groundwater data was Interpolated by calculating Inverse Distance Weighting (IDW) under the Spatial Analyst tool.
4. The resultant layer was reclassified based on the data in Table 4.2 using reclassify under the Spatial Analyst tool

Table 4.2: Depth to groundwater parameter rating

Depth to Water Table	
Range (m.bgl)	**Rating**
8 - 15	6
15 - 20	3
20 - 30	2
>30	1
Weight = 5	

4.2.2 Net recharge

The following procedures were followed when estimating R-parameter:

1. The net recharge shape file of Gauteng acquired from the Department of Water and Sanitation was added on ArcMap 10.8
2. The net recharge shape file was converted to raster using the Feature to Raster option under the Conversion tool
3. The resultant net recharge raster map was reclassified according to Table 4.3

Table 4.3: Net recharge parameter rating

Net recharge	
Range (mm)	**Ratings**
4 - 20	3
20 - 40	5
40 - 88	8
Weight = 4	

4.2.3 Aquifer media

The following procedures were followed when generating the A-parameter:

1. The 1:500,000 hydrogeological map (shape file) of South Africa by Barnard (1999) acquired from the Department of Water and Sanitation was added on ArcMap 10.8
2. The shape file was converted to raster using the Feature to Raster option under the Conversion tool
3. Gauteng Province was extracted from the resultant raster by using Extract by Mask under the Spatial Analyst tool

4. The resultant map was reclassified according to Table 4.4 by using reclassify tool on the Spatial Analyst tool

Table 4.4: Aquifer media parameter rating (Description source: Barnard, 2000)

Aquifer media		
Type	**Description**	**Rating**
Karst	Fractured dolomite	10
Fractured	Quartzite, shale, conglomerate, sandstone	8
Intergranular and fractured	Granite, shale, mudstone, sandstone, quartzite, andesite, dunite, coal, porphyritic, diamictite, granodiorite, alluvium, colluvium, eluvium, gravel, dolerite, tuff, tonalite, nepheline syenite, nepheline-feldspar porphyry, lujaurite, microfoyaite, tinguaite, tuff, agglomerate, breccia, trachyandesite, greywacke, gabbro, serpentinite	7
Weight = 3		

4.2.4 Soil media

The following procedures were followed when generating the S-parameter:

1. The South African soil shape file acquired from ISRIC was added in ArcMap 10.8
2. The shape file was converted to raster using the Feature to Raster option in the Conversion tool

3. The soil representing Gauteng was extracted by using the Extract by Mask option under the Spatial Analyst tool
4. The resultant raster was reclassified by using reclassify under the Spatial Analyst tool. The reclassification was according to Table 4.5

Table 4.5: Soil media parameter rating

Soil media	
Range	**Rating**
Sandy loam	7
Sandy clay loam	5
Sandy clay	3
Sand	10
Loamy sand	8
Clay loam	2
Clay	1
Weight = 2	

4.2.5 Topography

The following procedures were followed when generating the T-parameter:

1. A Digital Elevation Model (DEM) representing the Gauteng Province was downloaded from United State Geological Survey (USGS) and loaded in ArcMap 10.8
2. The four DEMs which covered Gauteng were loaded and were connected using Mosaic to Raster under the Spatial Analyst tool.

3. The shape file of Gauteng was added in ArcMap and DEM was extracted using the Extract by Mask option under the Spatial Analyst tool
4. The slope percentage was calculated from the DEM using the Slope tool under the Spatial Analyst tool in order to identify the slope percentage
5. The resultant map was reclassified according to Table 4.6 using reclassify under the Spatial Analyst tool

Table 4.6: Topography parameter rating

Topography	
Range (%)	**Rating**
0 - 5	10
5 - 10	8
10 - 20	4
20 - 30	2
Weight = 1	

4.2.6 Impact of Vadose zone

The following procedures were followed when generating the I-parameter:

1. The shape file acquired from the Council for Geosciences which comprised the lithologies of Gauteng was added in ArcMap 10.8
2. The shape file was converted to raster using the Feature to Raster option under the Conversion tool
3. The resultant raster was classified using reclassify under the Spatial Analyst tool according to Table 4.7

Table 4.7: Impact of vadose zone parameter rating (modified from Lynch *et al.* (1994))

Impact of Vadose zone		
Groups	**Description**	**Ratings**
Ventersdorp Supergroup, Transvaal Supergroup (black reef Formation and Pretoria Group), Karoo Supergroup, Bushveld Complex	Sandstone, conglomerate, shale, quartzite, andesite, tuff, coal, tholeiite, melanorite, tonalite, agglomerate, siltstone, mudstone, diamictite, porphyritic felsite, alluvium	5
Witwatersrand Supergroup, and Dominion Group	Quartzite, shale, conglomerate, granodiorite, gabbro, serpentinite, dunite, pyroxenite, nebo-granite, granite granophyre, granite-gneiss	8
Chuniespoort Group	Dolomite	10
Weight = 5		

4.2.7 Hydraulic conductivity

The following steps were followed when generating the C-parameter:

1. The shape file representing the lithologies of the Gauteng Province was added in ArcMap 10.8
2. Hydraulic conductivity values of the different aquifer media were allocated to the aquifer media with reference to Table 4.8
3. The hydraulic conductivity added to the different aquifer were reclassified into three ranges, namely, <5 m/day, 5-10 m/day, and >100 m/day

Table 4.8: Hydraulic conductivity parameter rating (Source: Health, 1983)

Lithology description	**Hydraulic conductivity (m/day)**
Dolomite	100 - 10000
Shale	10^{-8} - 10^{-4}
Quartzite, granite, gabbro, gneiss, sepentinite, granodiorite, dolerite, tuff, tonalite, tholeiite, migmatite, rhyolite, synenite, andesite	10^{-8} - 10
Diamictite, conglomerate, sandstone, greywacke, siltstone, alluvium, mudstone	10^{-7} – 10^{-1}
Weight = 3	

4.2.8 Intrinsic vulnerability map

The following steps were followed when generating the intrinsic vulnerability map:

1. The seven rated DRASTIC parameters were uploaded in ArcMap 10.8 in order to calculate the DRASTIC index
2. The DRASTIC index was calculated by using Raster Calculator in the Spatial Analyst tool, using the DRASTIC index formula by Aller *et al.* (1987)
3. The resultant DRASTIC map was reclassified into three vulnerability classes using the reclassify option under the Spatial Analyst tool

The DRASTIC index was calculated, using Equation 4.1 below:

$$\text{DRASTIC index} = \text{DrDW} + \text{RrRw} + \text{ArAw} + \text{SrSw} + \text{TrTw} + \text{IrIw} + \text{CrCw} \quad (4.1)$$

Where r is the rating, and w is the weight

Weight

The values allocated to the DRASTIC factors are based on the fixed DRASTIC factor assigned by Aller *et al.* (1987). The value in which each DRASTIC factor weigh is based on the importance of that factor in comparison to other factors of the DRASTIC methods; hence the factor with a value of 5 would represent the highest importance, whereas a factor with a value of 1 would represent the least importance.

Range

The importance of the different ranges for each factor is classified based on the importance of each parameter with respect to other parameters of the DRASTIC method. The rating of the ranges is not constant as it depends on the researchers' knowledge about the significance of the different ranges in that hydrogeological setting.

4.2.9 Landfill-Specific Vulnerability Map

The following procedures were followed when constructing the specific vulnerability map:

1. A land use map of South Africa acquired from the Environmental Geographical Information System was loaded in ArcMap
2. The land use of Gauteng was extracted from the shape file of South Africa by using Extract by Mask in the Spatial Analyst tool
3. Landfills were separated from other land uses by using Extract by Attribute under the Spatial Analyst tool
4. The resultant landfill raster was reclassified by assigning it a value of 10.
5. Using the Sum Weighted tool, the reclassified layer and the intrinsic vulnerability layer were overlaid to produce a landfill-specific vulnerability map. The landfill layer was assigned a weight of 5, and the intrinsic vulnerability was assigned a weight value of 1

The specific vulnerability was estimated, using Equation 4.2 below:

$$\textbf{Specific vulnerability} = \textbf{DI} + \textbf{LrLw} \qquad (\mathbf{4.2})$$

Where:

DI = Intrinsic vulnerability layer

Lr = Rated land use parameter

Lw = Weighted land use parameter

4.2.10 DRASTIC validation by NO_3+NO_2-N

The following procedures were followed when generating the nitrate validation map:

1. NO_3+NO_2-N (nitrate + nitrite nitrogen) data for the period of 2000 – 2022 was acquired from the Department of Water and Sanitation. The average NO_3+NO_2-N values were calculated and the values were superimposed on the intrinsic vulnerability index map.
2. The distribution and concentration of NO_3+NO_2- as N was presented on the vulnerability index map by using the Graduated Symbols in quantities under the Layer Properties.

4.3 DRASTIC validation by field Investigation

4.3.1 Soil Samples

Soil samples were collected at twelve (12) points in Robinson and thirteen (13) points in the Marie Louise landfill site from a depth of 0.5 m to analyse trace elements of the topsoil of the two landfill sites. The soil samples were collected along with their geographical readings in the Robinson and Marie Louise landfill sites, as reported in Table 4.9 and Table 4.10. The soil was dug using a spade and carefully placed in a plastic bag, whereby they were further marked according to their location. The twenty-five 50 g samples were placed in an oven and dried at 50 °C to remove moisture and to prepare them for milling. The samples were thereafter taken to the Earth lab at the University of the Witwatersrand for trace elements analyses using X-ray fluorescence (XRF). The results of the concentration levels of different trace elements were displayed using visual representations.

4.3.2 Borehole purging

Before collecting the water samples for environmental isotope and hydrochemistry analyses, the boreholes were purged to remove stagnant water and to collect samples whose chemistry is an actual representative of the natural condition of groundwater. To ensure the efficiency of purging, the pH and electric conductance needed to be monitored during purging, when these parameters had stabilised, the samples were collected. The purging of groundwater was conducted by using a polyethene bailer and a pump.

Figure 4-1: Measuring physicochemical parameters in the Marie Louise landfill site

4.3.3 Water samples

Water samples were collected for tritium, stable isotopes, and water chemistry analyses. Tritium and water chemistry samples were collected in 1 litre PVC bottles and 500 ml PVC bottles, respectively. At the Robinson landfill site, water samples were collected from boreholes, pond, and the leachate dam. Robinson landfill site has more than ten boreholes that were drilled for water monitoring; however, at the time of sampling, some boreholes were not accessible. At the Marie Louise landfill site, water samples were collected from boreholes and from the leachate pond. The other boreholes in the sites were either damaged or buried underneath. Prior to sampling, the bottles were rinsed at least five times to disinfect them. The samples were collected and placed into a cooler box with ice, and then they were transported to their designated laboratories for chemical analysis. For the tritium analysis, the samples were transported to the iThemba laboratory in Gauteng, whereas the stable isotope analysis was conducted at the Hydrogeological laboratory at the School of Geosciences at the University of the Witwatersrand. For the major ion and trace element analysis, samples were sent to the WaterLab in Pretoria. During groundwater sampling, the water level, the diameter and the casing were recorded by using a tape measure and a rope (Figure 4.2). For the hydrochemical facies analysis, a Piper diagram was generated to analyse the origin, evolution and mixing of water in the different landfill sites.

The mean residence time for tritium was calculated, using Equation 4.2 below (Clark and Fritz, 1997):

$$\boldsymbol{T = -17.93 \times \ln\left(\frac{a_t{}^3h}{a_0{}^3h}\right)} \qquad (4.2)$$

Where:

T = mean residence time (MRT) in years

$a_t{}^3H$ = residual activity remaining after decay overtime

$a_0{}^3H$ = initial tritium unit

Table 4.9: Geographical locations of the soil samples collected in Marie Louise landfill

Sample Name	**Longitude**	**Latitude**	**Elevation**
ML1	27.884177	-26.19309	1723
ML2	27.88505	-26.193379	1718
ML3	27.886627	-26.19137	1724
ML4	27.88719	-26.189983	1705
ML5	27.881202	-26.191327	1722
ML6	27.880856	-26.189172	1720
ML7	27.882078	-26.192958	1721
ML8	27.882068	-26.186525	1705
ML9	27.880101	-26.190642	1722
ML10	27.883930	-26.187622	1723
ML17	27.881087	-26.18834	1702
ML19	27.883053	-26.186885	1730
ML16	27.88135	-26.191572	1702

Table 4.10: Geographical locations of the soil samples collected in Robinson landfill

Sample Name	**Longitude**	**Latitude**	**Elevation**
RB1	28.039928	-26.235892	1722
RB2	28.038337	-26.236377	1727
RB3	28.037613	-26.236658	1722
RB4	28.034428	-26.237393	1725
RB5	28.032951	-26.237027	1721
RB6	28.034882	-26.236278	1727
RB7	28.040657	-26.231193	1723
RB8	28.039235	-26.23679	1722
RB18	28.038528	-26.228766	1726
RB9	28.032346	-26.233775	1722
RB12	28.033635	-26.231947	1721
RB19	28.040622	-26.234286	1722

Figure 4-2: Measuring hydrochemical parameters in the Robinson landfill site

CHAPTER 5: RESULTS AND DISCUSSIONS

5.1 Drastic Method

5.1.1 Depth to Water table

The depth to groundwater data was acquired from 342 monitoring boreholes from the Department of Water and Sanitation National Groundwater Archive. Figure 5.1 shows the spatial distribution of boreholes interpolated on the shapefile of Gauteng Province using the Inverse Distance Weighted (IDW) tool to generate the depth to groundwater map of the study area presented in Figure 5.2. As depicted in Figure 5.1, the monitoring boreholes are not spatially distributed and are clustered around the central region of the Province.

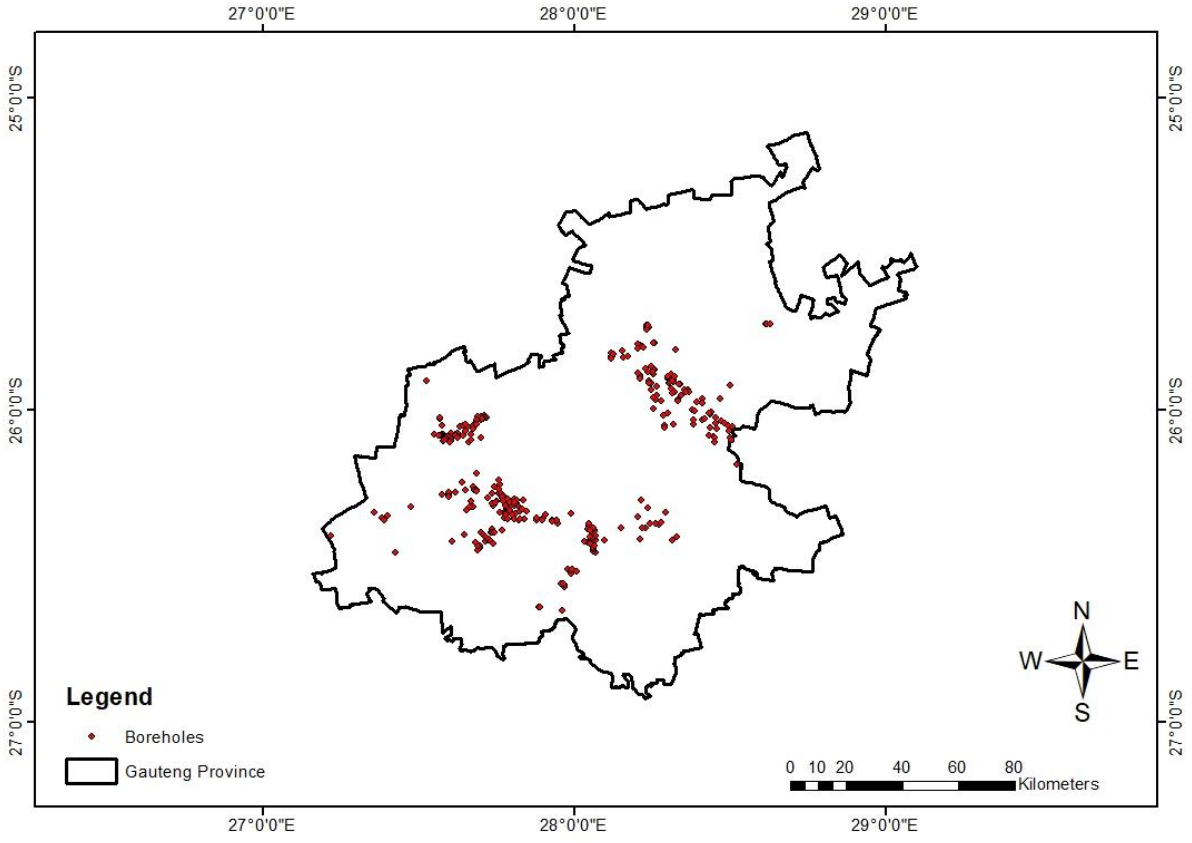

Figure 5-1: Spatial distribution of boreholes

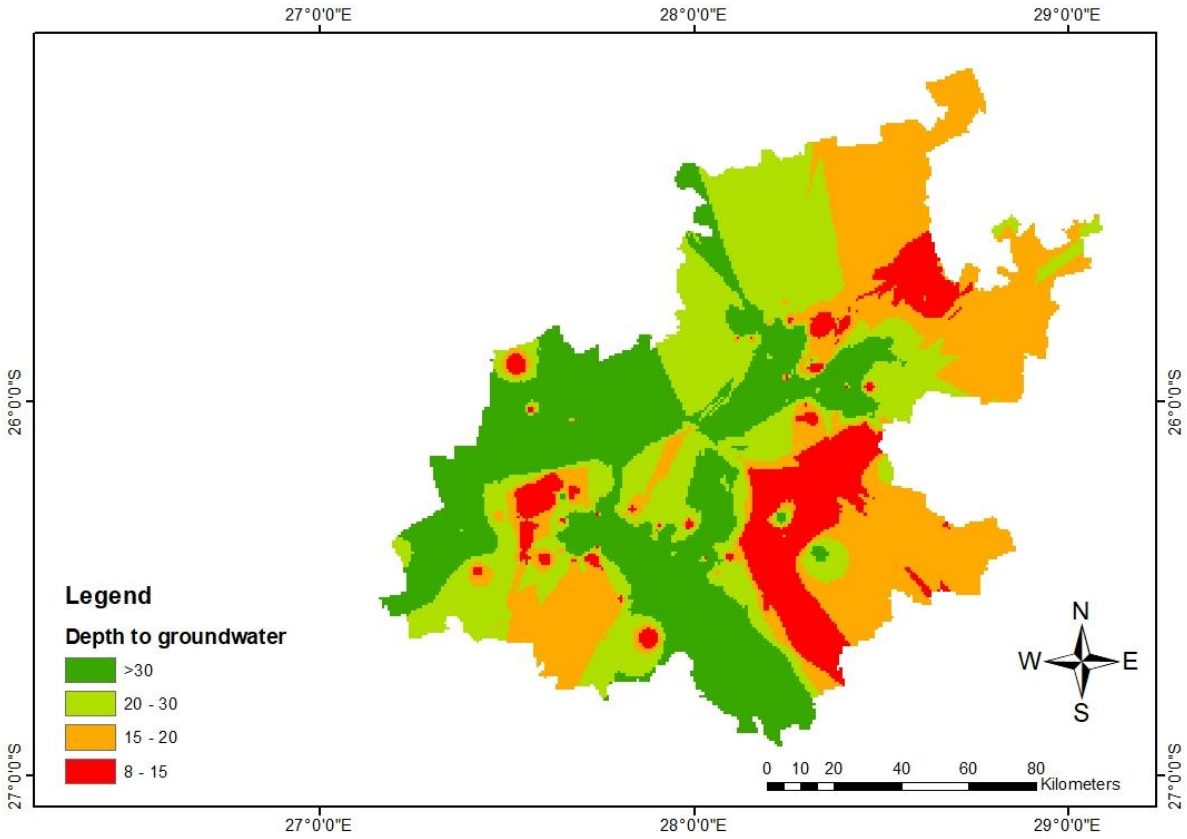

Figure 5-2: The depth to groundwater ranging between 8-15 m.b.g.l, 15-20 m.b.g.l, 20-30 m.b.g.l, and >30 m.b.g.l in red, orange, light green, and deep green, respectively.

The depth to groundwater in the Gauteng Province ranges between 8 to 30 m.b.g.l (Figure 5.2). The northeast and southeast regions have a groundwater level ranging between 15-20 m.b.g.l and 8-15 m.b.g.l, whereas the western part of the Province is dominated by a depth to groundwater >30 m.b.g.l. The longer distance that contaminants would have to travel allows attenuation processes such as adsorption and sorption to occur, which can prevent the migration of contaminants along the groundwater flow path (Aller *et al.*, 1987). For this reason, a groundwater depth greater than 30m was ranked less vulnerable and allocated a rating of 1 (Figure 5.3). The lowest groundwater depth in the Province range between 8 – 15 m. This range was allocated a rating of 6, as the travel distance is relatively shorter. Given the high water pressure in Pretoria and the semi-confined aquifers in Johannesburg that vary a lot, the depth to groundwater is expected to be different in accordance with the differences in aquifers. The data obtained from the National Groundwater

Archive does not indicate if the water level >30 are from pumping wells at the time of measurements.

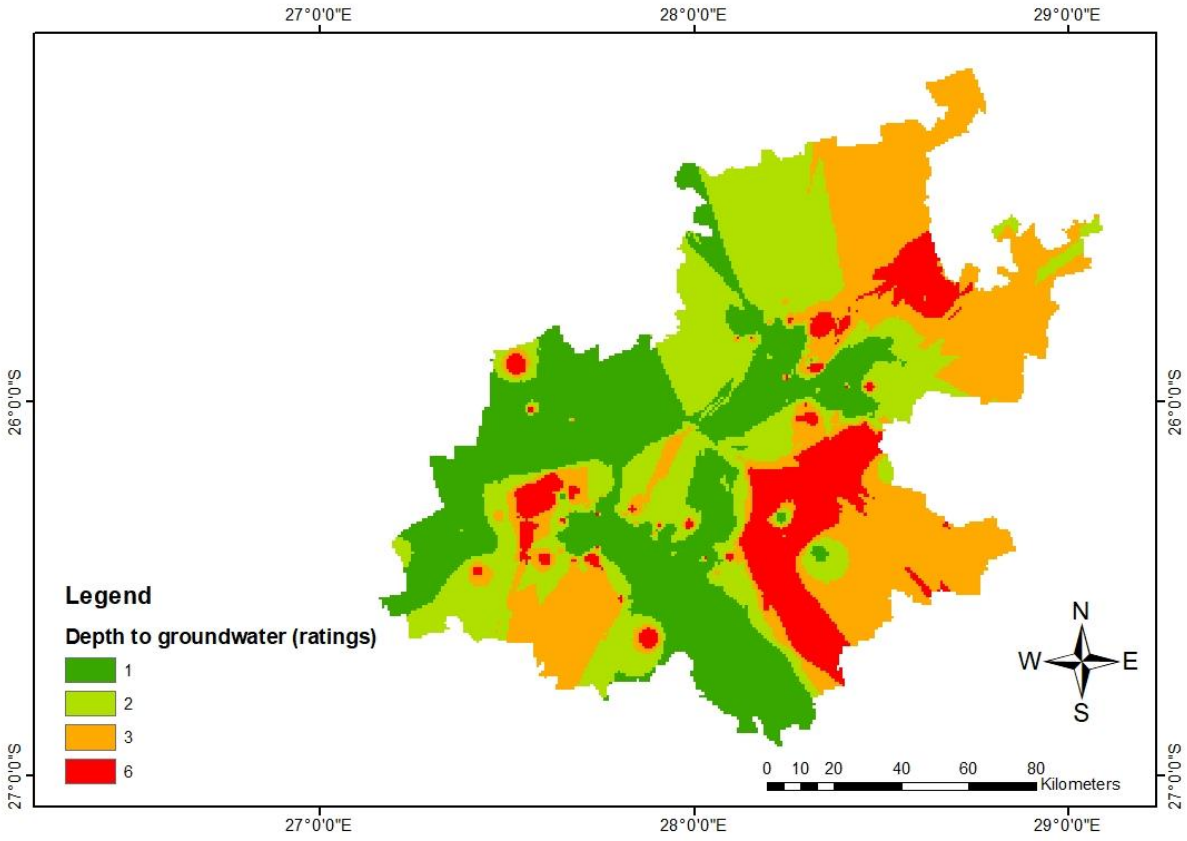

Figure 5-3: The depth to groundwater ratings of 1 (green), 2 (light green), 3 (orange), and 6 (red).

The percentage composition of depth to groundwater is presented in Figure 5.4. Moderately vulnerable areas cover 11% of the study area and were assigned a rating of 6 which are represented in red in Figure 5.4. Areas with low vulnerability have a rating of 1-3 and cover 89% of the study area. The low vulnerability areas are shown in deep green, light green, and orange for the rating of 1, 2, and 3, respectively.

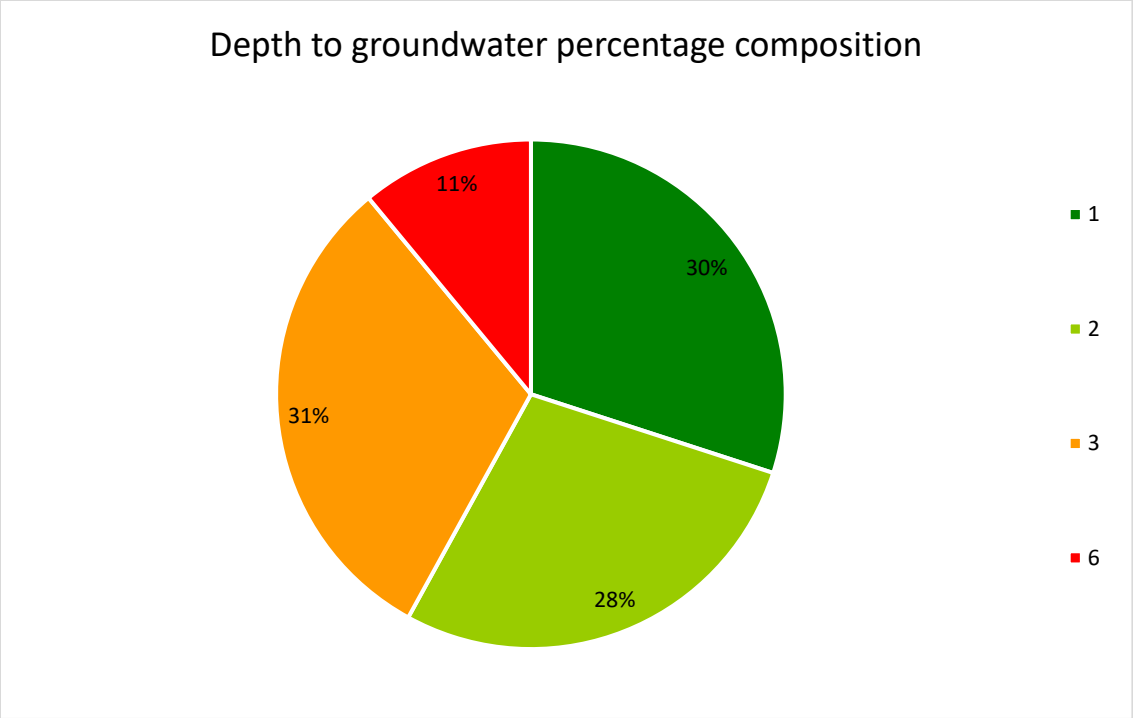

Figure 5-4: The percentage composition of depth to groundwater shows a rating of 1, 2, 3, and 6 covering 30%, 28%, 31%, and 11% of the Province, respectively.

5.1.2 Net Recharge

A South African recharge map, which was used to estimate the net recharge for the Gauteng Province, was acquired from the Department of Water and Sanitation (DWS). The Department of Water and Sanitation used the Chloride Mass Balance method to estimate the net recharge of South Africa. As demonstrated in Figure 5.5, the estimated net recharge range is between 4-88 mm/y. Although the Central Bushveld (north of Gauteng) receives rainfall ranging between 500-750 mm/y, whereas the Moist Highveld Grassland (south of Gauteng) receives rainfall ranging between 600-800 mm/y (SAWS, 2021), the net recharge depicted in Figure 5.5 is relatively low when compared to the annual rainfall that the north and south regions receive. Recharge is influenced by precipitation intensity, duration, amount; evapotranspiration; flow dynamics; and karst features, amongst other factors. Springs associated with dykes and tectonic depression in dolomites, and sinkholes that form from dissolution cavities, are some of the karst features that influence groundwater recharge in Gauteng. The presence of fractures and dykes also influences flow dynamics which may have ultimately influenced groundwater flow dynamics. Given that Gauteng receives most of its rainfall in summer, winter seasons contribute less to recharge since the rate of recharge relies on rainfall amount. Figure 5.5 shows three recharge ranges: 4 – 20 mm/year, 20 – 40 mm/y, and 40 – 88 mm/y.

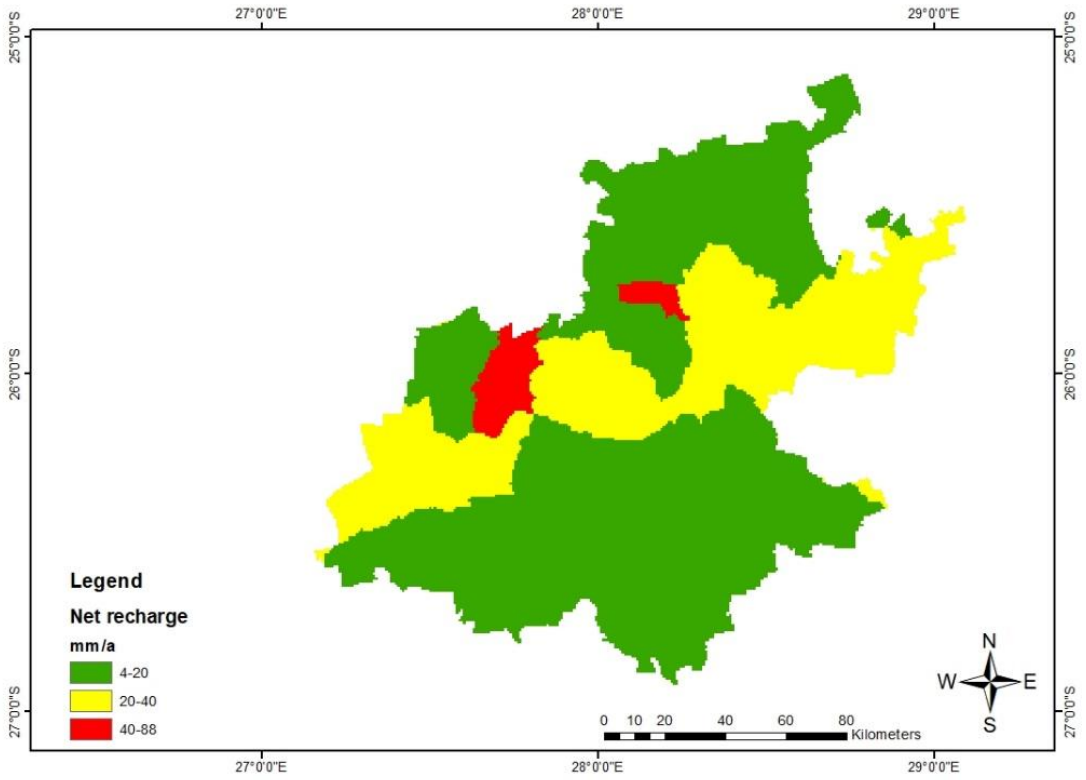

Figure 5-5: Recharge range map showing a net recharge of 4-20 mm/a, 20-40 mm/a, and 40-88 mm/a in green, yellow, and red, respectively.

A rating of 3 was assigned to regions with recharge ranging between 4-20 mm/y in the north and south regions (Figure 5.6). Low recharge hinders the movement of contaminants with water; hence areas with a rating of 3 are classified as less vulnerable. A rating of 5, which represents moderate vulnerability, was assigned to areas that receive recharge ranging between 20-40 mm/y. The moderately vulnerable areas are situated in the northeast, southwest, and central part of the Province. Areas that receive high recharge cover a small portion of the west and central north regions. This recharge range (40-88 mm/y) was assigned a rating of 8. Recharge is the main transporter of contaminants. Since high recharge promotes the transportation of contaminants, the vulnerability of aquifers to pollution in the area, with recharge ranging between 40-88 mm/y, is expected to be high. Recharge is responsible for the leaching and contaminant transportation from the surface to the aquifer. The dilution and dispersal of contaminants in unsaturated and saturated

zones depend on the amount of recharge. The net recharge data and the aquifer type (Figure 5.8) may not match because of the different conduit in the aquifers that affects the net recharge rate.

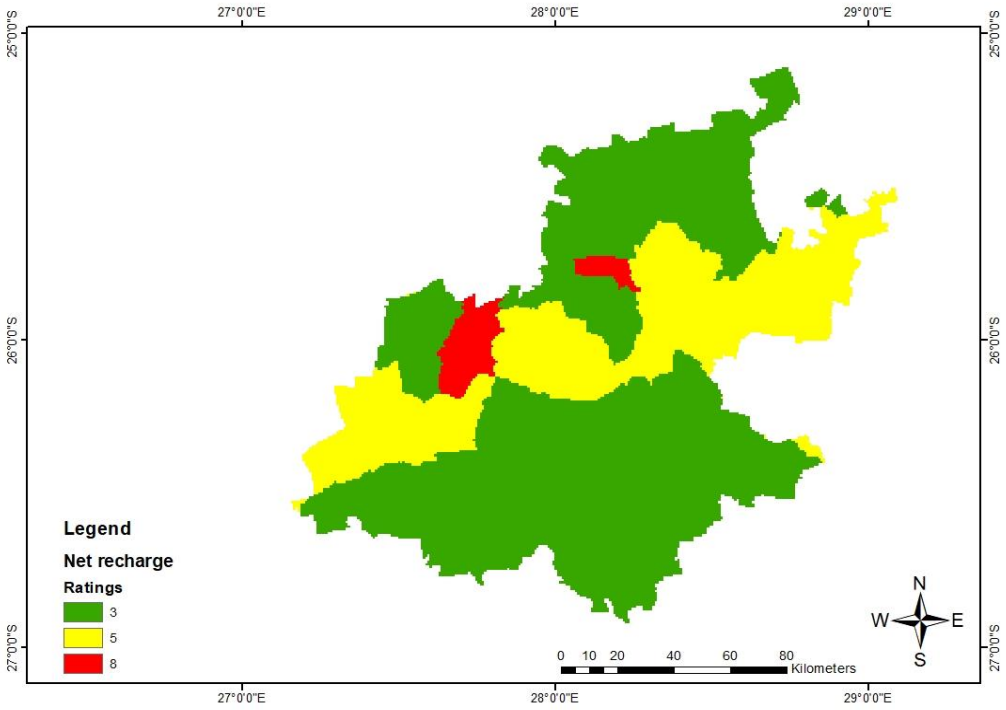

Figure 5-6: Recharge map showing low (3), moderate (5), and high vulnerability (8).

The percentage composition of net recharge is presented in Figure 5.7. A small portion of the Province (3%) has a vulnerability rating of 8, indicating high recharge and pollution vulnerability. On the other hand, 30% of the study area has a moderate vulnerability rating of 5, whilst 67% of the study area is represented by a low vulnerability rating of 3.

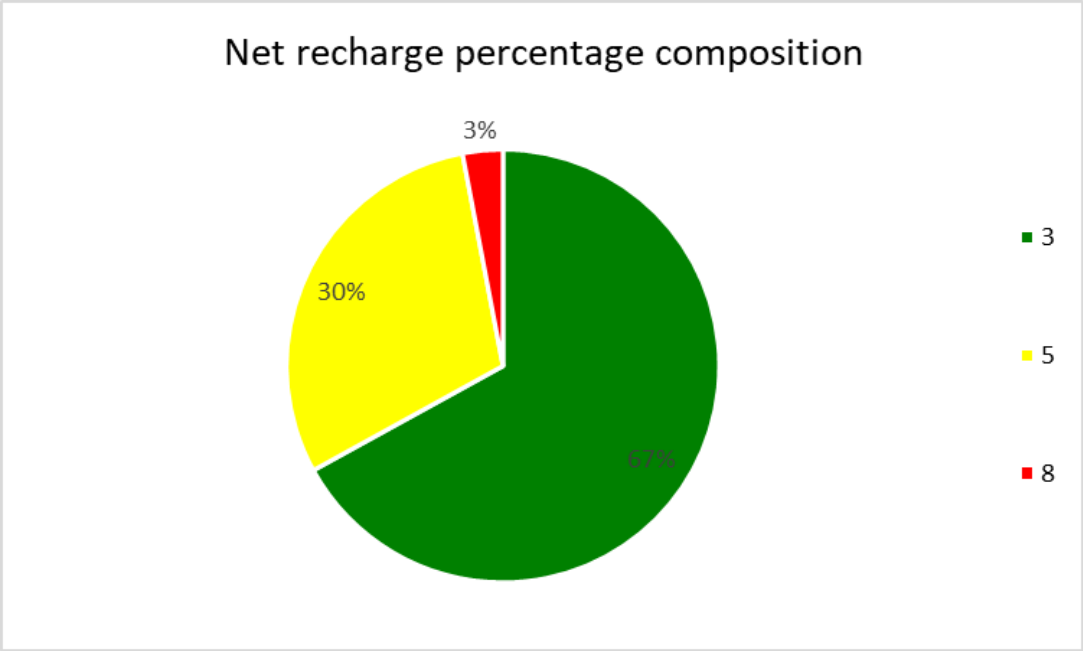

Figure 5-7: Percentage composition of net recharge showing areas with low (green), moderate (yellow), and high vulnerability (red).

5.1.3 Aquifer Media

The 1:500,000 hydrogeological map of South Africa by Barnard (1999) which showed the groundwater occurrence and the aquifer yield acquired from the Department of Water and Sanitation (DWS) as a shapefile was used to generate the aquifer media map of the Gauteng Province (Figure 5.8). As depicted in Figure 5.8 below, the Gauteng Province has three aquifer media, namely, karst, fractured, and, intergranular and fractured. The Province is dominated by the intergranular and fractured aquifer. Karst aquifers of dolomite overlapped by fractured aquifers can be observed in the southwest and central regions of Gauteng.

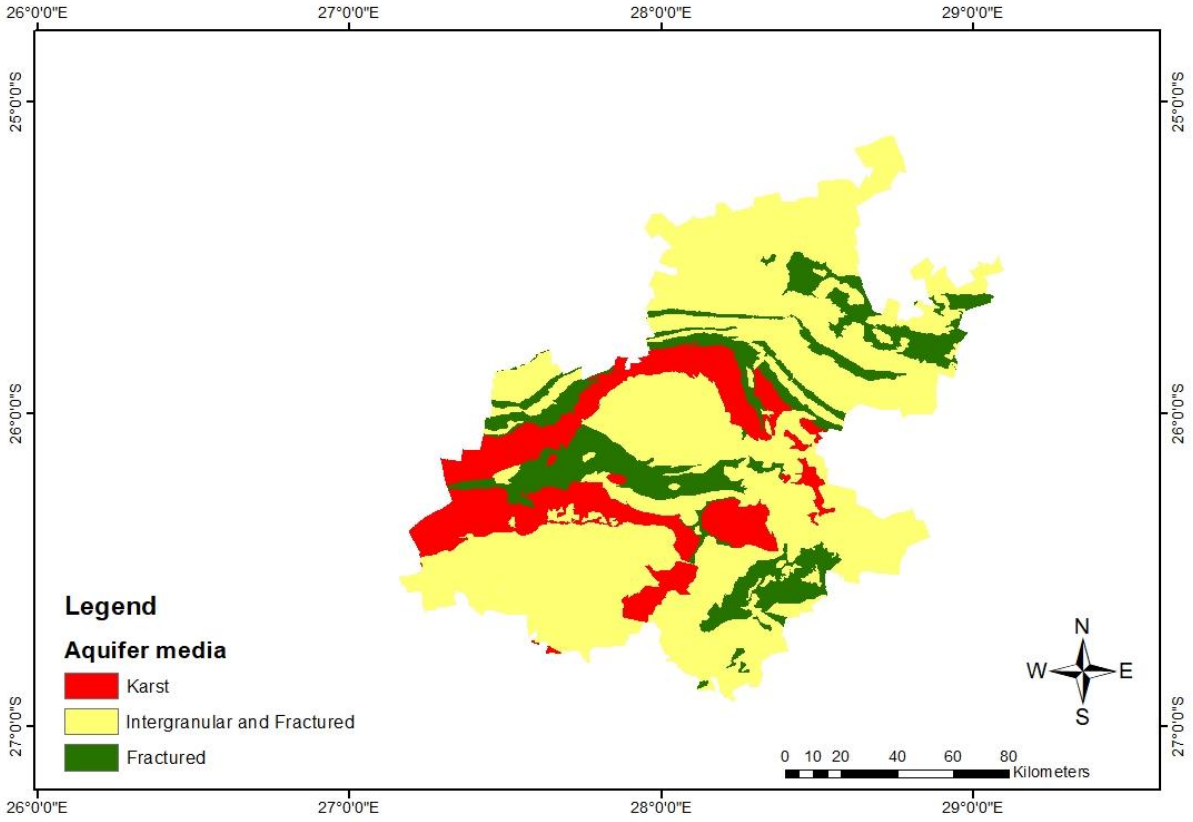

Figure 5-8: Aquifer media map showing karst aquifer, intergranular and fractured, and fractured aquifers in red, yellow, and green, respectively.

The ratings assigned to the aquifer media of the study area are depicted in Figure 5.9. The karst aquifers of Malmani dolomite are characterised by dissolution cavities and have a high groundwater yield (Abiye, 2011, Abiye *et al.*, 2015). Dolomites have numerous fractures and cavities that may serve as effective recharge zones, which may potentially transport contaminants. For this reason, the dolomite aquifers were assigned a rating of 10.

Fractured aquifers are characterised by fractures, fissures, and joints of the granitic gneiss and quartzite which play a role in groundwater and contamination circulation. Fractures create permeable avenues for contamination to move. According to Morris *et al.* (2003), highly fractured aquifers with shallow water tables provide little opportunity for contaminant attenuation and are therefore linked to extreme vulnerabilities. The level of groundwater contamination would therefore depend on the degree of fractures and the depth to groundwater. For these reasons, fractured aquifers were assigned a rating of 8, representing high vulnerability. The fractured and intergranular aquifers are hydraulically interlinked, with fractured aquifer overlying the intergranular aquifer (Barnard, 2000; Abiye, 2011; Abiye *et al.*, 2015). These aquifers were assigned a rating of 7, which represents moderate-high vulnerability.

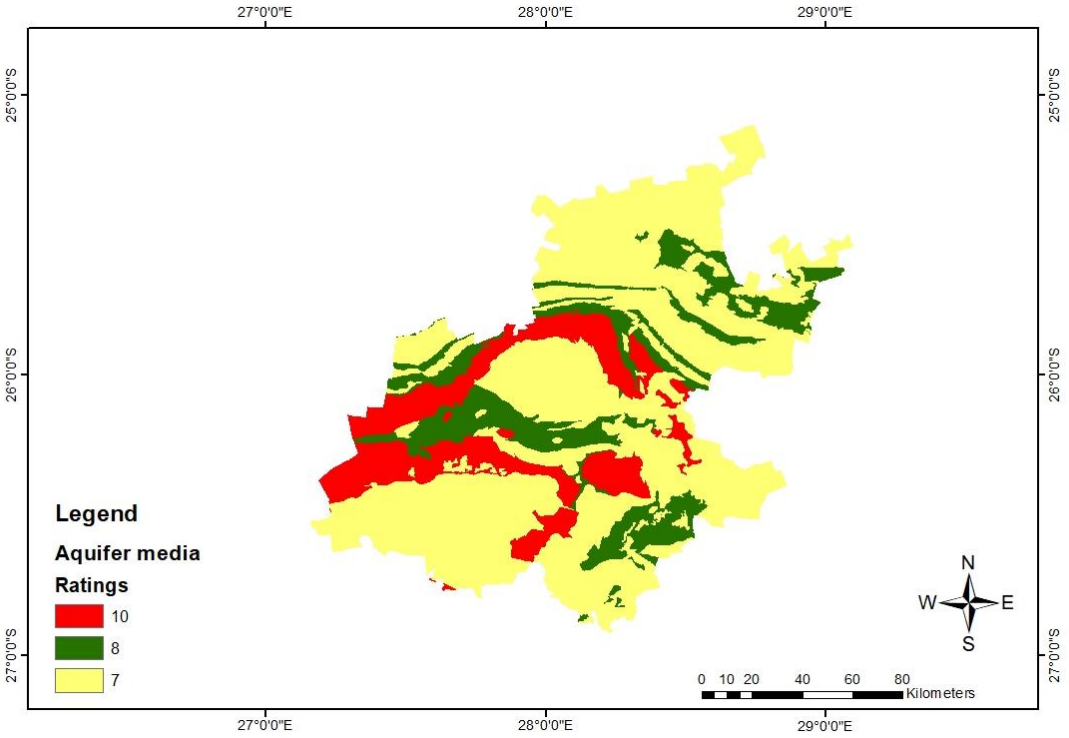

Figure 5-9: Aquifer media map showing a rating of 10 (dolomite), 7 (intergranular and fractured), and 8 (fractured).

The percentage composition of aquifer media is presented in Figure 5.10. The area that has highly vulnerable aquifer media covers 17% of the Province and is represented by a rating of 10. The aquifer media with a rating of 7 covers 66% of the study area whilst the aquifer media with a rating of 8 covers 17% of the study area.

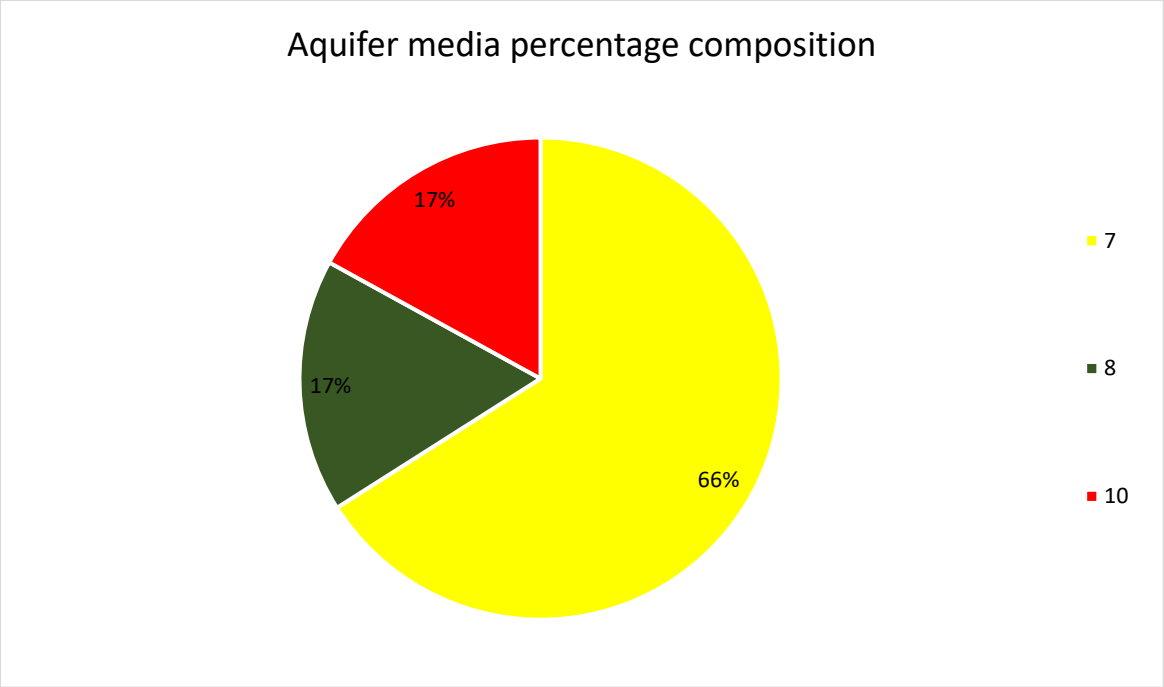

Figure 5-10: Percentage composition of aquifer media showing dolomite in red, intergranular and fractured aquifer in yellow, and fractured aquifer in green.

5.1.4 Soil Media

Gauteng Province is dominated by loamy sand, which covers most parts of the south and northeast regions of the Province (Figure 5.11). Clay covers a small part of the southwest region, whilst a combination of sandy clay loam, clay loam, and sandy clay dominates the north region. As depicted in Figure 5.11, the central part of the Province consists of sand.

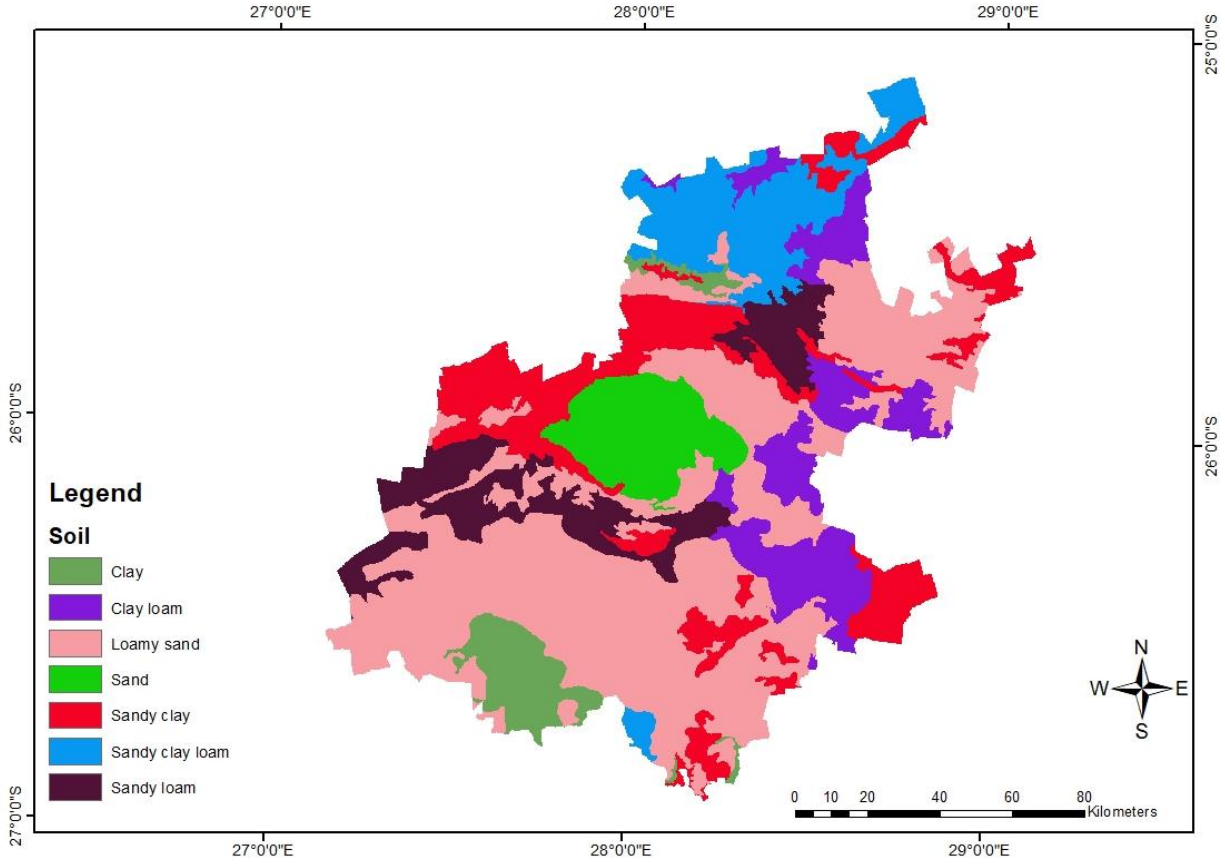

Figure 5-11: Soil media map showing clay in dark green, clay loam in purple, loamy sand in pink, sand in light green, sandy clay in red, sandy clay loam in blue, and sandy loam in maroon.

Due to the absence of clay and silt in loamy sand, loamy sand was allocated a rating of 8, which demonstrate high vulnerability. Since clay can restrict the movement of contaminants, it was assigned a vulnerability rating of 1, which indicates low vulnerability. The north region is dominated by a combination of sandy clay loam, clay loam, and sandy clay, with a rating of 5, 2, and 3, respectively (Figure 5.12). According to the soil textural classification chart (Soil

conservation service, 1951), clay loam consists of 15 - 55% silt and 27 - 40% clay. The high percentage of clay is essential in reducing the permeability of contamination as the presence of fine-textured material restricts contamination movement. Sand with a rating of 10 lacks silt and clay content which can aid in the attenuation of contamination. Sandy loam in the north and west region of the Province has relatively low clay content, which can increase the migration of contamination. For these reasons, it was allocated a rating of 7. Given that the soil media has great depth, attenuation processes such as filtration, biodegradation, and volatilization can occur (Aller *et al.*, 1987).

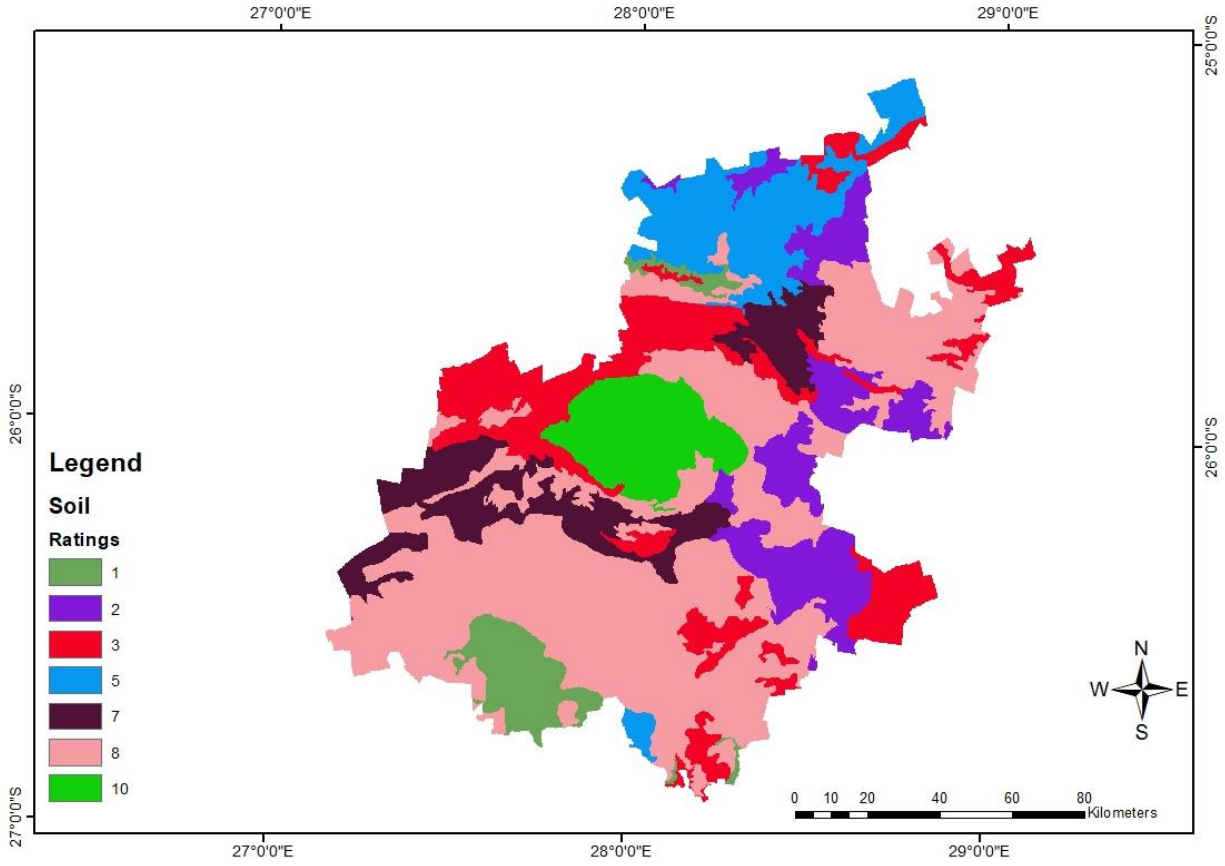

Figure 5-12: Soil media map showing ratings of 1 (clay), 2, (clay loam) 3 (sandy clay), 5 (sandy clay loam), 7 (sandy loam), 8 (loamy sand), and 10 (sand).

The percentage composition of the soil is demonstrated in Figure 5.13. Soil composition that is highly vulnerable to pollution covers 60% of the Province and is represented by a rating between 7-10. Soil compositions with low vulnerability to pollution cover 31% of the Province and is therefore represented by a rating of 1-3. 9% of the Province comprises soil that is moderately vulnerable to pollution, with a rating of 5. The majority of the study area comprises soil that is highly susceptible to pollution.

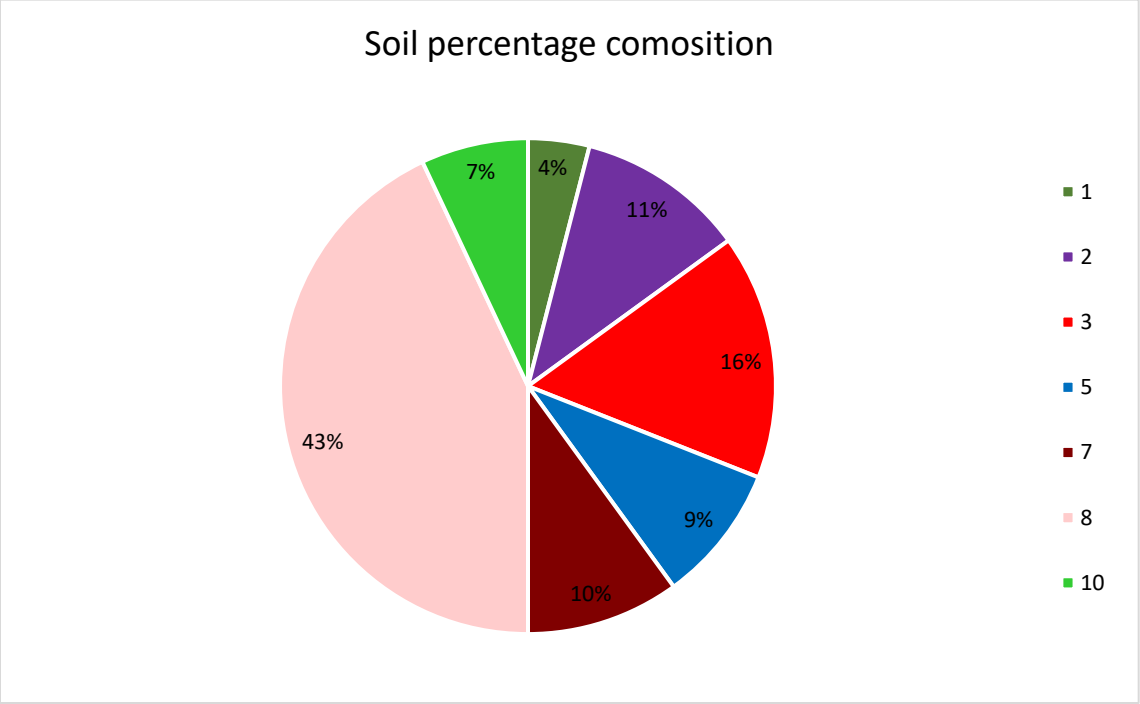

Figure 5-13: Percentage composition of clay, clay loam, loamy sand, sand, sandy clay, sandy clay loam, and sandy loam with ratings of 1, 2, 8, 10, 3, 5, and 7, respectively.

5.1.5 Topography

The slope of the study area was estimated using Digital Elevation Model (DEM) acquired from the United State Geological Survey (USGS). As demonstrated by Figure 5.14, the slope of the Gauteng Province varies between 0-30 %. The Province is dominated by a range of 0-5%, followed by a range of 5-10%.

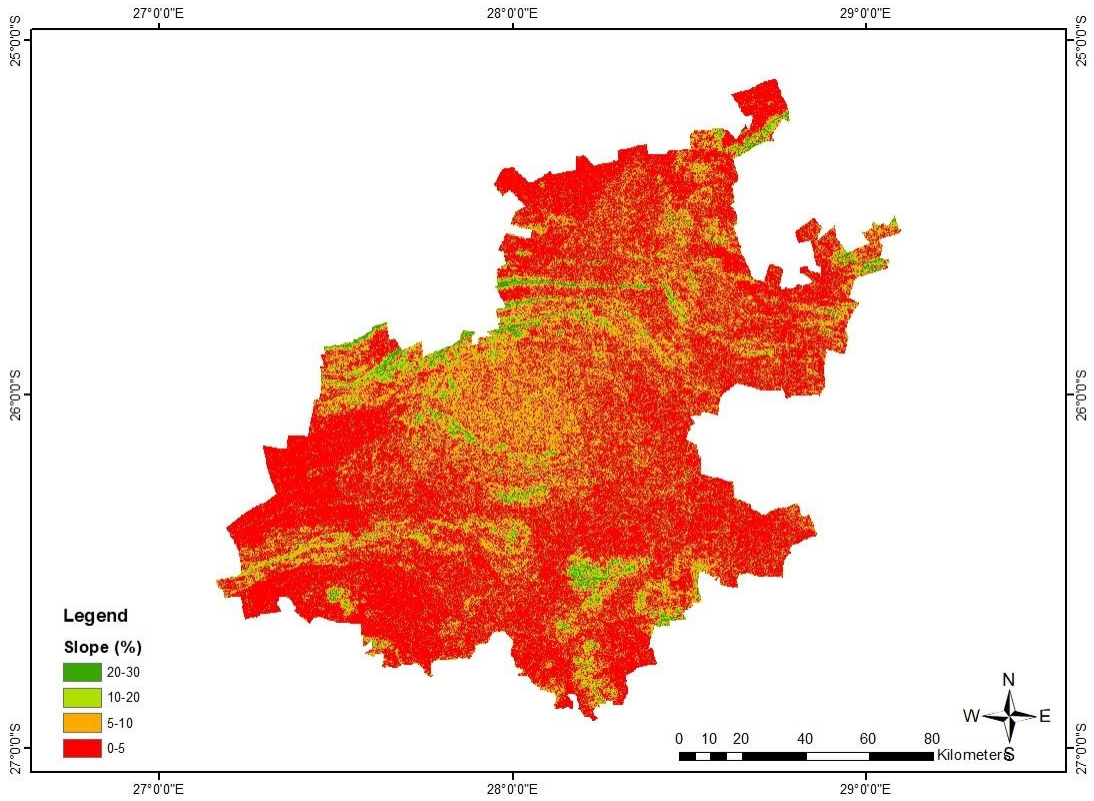

Figure 5-14: Topography (slope) ranging between 0-5%, 5-10%, 10-20%, and 20-30%.

Figure 5.15 presents the vulnerability ratings assigned to the slope map. Regions with a slope range of 0-5% are considered highly vulnerable to pollution and therefore were assigned a rating of 10. This is because gentle slopes have less surface runoff and greater water-holding capacity, creating greater chances of infiltration. Regions with a slope range between 20-30% were allocated a vulnerability rating of 2 because steep slopes favour runoff over infiltration, which ultimately decreases contaminant movement to the underlying aquifer. Some parts of the western and southern regions of the Province have a slope that ranges between 10-20 %, which was assigned a rating of 4, which represents less vulnerability to groundwater pollution. The likelihood of high

surface runoff and low infiltration increases with topography. Nevertheless, the movement of water and the processes of rainfall-runoff and infiltration in the local hydrogeological system is greatly influenced by topography.

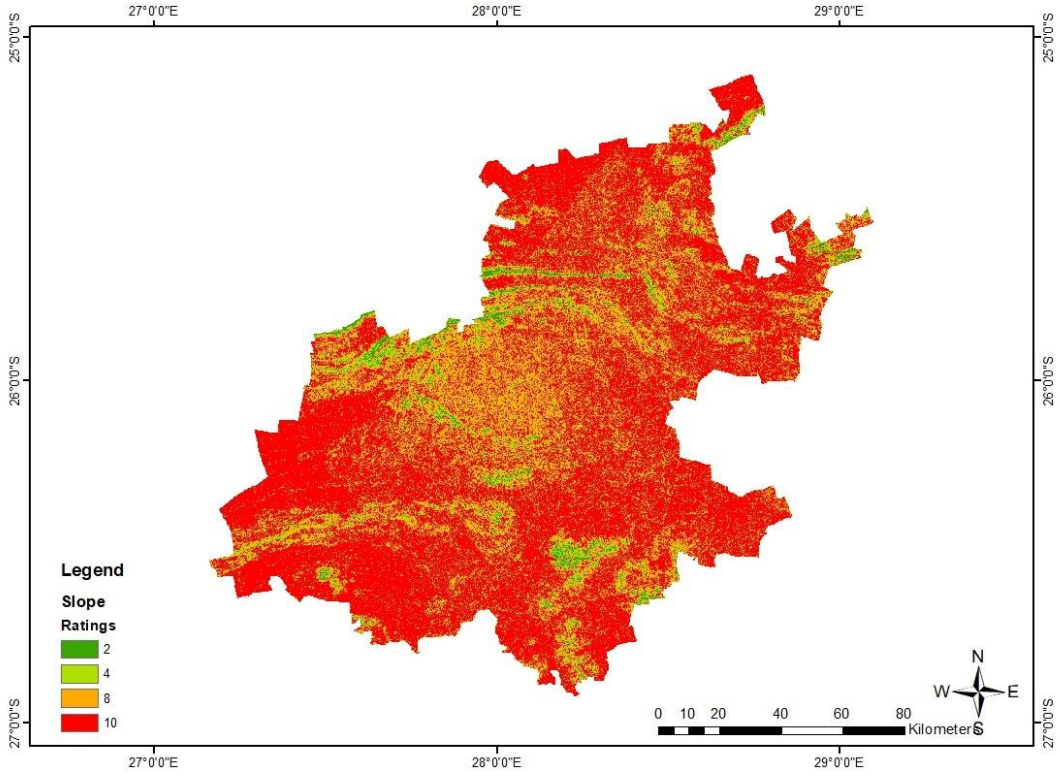

Figure 5-15: Slope map showing a rating of 2 in green, 4 in light green, 8 in orange, and 10 in red.

62% of the Province comprises a gentle slope which is associated with high vulnerability to pollution. Steep slopes with a rating of 2 and 4 which represents the low vulnerability of the aquifer to pollution cover 10% of the Province (Figure 5.16). Areas with a rating of 8 covers 28% of the Province.

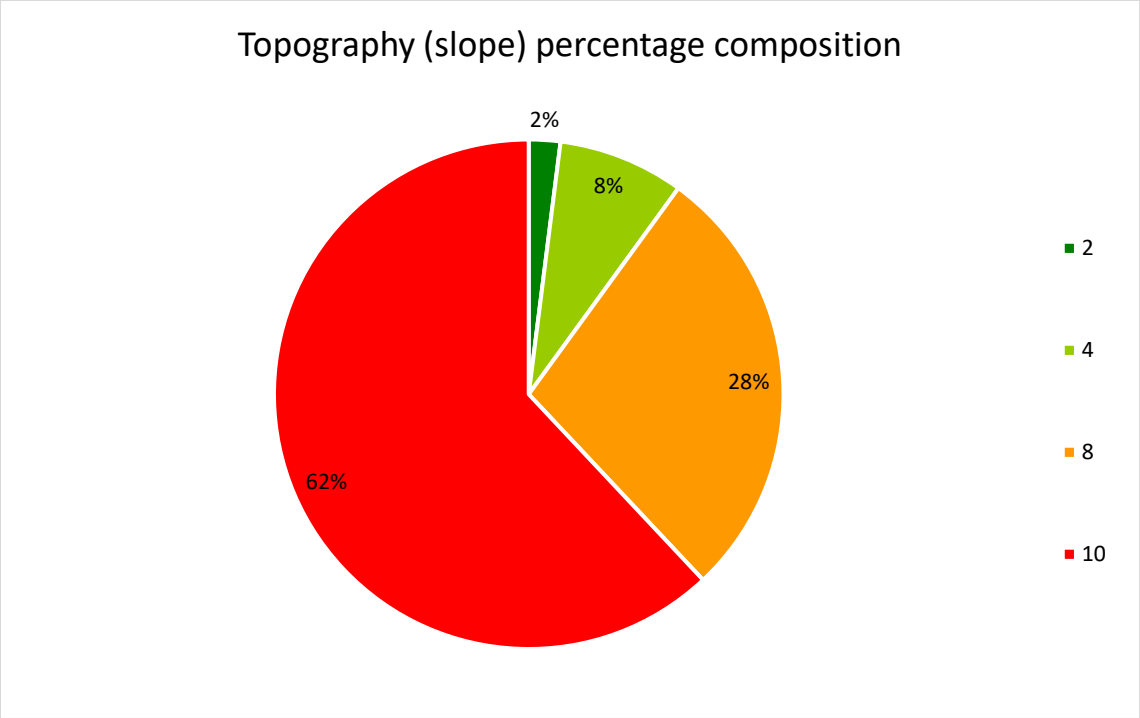

Figure 5-16: Percentage composition of topography (slope) with ratings of 2, 4, 8, and 10 covering 2%, 8%, 28% and 62% of the Province, respectively.

5.1.6 Impact of vadose zone

The shapefile with the lithology of South Africa acquired from the Council for Geosciences was used to identify the dominant lithology, with reference to Lynch *et al.* (1994), and Musekiwa and Majola (2013). As depicted in Figure 5.17, the majority of the study area is represented by sandstone, conglomerate, shale, quartzite, andesite, tuff, tholeiite, melanorite, tonalite, agglomerate, siltstone, mudstone, diamictite, porphyritic felsite, and alluvium of the Ventersdorp Supergroup, Transvaal Supergroup (Black Reef Formation and Pretoria Group), Karoo Supergroup, and the Bushveld Complex. The central part and a small portion of the north and southeast are represented by quartzite, shale, conglomerate, granodiorite, gabbro, serpentinite, dunite, pyroxenite, Nebo-granite, granite granophyre, and granite-gneiss of the Witwatersrand Supergroup and Dominion Group. Because of the complexity of the Malmani dolomite, dolomite was separated and assigned a higher rating from all the other lithologies.

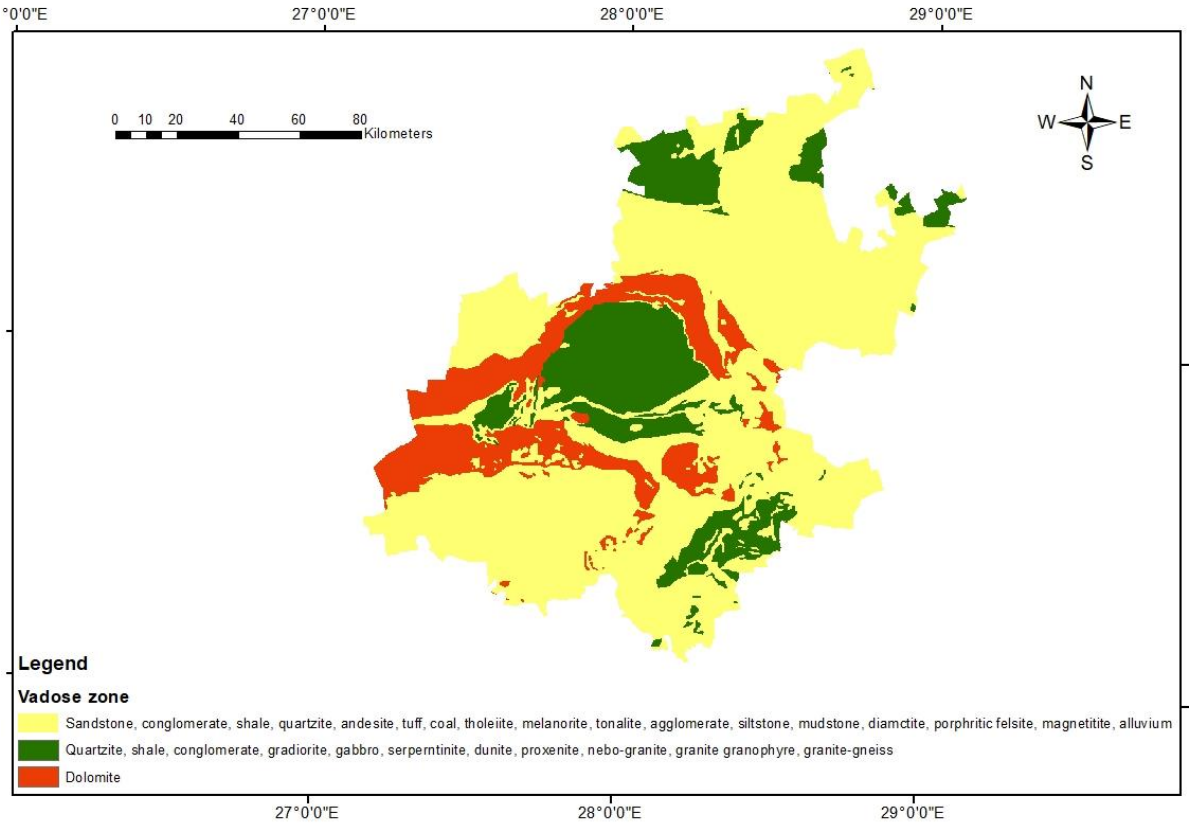

Figure 5-17: Vadose zone map showing the different vadose zones in yellow, green, and red.

The parameter I was referred to as the unsaturated zone, which consists of pores that are filled with water and air, where chemical and physical processes such as dispersion, biodegradation, and volatilisation take place (Moges and Dinka, 2021). The vadose zone serves as a crucial buffer of water and contaminants (Jahan *et al.*, 2018). Sandstone, conglomerate, shale, quartzite, andesite, tuff, tholeiite, melanorite, tonalite, agglomerate, siltstone, mudstone, diamictite, porphyritic felsite, magnetitite, and alluvium of the Ventersdorp Supergroup, Transvaal Supergroup (Black Reef Formation and Pretoria Group), Karoo Supergroup, and Bushveld Complex was assigned a rating of 5, which represents moderate vulnerability. Quartzite, shale, conglomerate, granodiorite, gabbro, serpentinite, dunite, pyroxenite, nebo-granite, granite granophyre, and granite-gneiss of the Witwatersrand Supergroup and Dominion Group was assigned a rating of 8, which represents high vulnerability, whereas the Malmani dolomite is represented by a rating of 10, which indicates very high vulnerability to pollution (Figure 5.18). The grouping of the lithology was in accordance with the groupings by Lynch *et al.* (1994), and Musekiwa and Majola (2013).

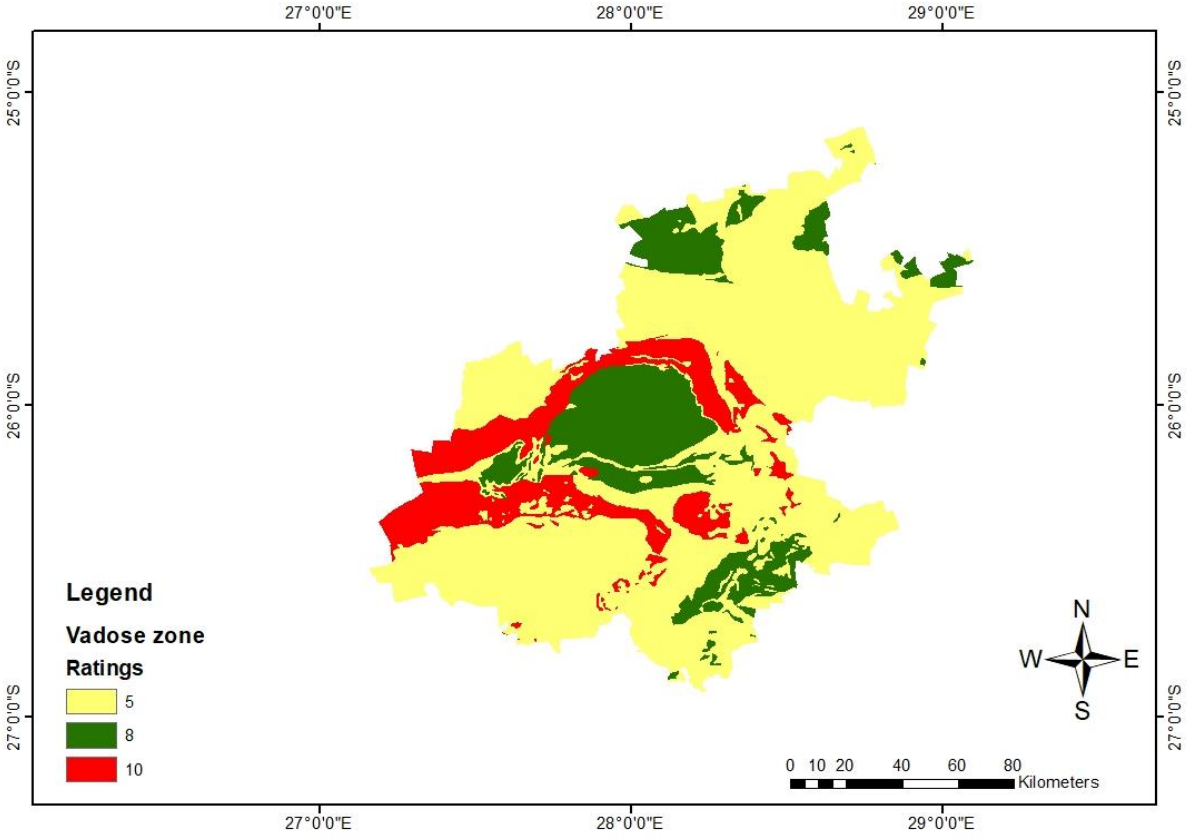

Figure 5-18: Vadose zone map showing ratings of 5 (yellow), 8 (green), and 10 (red).

As demonstrated in Figure 5.19, 67% of the Province has a vadose zone that is moderately vulnerable to pollution, which was assigned a rating of 5. The highly vulnerable areas cover 33% of the Province and are represented by a rating of 8 and 10.

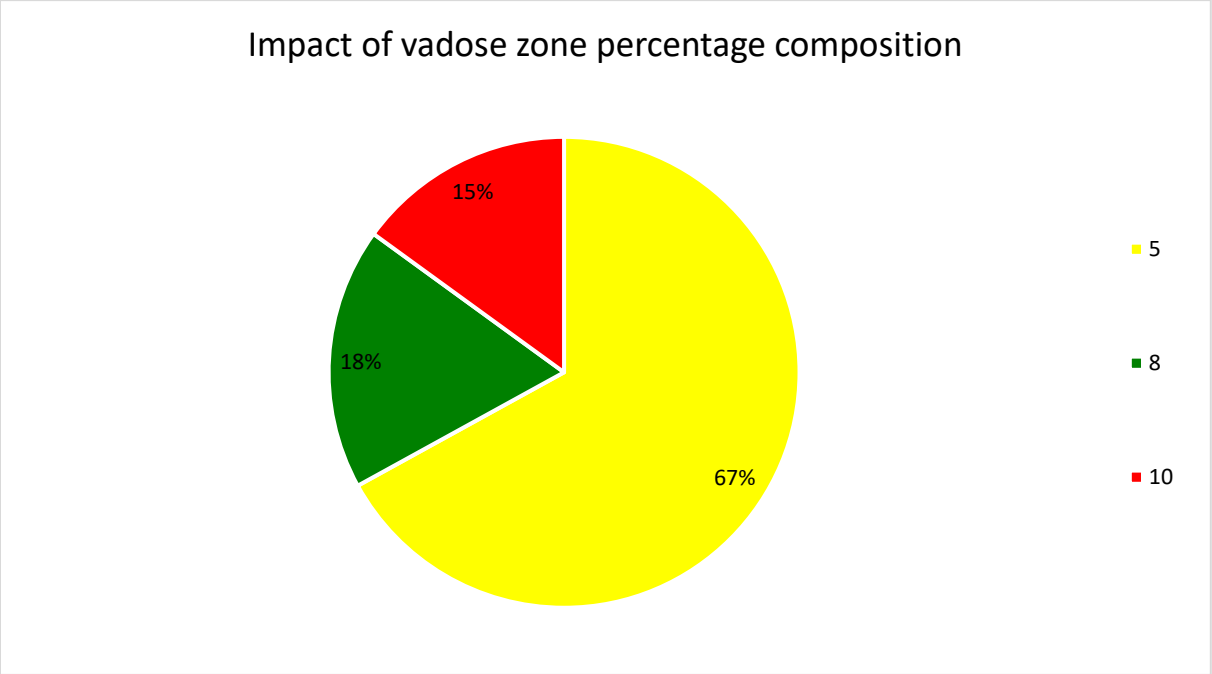

Figure 5-19: Percentage composition of vadose zone showing moderate (yellow), and high vulnerable (green and red) areas covering 67%, and 33% of the Gauteng Province, respectively.

5.1.7 Hydraulic conductivity

Due to the unavailability of hydraulic conductivity from field investigations, hydraulic conductivity values were acquired from Health (1983). The hydraulic conductivity of Todd and Mays (2005) and Health (1983) were compared, depicting similar ranges. Like Press (2020), Hydraulic conductivities from Health (1983) were used for this study. Hydraulic conductivity plays a direct role in groundwater and contaminant circulation; therefore, it was deemed significant for this parameter to be included in the estimation of the DRASTIC index. The hydraulic conductivity of the different lithologies in Gauteng Province is depicted in Figure 5.20 below. The study area is represented by three ranges: <5 m/day, 5-10 m/day, and > 100 m/day. Hydraulic conductivity with a range below 5 m/day is dominant in the north, east, and southwest regions. In contrast, hydraulic conductivity greater than 100 m/day (dolomite) is in the southwest and overlaps the central regions of the Province. Hydraulic conductivity between 5-10 mm/day covers the central part and some parts of the north and south regions.

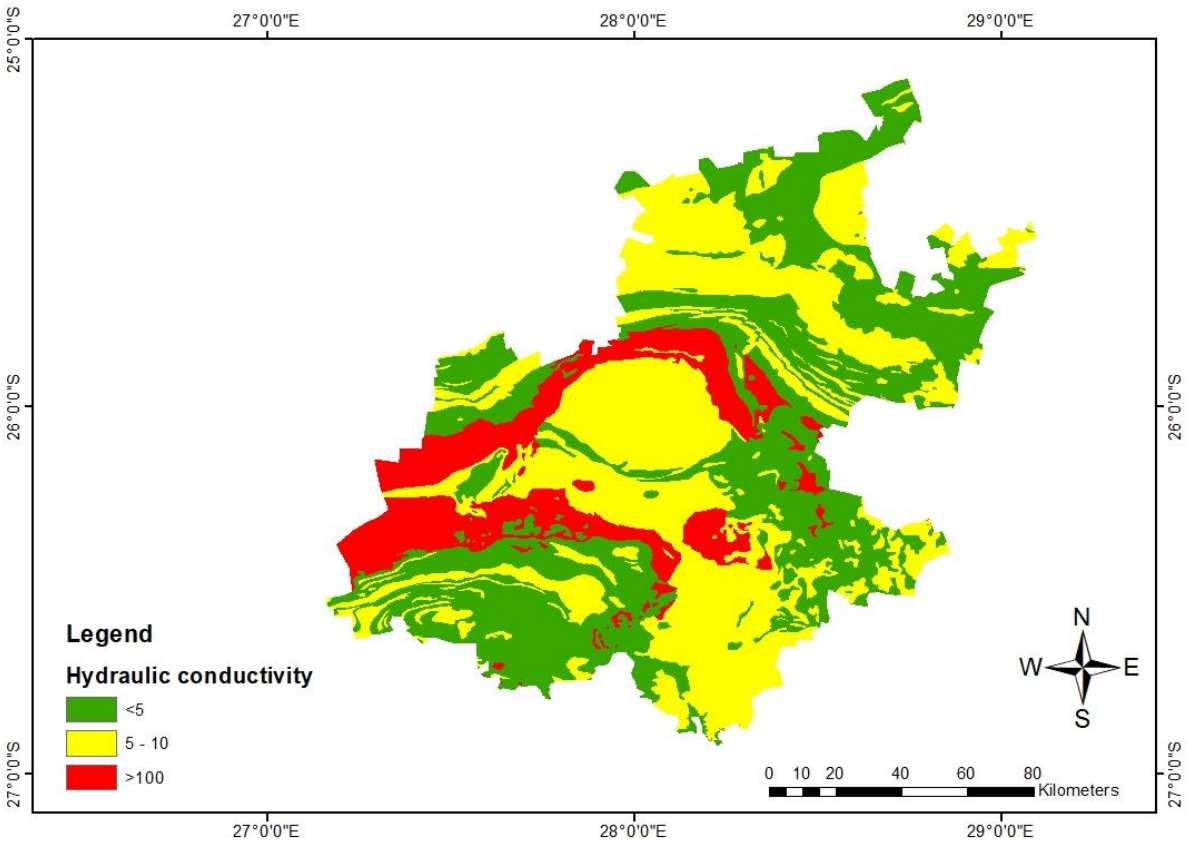

Figure 5-20: The range of hydraulic conductivity, <5 m/day in green, 5-10 m/day in yellow, and >100 m/day in red.

Hydraulic conductivity is a function of not only the porous medium through which the fluid moves, but of the fluid itself such as viscosity, density and acceleration due to gravity (Abiye, 2021). The presence of fractures or pores in an aquifer media controls the hydraulic conductivity of that aquifer media. The residence time of contaminants and attenuation processes are determined by hydraulic conductivity. Even so, the hydraulic conductivity is dependent on the water properties and the aquifer media (Younger, 2009). Rocks that permit water movement have high hydraulic conductivity, whereas rocks that restrict groundwater movement have low hydraulic conductivity. In this study, dolomite, known for its dissolution cavities and high permeability with a hydraulic conductivity between 1×10^4 - 1×10^2 m/day, was assigned a vulnerability rating of 10 since contaminants are likely to move in dolomite.

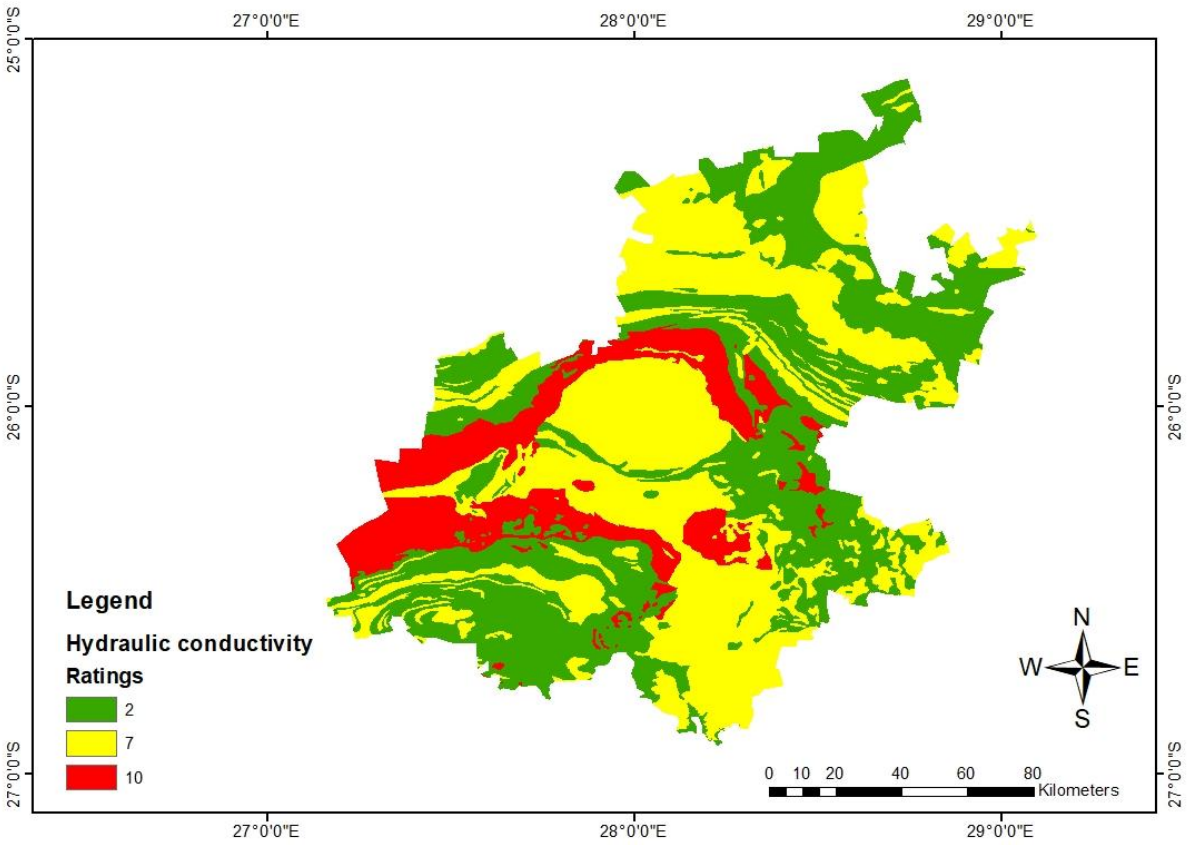

Figure 5-21: Hydraulic conductivity map showing a rating of 2 in green, 7 in yellow, and 10 in red.

The percentage composition of hydraulic conductivity is presented in Figure 5.22. High hydraulic conductivity with a vulnerability rating of 10 covers 14% of the Province. 43% of the study area comprises low hydraulic conductivity with a rating of 2, whilst hydraulic conductivity with a rating of 7 represents 43% of the study area.

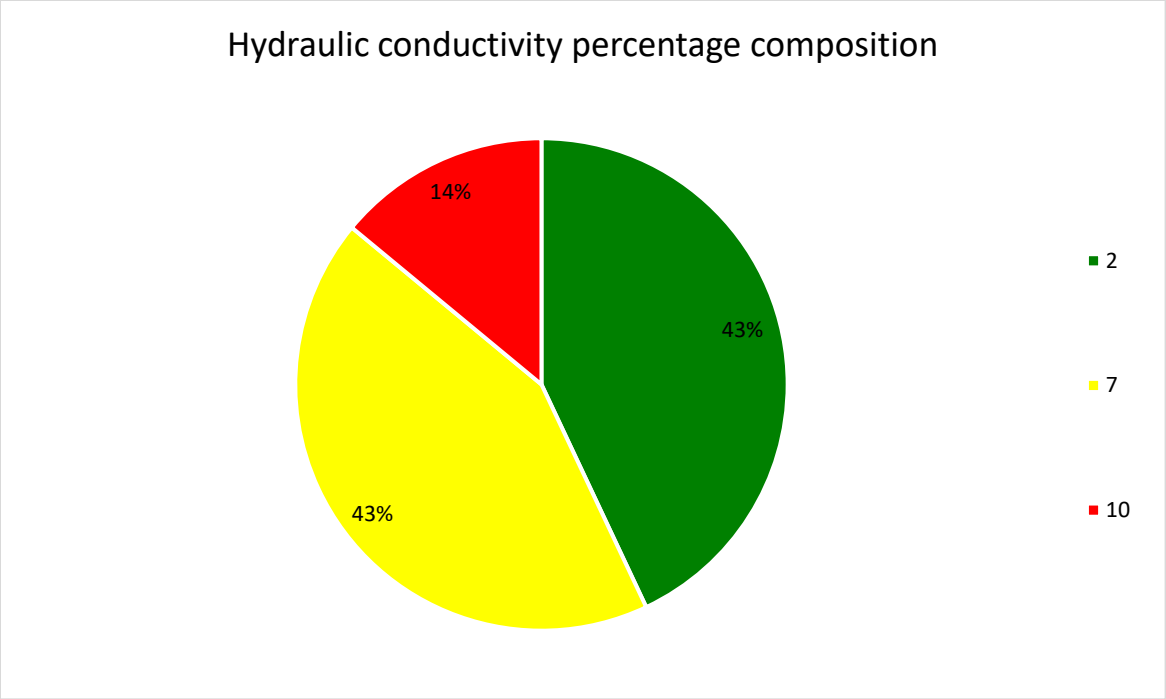

Figure 5-22: The percentage composition of hydraulic conductivity with ratings of 2 and 7 each covering 43% of the Province and a rating of 10 covering 14% of the Province.

5.1.8 Intrinsic vulnerability

The DRASTIC index was estimated using the ratings of the seven parameters. The DRASTIC index was grouped into three ranges: 77-111, 111-140, and 140-190, ranked as low, moderate, and high vulnerability, respectively (Figure 5.23).

High vulnerable areas are exposed in the karst aquifers of Malmani dolomite, which is characterised by dissolution cavities that act as recharge zones. The dissolution cavities are responsible for groundwater circulation and pollution movement. These aquifers have high hydraulic conductivity that allows the movement of groundwater and contaminants. The highly vulnerable areas consist of loamy sand/sandy loam and low slopes (southwest). The inability of this soil's properties to aid in attenuating contamination is one reason for high vulnerability, as the absence of clay and silt increases the movement of contaminants. If some of the contaminants are not attenuated by dilution, dispersion, mechanical filtration, volatilization, sorption, or ion exchange, the contaminants may be carried into the aquifer. The highly vulnerable area is also characterised by permeable vadose zone and high hydraulic conductivity.

The moderately vulnerable areas are exposed in the fractured and weathered crystalline rocks of granitic gneiss and quartzite; the Wilge River Formation; and the Nebo granite. The fractures create a path for the movement of contaminants, increasing the vulnerability of the aquifer. The variation of groundwater depth in different aquifers also influences groundwater pollution and aquifer vulnerability in the Gauteng Province. The moderately vulnerable areas are also exposed in areas with low topography. Low topography increases the chance of pollution potential as infiltration is favored over runoff, increasing the chances of water infiltrating into the subsurface environment. If there is no adequate clay soil to aid in the immobilisation of contaminants, the vulnerability of groundwater to pollution increases; in this case, the soil media is sand in the center with a rating of 10 and loamy sand in the southwest and northeast regions. Furthermore, some regions of the moderately vulnerable area receive an annual recharge of 20-40 mm/year. Rainwater carries pollution, and if the recharge is high, the movement of pollution increases as pollution moves with rainwater. Low vulnerable areas are exposed in some parts of the north, south, and east regions represented by low net recharge.

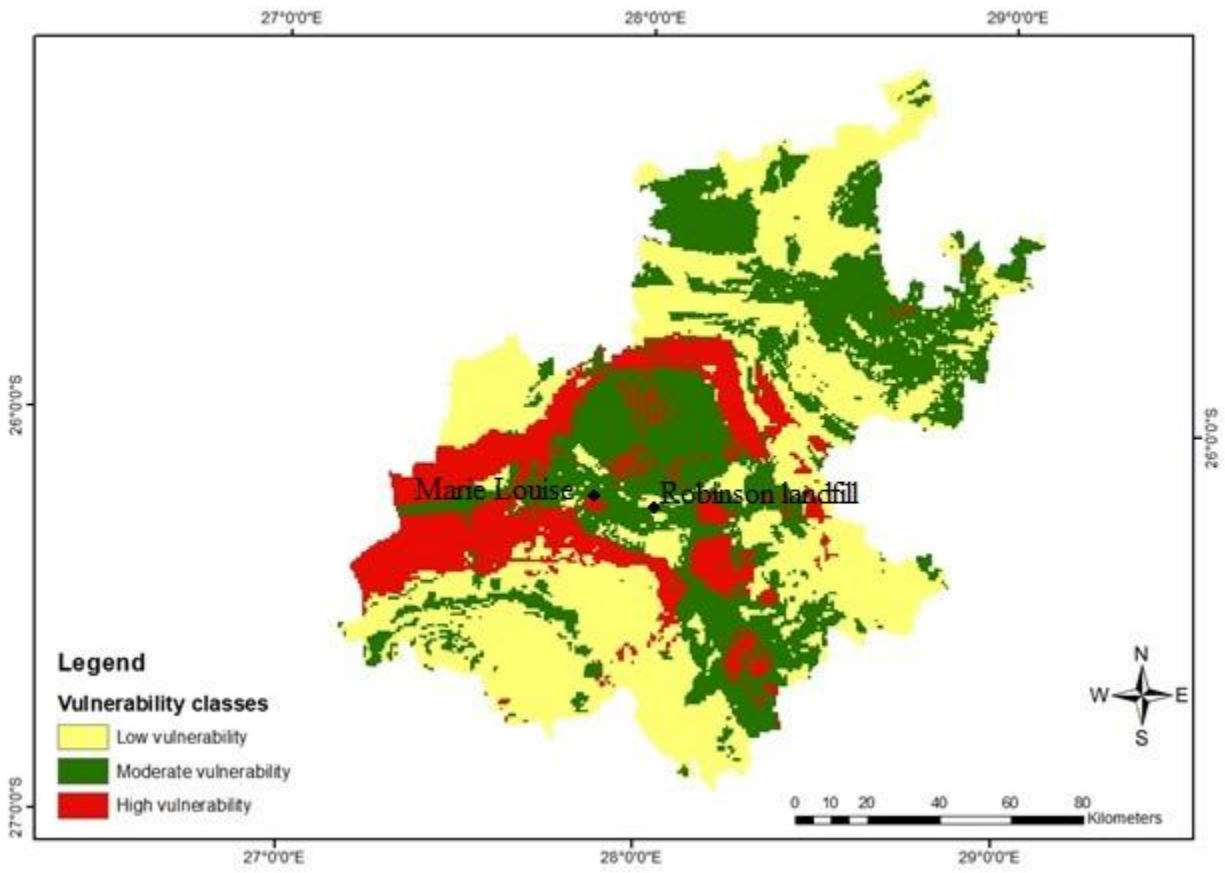

Figure 5-23: Intrinsic vulnerability map showing low, moderate, and high vulnerability in yellow, green, and red, respectively.

The percentage composition of intrinsic vulnerability is presented in Table 5.1 and Figure 5.24. Low vulnerable areas cover 46% (8313 km^2) of the Province, whilst 37% (6685 km^2) of the Province is moderately vulnerable to groundwater pollution. Areas that are highly vulnerable to groundwater pollution cover 17% (3122 km^2) of the Province.

Table 5.1: Vulnerability classes, area and percentage

Vulnerability classes	Area (km^2)	Percentage (%)
Low vulnerability	8313	46
Moderate vulnerability	6685	37
High vulnerability	3122	17

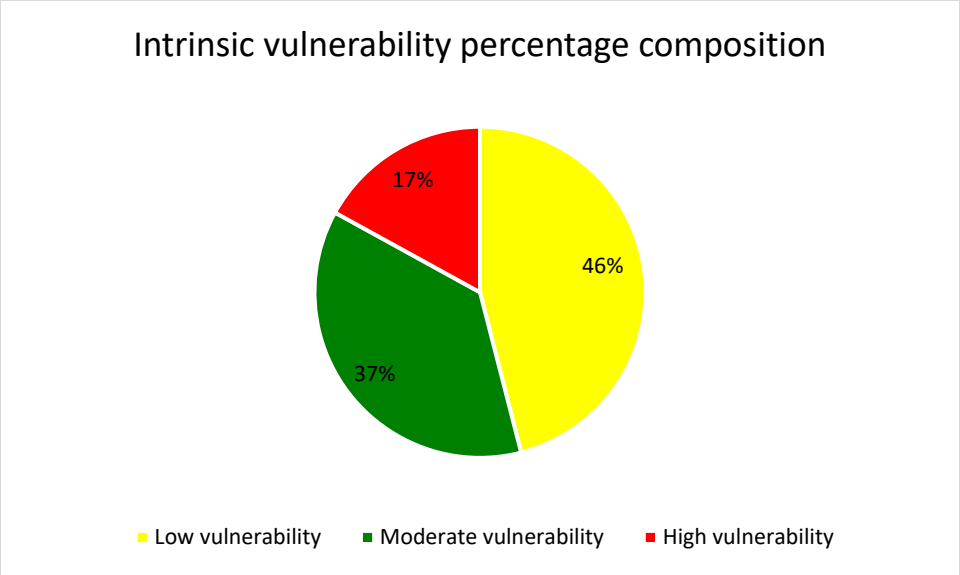

Figure 5-24: The percentage composition of intrinsic vulnerability showing low, moderate, and high vulnerable areas covering 46%, 37%, and 17% of the Province, respectively.

The intrinsic vulnerability map serves as a screening tool that will assist in the proper planning and designs of the future establishment. By using the intrinsic vulnerability map, proper monitoring can be enforced on landfill sites that are situated in regions where the underlying aquifer is highly vulnerable to pollution, whilst monitoring can be enforced in those landfills that are located in moderately vulnerable regions.

Areas with high intrinsic vulnerability to groundwater pollution require the implementation of strict measures and laws that will help safeguard the groundwater quality of the underlying aquifer. Given that Malmani dolomite, which is popular for its high groundwater yield, is highly vulnerable, thorough monitoring of landfills located within the Malmani dolomite needs to be conducted. In addition, areas that are classified as moderately vulnerable should not be neglected as these areas have the potential to become highly vulnerable if more waste sites are established, especially now that illegal dumping of waste is increasing as a result of the increase in informal settlements.

5.1.9 Landfill-Specific vulnerability map

Figure 5.25 depicts the locations and spatial distributions of the landfills in the Gauteng Province acquired from the Gauteng Department of Agriculture and Rural Development (GDARD). The presented landfill sites are only for landfills that are licensed. Even so, there is illegal waste dumping in the province because of the increase in informal settlements caused by the ever-expanding population. As shown in Figure 5.25, there is a scarcity of landfilling airspace in the Province. Most of the landfill sites are located within moderately vulnerable areas characterised by permeable soil type, and lithology with high hydraulic conductivity, which makes the underlying aquifers at high risk of being polluted by landfill leachate. Both Marie Louise and Robinson landfill sites which are situated in the Central Rand Group which according to the intrinsic vulnerability map is in the moderately vulnerable area will be used to further validate the DRASTIC index map in that area.

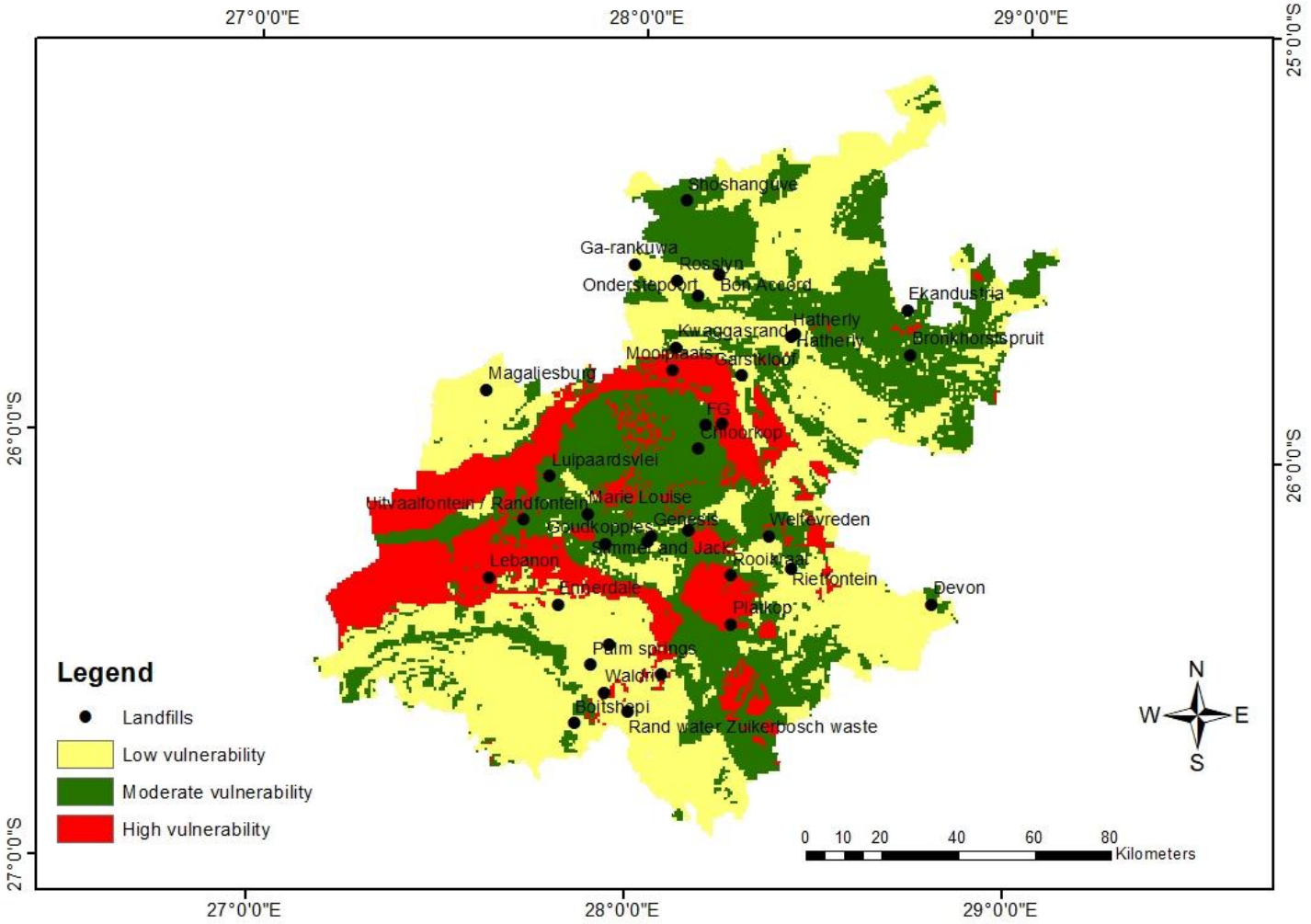

Figure 5-25: Spatial distribution of landfills in low, moderate, and high vulnerability areas

Specific vulnerability demonstrates the vulnerability of the aquifer to a particular anthropogenic activity. A land use map acquired from the Environmental Geographical Information System (EGIS) was computed in ArcMap, where landfills was separated from other land use and thereafter assigned a rating of 10 and a weight of 5. The landfill-specific vulnerability map depicted in Figure 5.27 has four classes, namely, low vulnerability (77 - 111), moderate vulnerability (111 - 140), high vulnerability (140 - 190), and very high vulnerability (>190). The specific vulnerability map shows high vulnerability in areas that have Malmani dolomite, high hydraulic conductivity, gentle slope, and loamy sand. Moderately vulnerable areas are within fractured aquifers (north region), and fractured/weathered aquifers (granite and gneiss) in the central regions. Moderately vulnerable areas are also associated with gentle slopes, permeable vadose zone, and sand soil type (central region). Landfills situated within moderate and highly vulnerable areas have a high chance of negatively affecting the water quality of the underlying aquifer. Very high vulnerable regions (>190) are in the central region, north region, and some parts of the south regions. The landfill-specific vulnerability map and the intrinsic vulnerability map are similar as a result of the scale and the size of the study area being large, making the landfill less visible, spatially. Even though the weight (5) and rating (10) were assigned for landfill sites, the landfill-specific vulnerability map shows minor differences from the intrinsic vulnerability map as the landfill sites are point data (Figure 5.25, Figure 5.26). The landfill sites extracted from the land use map depicted in Figure 5.26 are not easily visible which is the reason for the minor differences between the specific and intrinsic vulnerability map. Even so, the difference between the two maps is shown by the >190 vulnerability index.

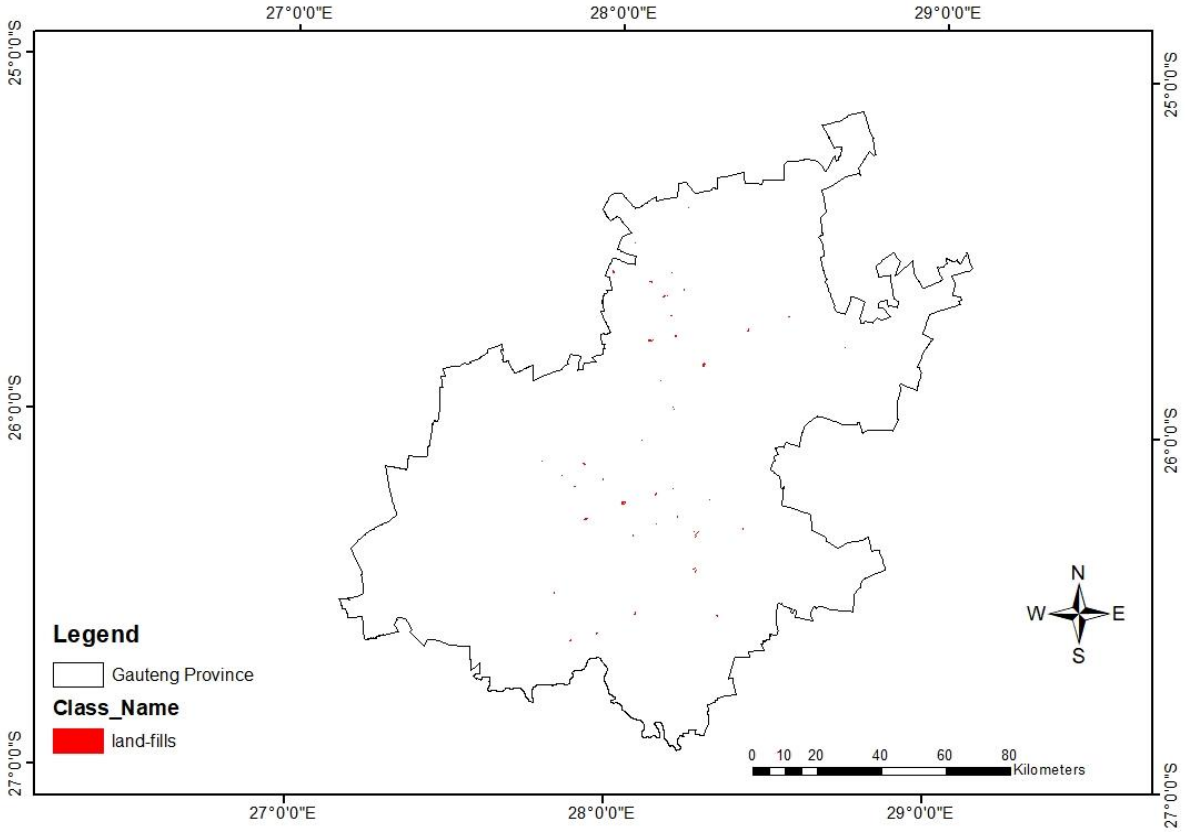

Figure 5-26: Landfills in the Gauteng Province extracted from the land use map (source: Environmental Geographical Information system)

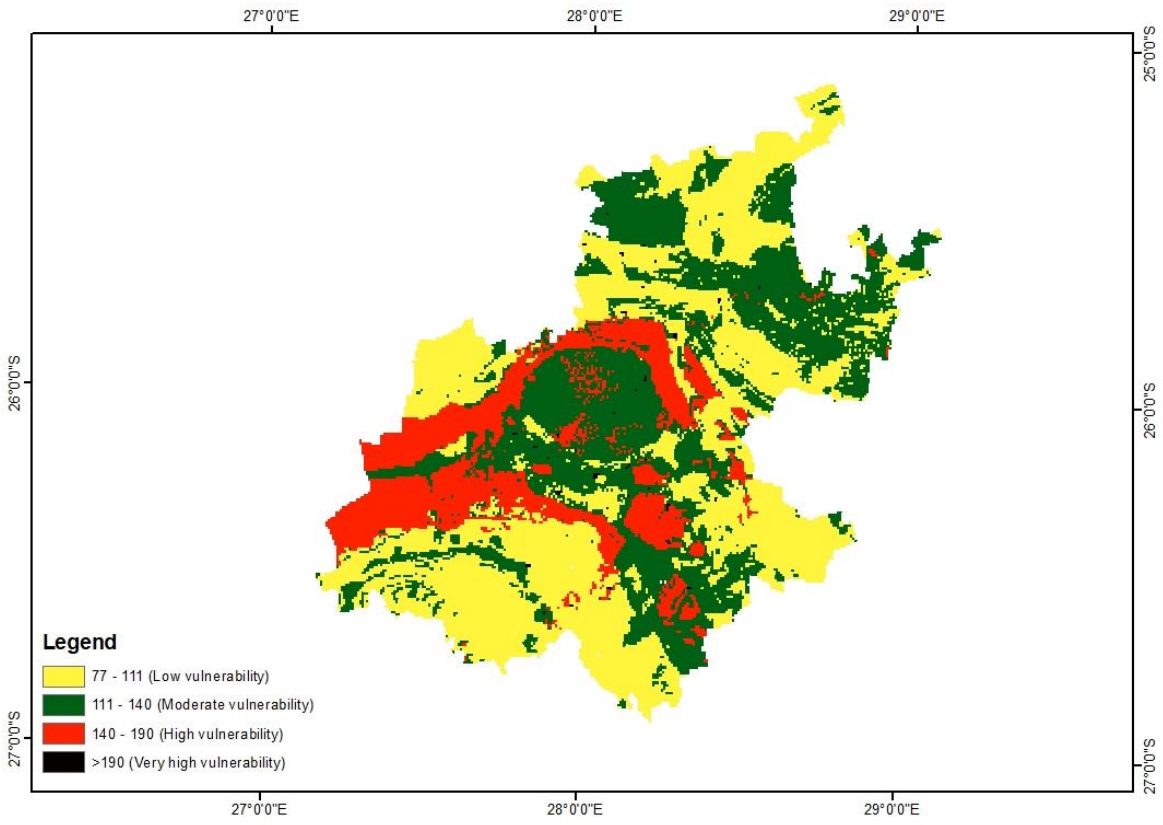

Figure 5-27: Landfill-specific vulnerability map showing DRASTIC index ranging from 77-111 (low vulnerability), 111-140 (moderate vulnerability), 140-190 (high vulnerability), and >190 (very high vulnerability).

5.2 DRASTIC validation – NO_3+NO_2 as N

Due to its extremely low presence in groundwater under natural conditions, nitrate is frequently used as a validation parameter in the assessment of groundwater vulnerability (Hasan *et al.* 2019). Pollutant sources like agricultural practices and urban waste can be identified by analysing the concentrations of nitrate in groundwater. Nitrate has been used to validate the DRASTIC method in studies done by Tilahun and Merkel (2009); Wang *et al.* (2012); Kumar *et al.* (2014); Hosseini and Seremi (2018) and; Moges and Dinka (2021). To validate the DRASTIC index, average nitrate and nitrite reported as nitrogen (NO_3+NO_2-N) acquired from the Department of Water and Sanitation were used. These data were superimposed on the intrinsic vulnerability map to analyse the NO_3+NO_2-N distribution. As depicted in Figure 5.28, groundwater sampling for NO_3+NO_2-N is concentrated in the southwest, north, and the central region of the study area where there is high NO_3+NO_2-N concentration (9.85-16.83 mg/l) whereas the northeast and southeast regions of the study area are not represented by any NO_3+NO_2-N concentration. The absence of NO_3+NO_2-N in the northeast and southeast regions can be attributed to the lack of sampling or monitoring of boreholes situated in these regions. NO_3+NO_2-N concentration ranging between 5.76-9.85 mg/l is evident in the north, west, and central regions whereas NO_3+NO_2-N concentration ranging between 0.02-0.90 mg/l can be observed in the low, moderate, and high vulnerable areas. The extent to which NO_3+NO_2-N occurs allows the analysis of NO_3+NO_2-N concentrations and the identification of areas of high priority. The lack of groundwater sampling in the northeast and southeast regions inhibits performing a thorough analysis of the extent of NO_3+NO_2-N concentrations in groundwater. Nevertheless, highly vulnerable regions characterised by high hydraulic conductivity, fractured-karst aquifers, permeable vadose zone, and sandy loam/loamy sand have elevated NO_3+NO_2-N concentrations. More NO_3+NO_2-N data are required to strengthen the validation of the intrinsic map.

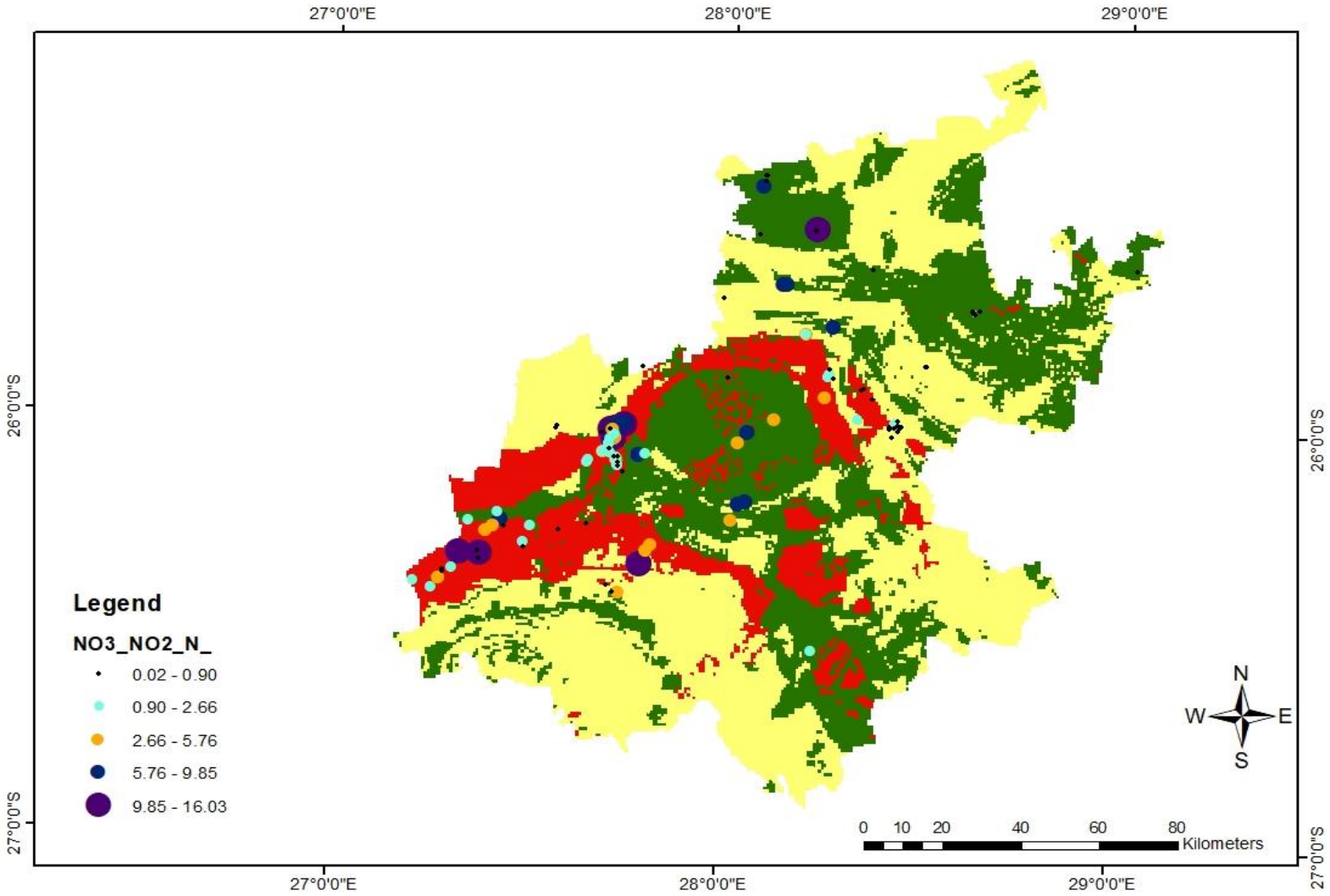

Figure 5-28: Average NO_3+NO_2 as N

5.3 DRASTIC method validation

5.3.1 Marie Louise landfill

5.3.1.1 Field parameter

The results of the physicochemical parameters are depicted in Table 5.2. Electrical Conductivity (EC) and Total Suspended Solids (TDS) for the samples collected at Marie Louise range between 26-458 mS/m and 196-3562 mg/l, respectively. The lowest EC and TDS were recorded by sample GMLS07 with EC and TDS values of 26 mS/m and 196 mg/l, respectively. Sample GMLS11 and GMLS10 have elevated EC values of 348 mS/m and 263 mS/m, and TDS values of 2966 mg/l and 1865 mg/l, respectively, which suggests possible leachate pollution as these boreholes are relatively shallow as depicted in Figure 5.30. Borehole GMLS15 has a high TDS concentration of 1960 mg/l, which is likely from the deep circulation of water, with longer residence time leading to mineral dissolution from rock-water interaction. This is also supported by the deep groundwater depth of borehole GMLS15 as depicted in Figure 5.30. The pH of the samples ranges between 5.8-7.6, with the pH of 5.8 falling below the recommended range of 6.5-9.2 by WHO (2008) and 6.0-9.2 by DWAF (1996). All the samples consist of TDS greater than the permissible TDS of 100-500 mg/l by WHO (2003), except for GMLS07. Borehole GMLS16 has a pH value of 5.8 which represents alkaline water, possibly from the iron released from mineralised shale, as shale is one of the dominant lithology (Figure 5.32). Marie Louise is located in an area with a fractured aquifer, permeable vadose zone with a hydraulic conductivity assigned a rating of 7, and loamy sand with little clay content. These hydrogeological factors make the underlying groundwater moderately vulnerable to pollution. As a result, the pollution of groundwater shown by the high TDS in some of the boreholes is likely anticipated as the underlying environment is moderately vulnerable to pollution.

Table 5.2: Physicochemical parameters of samples collected at Marie Louise landfill

Description	Sample Name	Electrical Conductivity (mS/m)	pH	TDS (mg/l)
Groundwater	GLMS 07	26	6.4	196
Groundwater	GLMS 09	235	6.5	1195
Groundwater	GLMS 11	348	7.2	2966
Groundwater	GLMS 16	92	5.8	564
Leachate dam	DMS1	458	7.5	3562
Groundwater	GMLS 10	263	6.9	1865
Groundwater	GMLS 15	358	7.6	1960

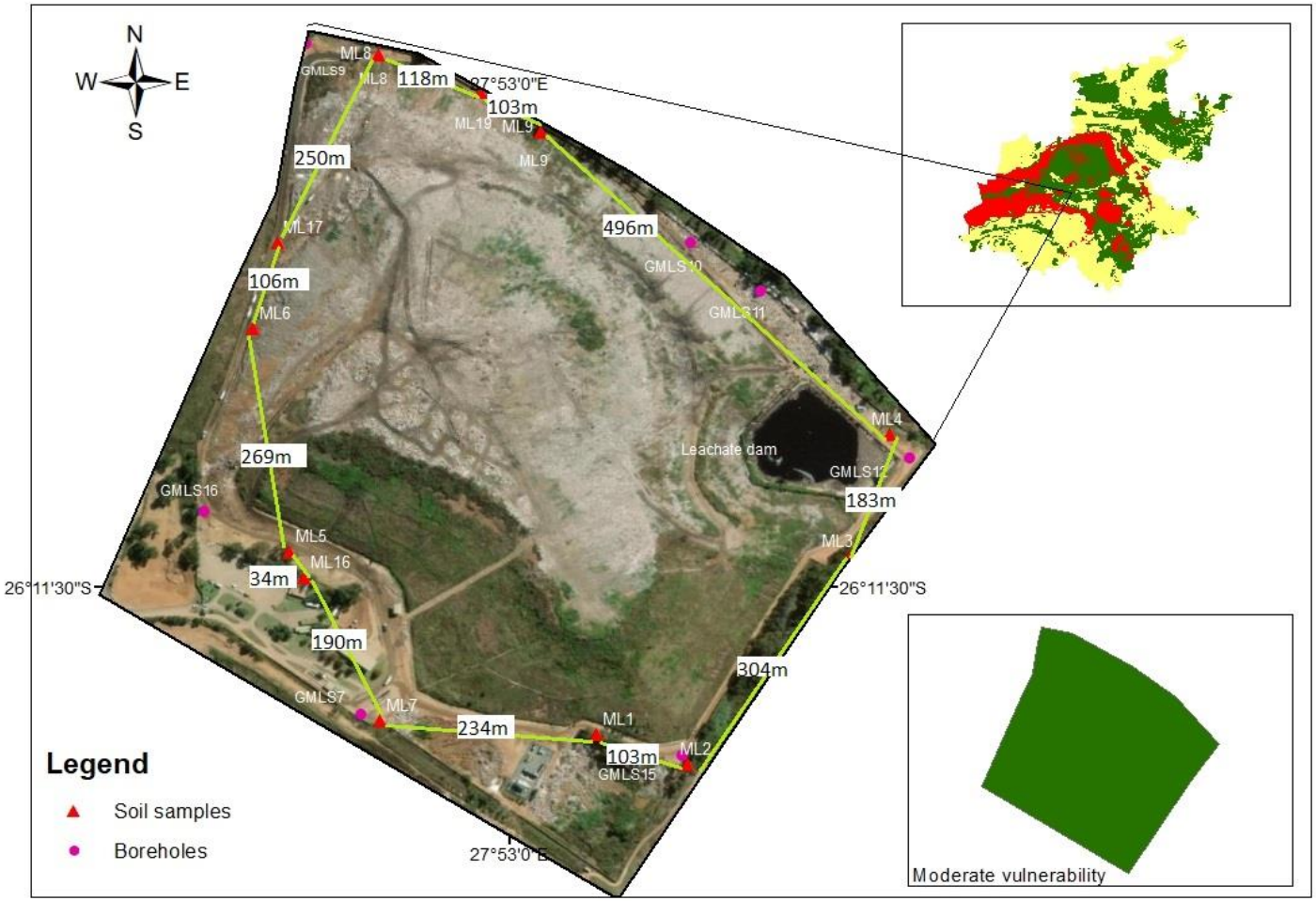

Figure 5-29: Sampling locations and distance between soil samples collected at Marie Louise

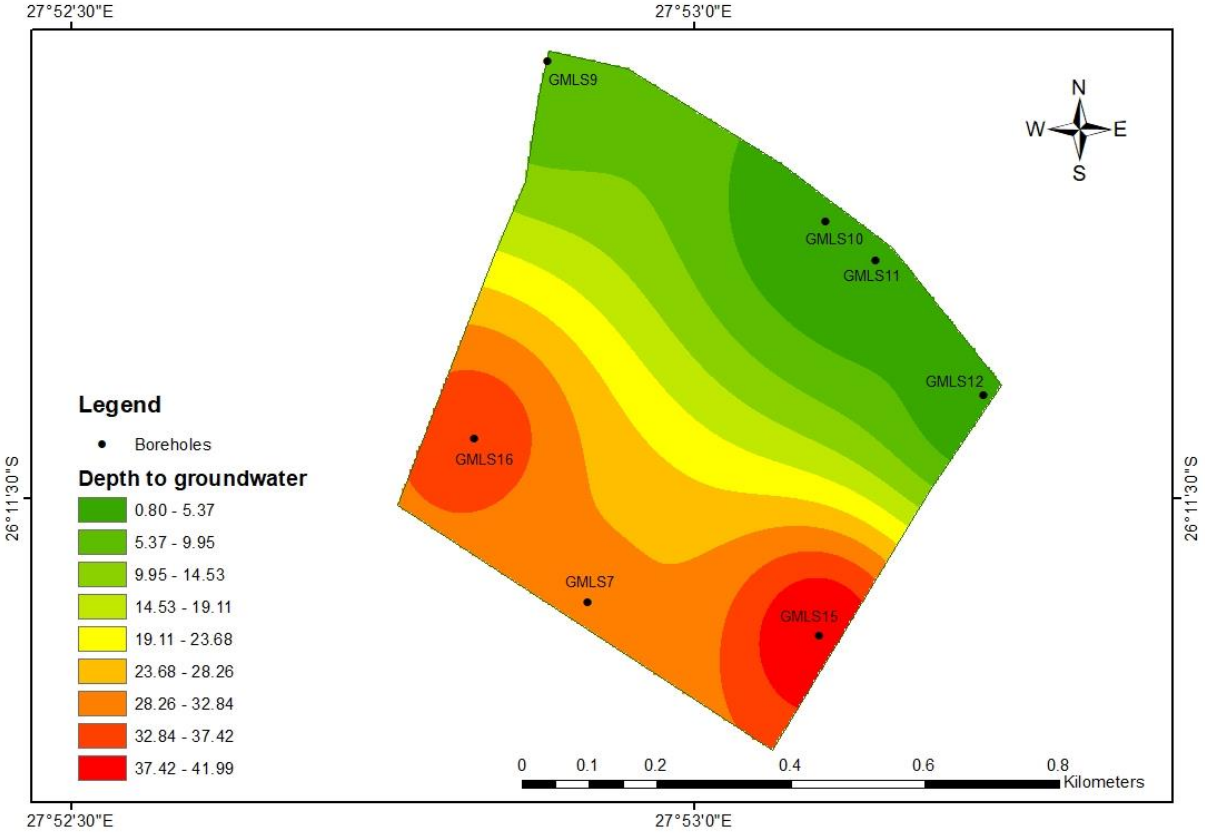

Figure 5-30: Depth to groundwater for Marie Louise (monitoring wells)

5.3.1.2 Stable isotopes of water

Stable isotopes have been used in various studies across South Africa for the better management of groundwater by assessing the interaction of groundwater and surface water (Abiye *et al.*, 2015), assessing the flow dynamics and recharge dynamics in the Johannesburg crystalline rocks (Abiye *et al.*, 2011) and the groundwater recharge of the dolomite karstic and crystalline aquifers (Leketa *et al.*, 2018). To interpret the different isotopic signatures of the water samples collected at Marie Louise landfill, the Johannesburg Local Meteoric Water Line (δ^2H=6.7; $\delta^{18}O$ + 10‰) by Leketa *et al.* (2018) and the Global Meteoric Water Line (δ^2H = 8 $\delta^{18}O$ + 10‰) by Craig (1961) were used. All the samples, except the rainwater sample, have highly depleted isotopic signatures, with borehole GMLS 16 comprising the highest depleted isotopic signatures (-24.6‰ for δ^2H and -5.80‰ for $\delta^{18}O$), followed by borehole GMLS 7 with -19.5‰ for δ^2H and -3.87‰ for $\delta^{18}O$. The

high depletion in isotopic signatures from all the samples indicates that these boreholes were recharged by precipitation sourced from high altitudes during cold seasons. On the other hand, the enriched isotopic signatures in the rainfall sample suggest that rainfall occurred from low altitude during warm seasons. In addition, the samples show differences in isotopic signatures, which suggest a variation of recharge episodes.

Table 5.3: Stable isotope results from samples collected at Marie Louise

Sample Name	**δ^2H (‰)**	**±‰**	**δ^{18}O (‰)**	**±‰**	**D-EXCESS**
Rainwater	10.4	1.4	-0.91	0.1	16.51
GML09	-16.3	4.1	-3.19	0.3	5.10
GMLS16	-24.6	0.3	-5.80	0.1	14.22
GMLS07	-19.5	0.9	-3.87	0.2	6.41
GMLS10	-9.0	0.4	-3.61	0.0	15.20

The impact of leachate pollution in borehole GMLS10 revealed by the high tritium unit (Table 5.4), correlates with the discovery of Fritz *et al.* (1976) where the samples with heavy isotopic composition (less depleted) were the most polluted, which can be related to gas exchange in the landfill. The source for pollution in borehole GMLS10 is likely from landfill leachate that has intercepted the loamy sand, the permeable vadose zone, and the fractured aquifer media which has a high hydraulic conductivity assigned a rating of 7. Given that the Marie Louise landfill site is located in a moderately vulnerable area, as depicted in Figure 5.23, pollution is expected.

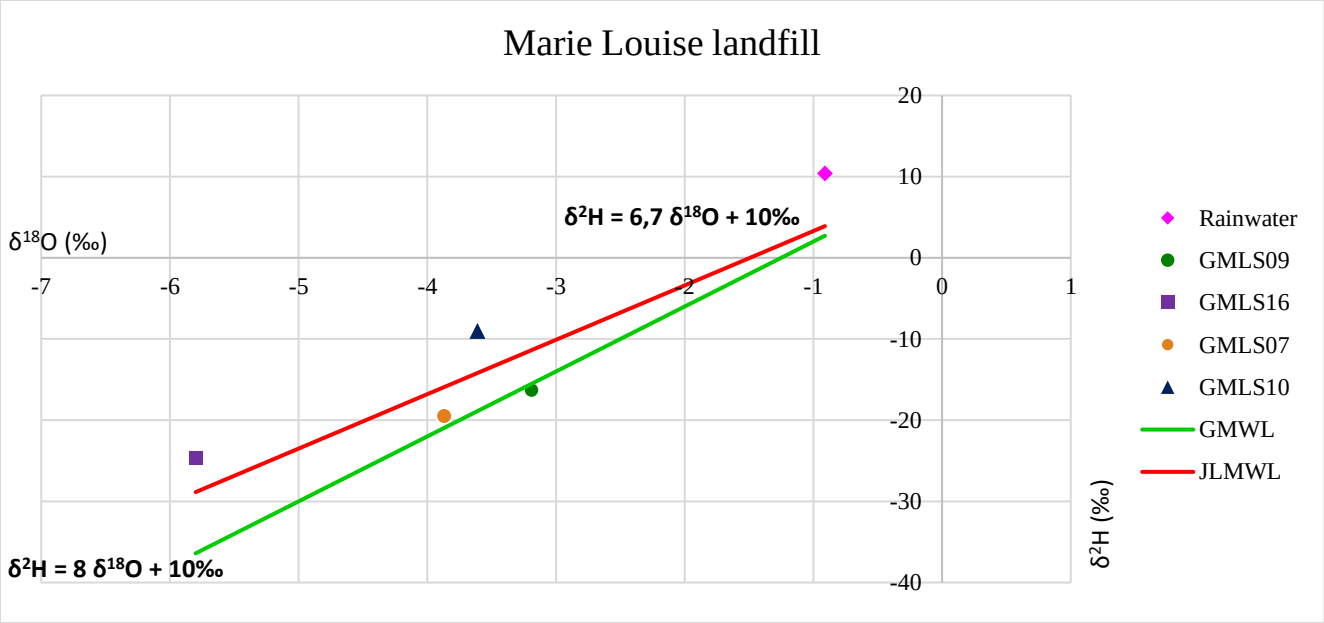

Figure 5-31: Stable isotopes of groundwater in Marie Louise landfill

5.3.1.3 Tritium

Tritium is a useful radioactive isotope for assessing groundwater flow dynamics and identifying recent and ancient recharge. It has been applied in South Africa to identify and trace groundwater pollution by landfill leachate (Verhagen *et al.,* 1991). A study by Abiye *et al.* (2015) used tritium to identify mining impact in the surface and groundwater of the fractured crystalline aquifer and aquifers of Malmani dolomite in Johannesburg. A mean tritium unit of 5.6 ± 0.4 TU for the Johannesburg rainfall was estimated which will be used in this study as a threshold for determining artificial tritium from the groundwater and surface water of the Marie Louise landfill site. As depicted in Table 5.4, GMLS 09 and GML 07 have ^{3}H of 3.3 TU and 4.0 TU, respectively. The low ^{3}H suggests longer groundwater circulation because of low rock permeability, which ultimately represents old water. The low tritium may also be from rainfall. Furthermore, the aforementioned boreholes have tritium units below 5.6 TU, which implies that there is no artificial tritium or landfill leachate pollution. Sample GMLS 16, GMLS 10, and GMLS 11 have 22.4 TU, 64.8 TU, and 111.6 TU, respectively, which exceeds that of rainfall (2.2 TU) and Johannesburg rainfall (5.6 TU.). Such extensively high ^{3}H represents artificial ^{3}H, suggesting pollution from landfill leachate. The high tritium unit in boreholes GMLS11 and GMLS10 indicates landfill leachate that seeped into the environment. Pollution in these boreholes is supported by chemical analysis results, which demonstrate high TDS and high ammonia concentrations. The leachate dam (DMLS01) also has high tritium (236 TU).

Table 5.4: Tritium results of water samples collected in Marie Louise landfill

Laboratory Number	**Sample Identification**	**Tritium**	
		(T.U.)	**±**
WITS 1529	DMLS 01	236.0	56.0
WITS 1530	GMLS 07	4.0	0.4
WITS 1531	GMLS 09	3.3	0.3
WITS 1532	GMLS 10	64.8	2.0
WITS 1533	GMLS 11	111.6	3.1
WITS 1534	GMLS 16	22.4	0.9
WITS 1541	Marie Louise Rain	2.2	0.3

As depicted by the intrinsic aquifer vulnerability map (Figure 5.23) and the landfill-specific vulnerability map (Figure 5.27), the Marie Louise landfill site lies in moderately vulnerable areas, where the soil and vadose zones are permeable, with a high hydraulic conductivity assigned a rating of 7. The pollution of the underlying groundwater in Marie Louise landfill shown by the presence of artificial tritium higher than the permissible environmental tritium in sample GMLS11 and GMLS10 is a result of the aforementioned hydrogeological parameters which have little ability to restrict the movement of pollution to the aquifer, making the underlying groundwater vulnerable to pollution. The presence of pollution validates the results obtained from the aquifer vulnerability map and the landfill-specific vulnerability map which indicates that the environment of the underlying system is moderately vulnerable to pollution and therefore to some degree unable to protect itself from pollution as the soil and vadose zone are permeable.

5.3.1.4 Hydrochemical facies

Table 5.5 presents the major ion results that were measured from the surface water, groundwater, and leachate dam samples collected at the Marie Louise landfill site. The cations and anions results were used to plot the Piper diagram to identify the major water chemistry and possible mixing. As depicted in Table 5.5, GMLS11 and the leachate dam demonstrated elevated alkalinity, bicarbonate, chloride, and sodium concentrations. The elevated chloride concentration is possibly from landfill leachate as this borehole is located adjacent to the waste pile where leachate runs off, and has a shallow groundwater depth that makes it highly prone to contamination. The high total alkalinity and bicarbonate in borehole GMLS11 can be linked to CO_2 from the atmosphere or soil. The pollution of GMLS11, possibly from landfill leachate is supported by the high tritium and TDS concentrations. The elevated calcium concentrations in borehole GMLS9 and GMLS11 is likely from rocks and soil. The Marie Louise landfill forms part of the Central Rand Group of the Witwatersrand Supergroup, which consists of shale and quartzite that are highly fractured and weathered which makes the underlying aquifer highly vulnerable to pollution. The highly fractured nature of the underlying aquifer increases the vulnerability of the underlying groundwater. This is supported by the DRASTIC index map produced in this study where it is demonstrated that the

Central Rand Group of the Witwatersrand Supergroup falls part of the moderately vulnerable areas. The presence of fractures in the quartzite creates channels for groundwater to occur which may potentially carry contaminants from landfills. Boreholes GMLS9, GMLS11, and GMLS16 have elevated sulphate concentrations. Since Marie Louise landfill was established in a mine tailing dump, the elevated SO_4 in the aforementioned boreholes is possibly from the dissolution of sulphate precipitates, namely, magnesium sulphate, gypsum, and anhydrite, which are common in mine tailing dumps and also from sources of calcium and magnesium (Masindi and Abiye, 2018). In Marie Louise, the highest ammonia is observed in samples GMSL09, GMLS11, and leachate dam (DMS01), with a concentration of 13 mg/l, 16 mg/l and 163 mg/l, respectively. Boreholes GMLS7 and GMLS16 both have an ammonia concentration of 0.1 mg/l. The high ammonia concentration in GMLS11 suggests contamination from landfill leachate.

Table 5.5: Marie Louise major ion results (mg/L)

Parameter	GMLS07	GMLS09	GMLS11	GMLS16	DMLS01
Total Alkalinity ($CaCO_3$)	28	20	488	12	2220
P-alkalinity ($CaCO_3$)	<5	<5	<5	<5	<5
Bicarbonate (HCO_3)	34	24	595	15	2706
Carbonate (CO_3)	<5	<5	<5	<5	<5
Chloride as (Cl)	16	61	417	20	1866
Sulphate as (SO_4)	49	2029	500	290	<2
Ammonia (N)	0.1	13	16	0.1	163
Sodium (Na)	7	138	256	8	998
Potassium (K)	1	5.3	146	1.6	845
Calcium (Ca)	15	428	206	63	142
Magnesium (Mg)	10	144	68	39	84

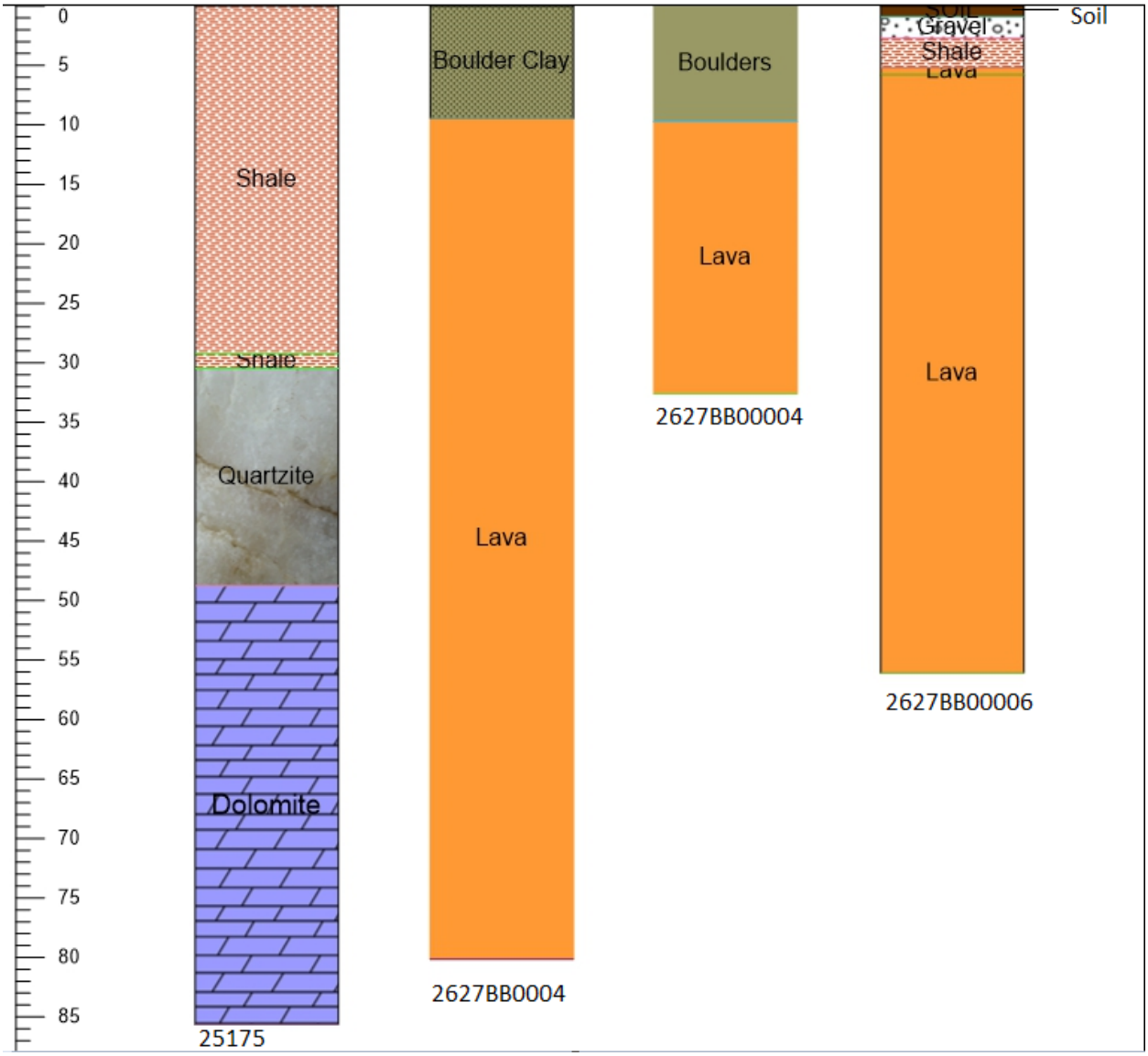

Figure 5-32: The underlying lithology in the Marie Louise landfill (source: constructed from the DWS National Groundwater Archive)

Various methods have been integrated in assessing the hydrogeological processes that affect the chemical composition of groundwater. For example, multivariate analysis, bivariate correlation analysis, Gibbs plot, Piper plots, and stoichiometric analyses have been integrated by Kumar *et al.* (2009), Rajesh *et al.* (2012), Tahoora *et al.* (2014), Luo *et al.* (2018) and Ntanganedzeni *et al.* (2018) in understanding the geochemical processes that impact the chemical components and groundwater quality of the different geological settings. This study used the Piper diagram to

analyse the source of water and to identify the main water type; the Gibbs diagram to identify geochemical processes such as precipitation, dissolution, and water-rock interaction; and bivariate correlation analyses to identify the relationship between the ions and to identify the dominant ion.

The chemical components of groundwater and leachate dam are presented in Figure 5.33 and Table 5.6. Four water types, namely, magnesium sulphate, calcium sulphate, sodium sulphate, and sodium chloride are identified for the water samples collected at Marie Louise landfill. Groundwater of samples GMLS7, GML09, GMLS11, and GMLS16 consisted of high sulphate concentration. There is no evidence of mixing as the plots are dispersed in different regions.

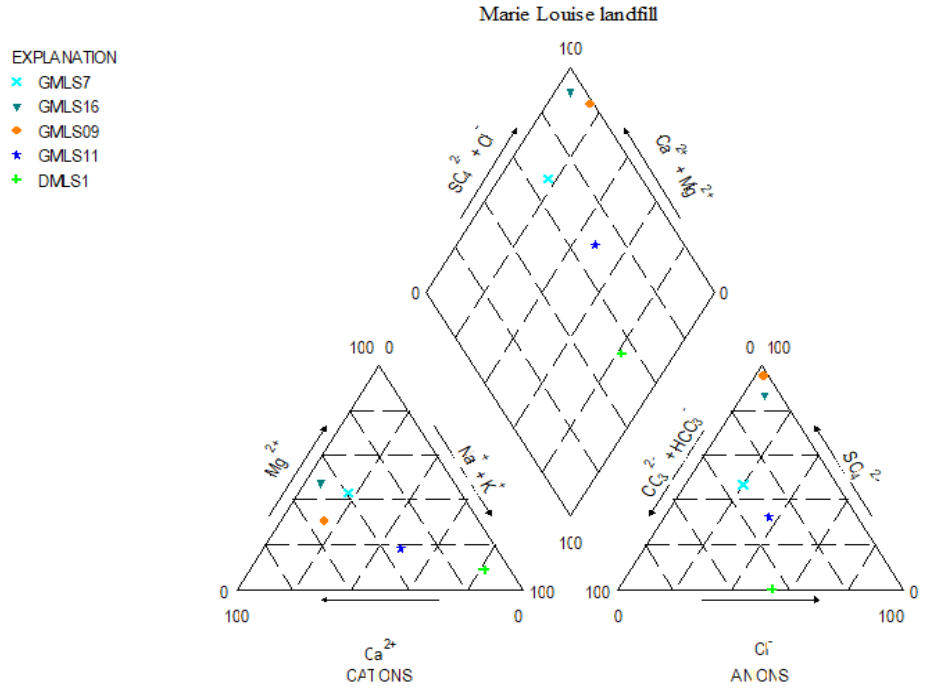

Figure 5-33: Hydrochemical facies of groundwater, and leachate in Marie Louise landfill.

Table 5.6: Hydrochemical facies of Marie Louise samples

Sample name	Water chemistry
GMLS07/GMLS16	Mg^{2+}- SO_4^{2-}
GMLS09	Ca^{2+}- SO_4^{2-}
Leachate dam (DMLS01)	Na^{+} - Cl^{-}
GMLS11	Na^{+} - SO_4^{2-}

The relationship between the major ions is presented in Figure 5.34. Sodium and chloride in Figure 5.34a and, Calcium and sulphate in Figure 5.34b show a strong correlation. This suggests that the two ions plotted against each other in Figure 5.34a and b derive from the same source. The source of the chemical component could be landfill leachate supported by the concentrations of TDS, tritium, and ammonia concentrations which indicate possible pollution that is likely from landfill leachate. A weak correlation is demonstrated in Figure 5.34c between calcium and chloride. The weak correlations suggest that the source contributing to the chemical composition of the two ions is not the same; hence the presence of chloride does not have any influence on calcium, nor does calcium has an influence on chloride.

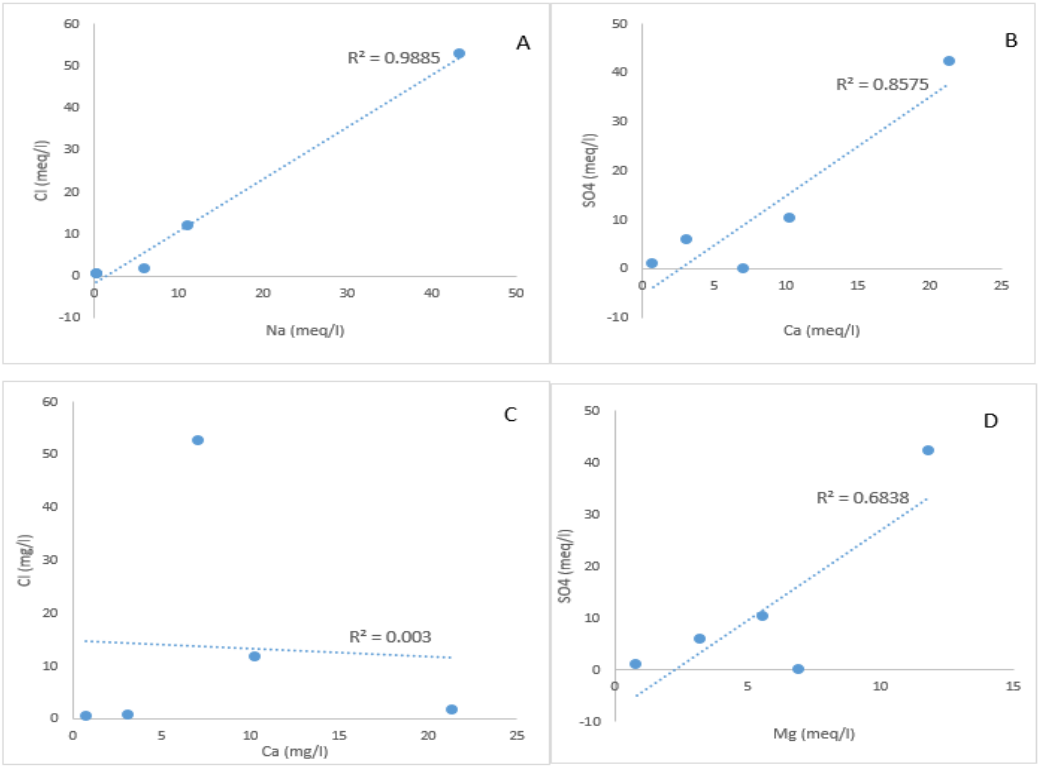

Figure 5-34: The Marie Louise landfill bivariate correlation

Several variables, such as the physical state of the aquifer, bedrock mineralogy, and weather conditions control groundwater chemistry. To illustrate the natural mechanisms controlling groundwater chemistry, Gibbs (1970) proposed the plotting of TDS versus $Na^+/(Na^+ + Ca^{2+})$ and $Cl^-/(Cl^-+HCO_3\text{-})$ for cations and anions, respectively. By plotting the TDS versus weight ratio of $Na^+/(Na^+ + Ca^{2+})$ and $Cl^-/(Cl^-+HCO_3\text{-})$, the main natural processes influencing groundwater chemistry mainly: 1) atmospheric precipitation, 2) rock weathering dominance, 3) evaporation and precipitation can be identified (Gibbs, 1970). The main factors controlling the chemical composition of the groundwater in the Marie Louise landfill site are rock weathering and evaporation dominance. As demonstrated by the Gibbs diagram in Figure 5.35, samples GMLS07 and GMLS16 fall within the rock dominance region, suggesting that rock weathering is the primary factor influencing the chemical composition of this groundwater. The groundwater chemistry of GMSL9 is influenced by evaporation. This is supported by the depicted stable isotopes in Figure

5.31 which depicts GMLS9 in the evaporation line/region. Samples DMLS01 amd GMLS11 which fall outside the bounded area are considered to be part of the evaporation dominance area as they are above the 1000 mg/l TDS concentration.

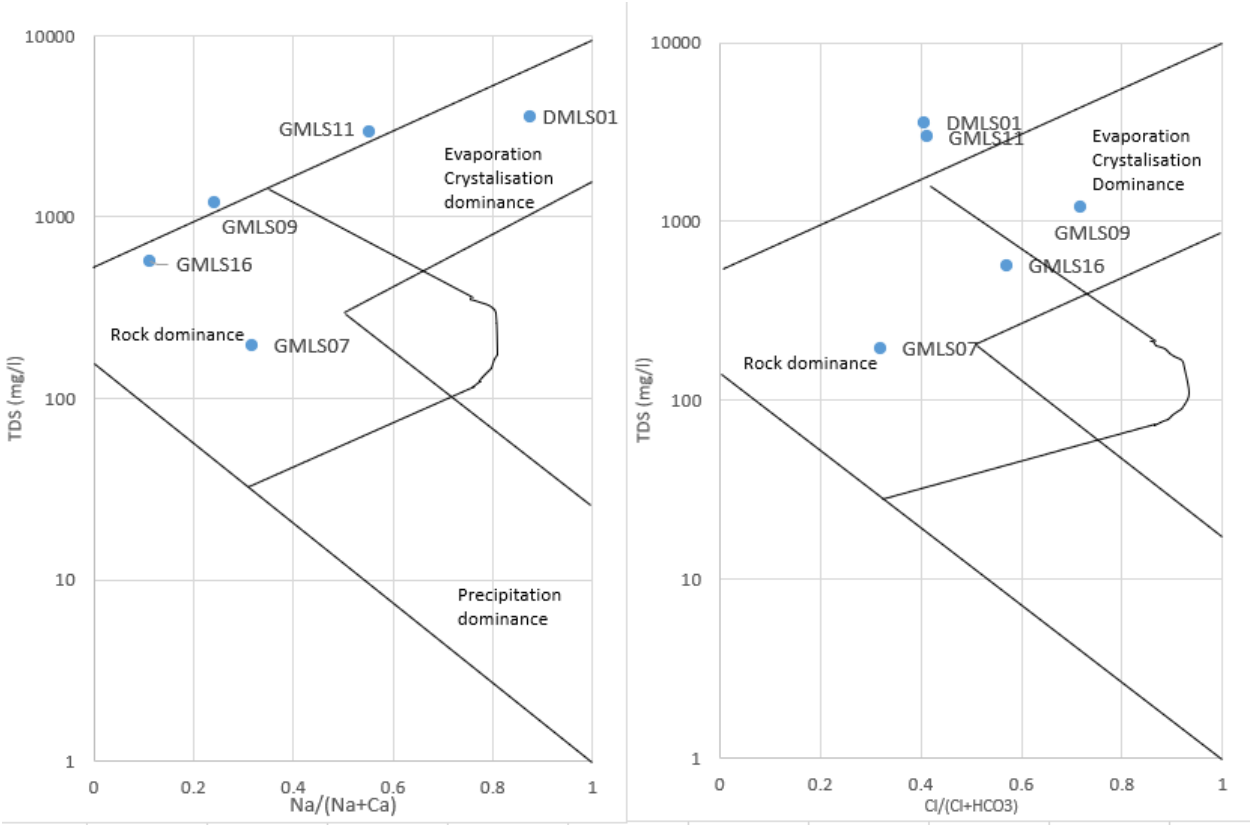

Figure 5-35: Gibbs diagram for the Marie Louise landfill site

5.3.1.5 Metals

The metal concentrations of soil samples collected at Marie Louise are presented in Table 5.7, Table 5.8, and Figure 5.36. The 13 soil samples collected from different sample points show the distribution of metal concentration across the Marie Louise landfill site. All the soil samples have high mean concentrations of Cr (313.42 ppm), Zr (185.82 ppm), and Ba (198.00 ppm). Cr is exceptionally high in samples ML9 (799.41 ppm) and ML2 (394.34 ppm). Sample ML2 lies in close range with borehole GMLS15 with a TDS of 1960 mg/l (Figure 5.29). Given the proximity of ML2, which has a high Cr concentration to borehole GMLS15, the groundwater of this borehole is likely to be contaminated if the toxic metals infiltrate the aquifer, especially since groundwater moves towards this point, as shown by the groundwater flow direction (Figure 5.37). Groundwater contamination is highly possible if the vadose zone is thin, as the travel distance for contaminants is less. The high concentration of the Cr, Zr and Ba metals is likely from leachate. Besides the high concentrations of Cr, Zr, and Ba in all the soil samples, the concentrations of Zn and Cu are high in some of the soil samples. The accumulation of these toxic metals can negatively impact groundwater if leachate flows into the unsaturated zone.

Table 5.7: Metal concentrations of soils collected in Marie Louise (ppm)

(ppm)	ML1	ML2	ML3	ML4	ML5	ML6	ML7	ML8	ML9	ML10	ML16	ML17	ML19
Sc	7.87	14.19	13.01	5.14	8.63	11.18	5.27	10.77	16.94	11.65	4.87	10.24	10.47
V	60.36	92.19	74.21	51.48	77.26	64.05	59.17	102.99	207.88	81.63	31.25	77.64	78.56
Cr	216.33	394.34	360.56	173.26	252.59	291.95	188.15	386.87	799.4	293.38	109.38	278.78	329.41
Co	18.36	40.55	199.93	14.14	12.96	18.6	1.47	19.58	8.76	23.28	3.56	16.81	11.71
Ni	68.24	53.12	443.53	42.02	58.6	45.12	22.23	71.08	78.92	63.94	17.06	46.11	58.66
Cu	89.04	43.32	118.22	34.82	27.31	59.79	20.62	84.63	60.81	109.71	18.05	43.31	70.99
Zn	255.25	33.21	511.89	55.24	25.91	98.8	12.92	108.17	35.54	266.84	29.47	60.31	71.08
Ga	6.97	11.02	10.39	8.26	6.76	9.62	5.14	11.19	16.83	9.43	3.04	9.89	7.64
Rb	21.82	34.05	26.63	20.72	18.35	62.03	15.07	50.79	30.8	42.12	10.76	62.61	32.08
Sr	36.76	108.03	42.93	15.55	46.14	130.6	7.49	72.96	15.85	78	6.08	84.48	83.59
Y	10.71	16.76	53.03	9.18	9.79	15.35	9.25	16.14	14.4	13.07	6.22	13.66	14.02
Zr	180.3	172.46	220.69	194.66	191.36	162.91	203.24	179.06	218.88	169.56	175.1	173.17	174.22
Nb	6.36	7.9	8.06	6.45	6.95	7.37	4.81	7.03	8.01	6.27	4.3	7.12	8.14
Mo	1.71	1.16	2.53	0.82	1.13	2.59	1.06	0.93	2.76	1.48	0.28	1.56	2.41
Ba	160.46	318.99	162.64	93.59	125.14	343.66	36.86	260.09	265.28	260.6	37.55	264.63	244.57
Pb	71.66	29.67	78.4	28.68	26.62	41.66	9.24	48.64	42.93	103.35	10.71	64.93	38.53
Th	4	6.72	14.19	3.06	3.68	6.3	3.45	4.48	4.34	3.56	5.79	11.56	11.01
U	11.92	1.64	135.1	3.61	1.7	2.52	dl	4.92	2.87	3.33	0.25	dl	1.84

As depicted by the soil map in Figure 5.11 and the vulnerability map in Figure 5.23, Marie Louise lies in a moderately-vulnerable area where the underlying soil has little clay and silt content that can decrease the movement and migration of metals. The high concentrations of Cr, Ba, and Zr are likely encouraged by the permeable soil. The Marie Louise landfill site also lies in an area with a permeable vadose zone where the metal in the soil is likely to migrate to the vadose zone and the water table, therefore contaminating the groundwater. The presence of Cr, Ba, and Zr metals amongst other metal concentrations in the soil is proof that the soil is permeable as the soil has elevated concentrations of Cr, Ba, and Zr. The elevated metal concentrations are likely to be transported to the vadose zone and the groundwater by the moving water.

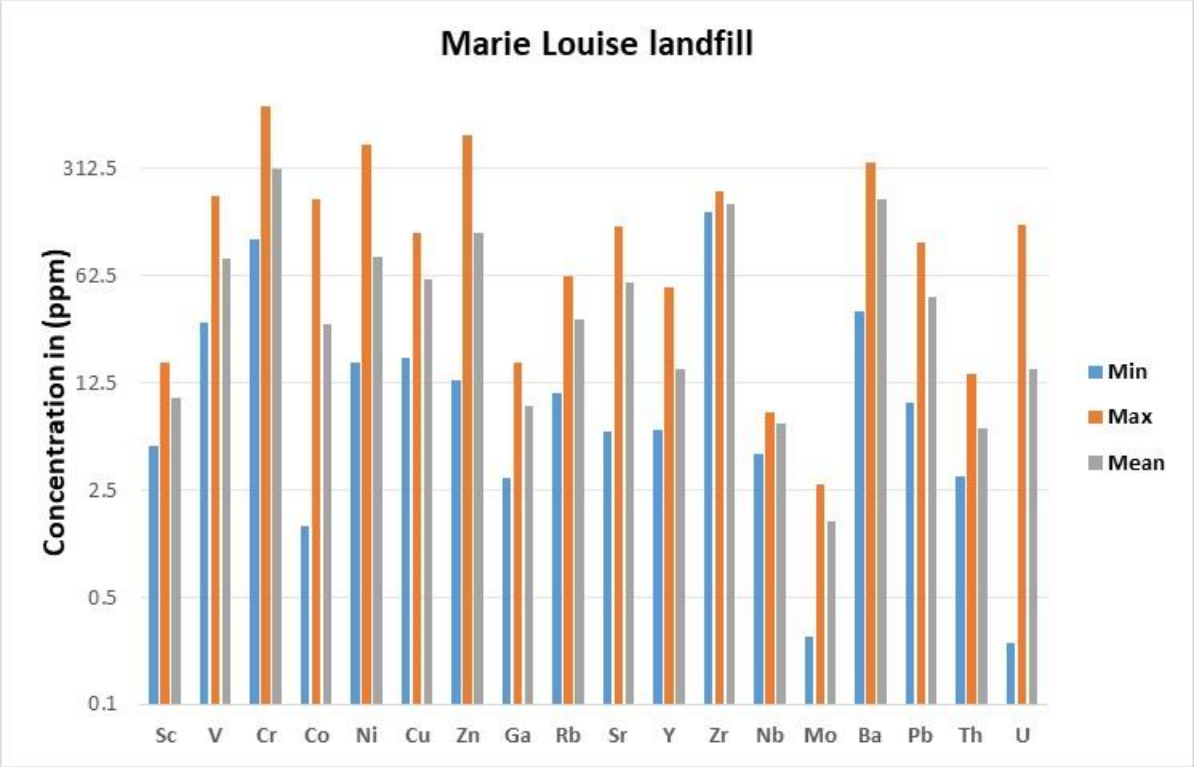

Figure 5-36: Metal concentration of soil samples collected at Marie Louise

Table 5.8: Minimum, maximum, and mean results of metals (Marie Louise)

Metal (ppm)	Min	Max	Mean
Sc	4.87	16.94	10.02
V	31.25	207.88	81.44
Cr	109.38	799.4	313.42
Co	1.47	199.93	29.98
Ni	17.06	443.53	82.20
Cu	18.05	118.22	60.05
Zn	12.92	511.89	120.36
Ga	3.04	16.83	8.94
Rb	10.76	62.61	32.91
Sr	6.08	130.6	56.04
Y	6.22	53.03	15.51
Zr	162.91	220.69	185.82
Nb	4.3	8.14	6.83
Mo	0.28	2.76	1.57
Ba	36.86	343.66	198.00
Pb	9.24	103.35	45.77
Th	3.06	14.19	6.32
U	0.25	135.1	15.43

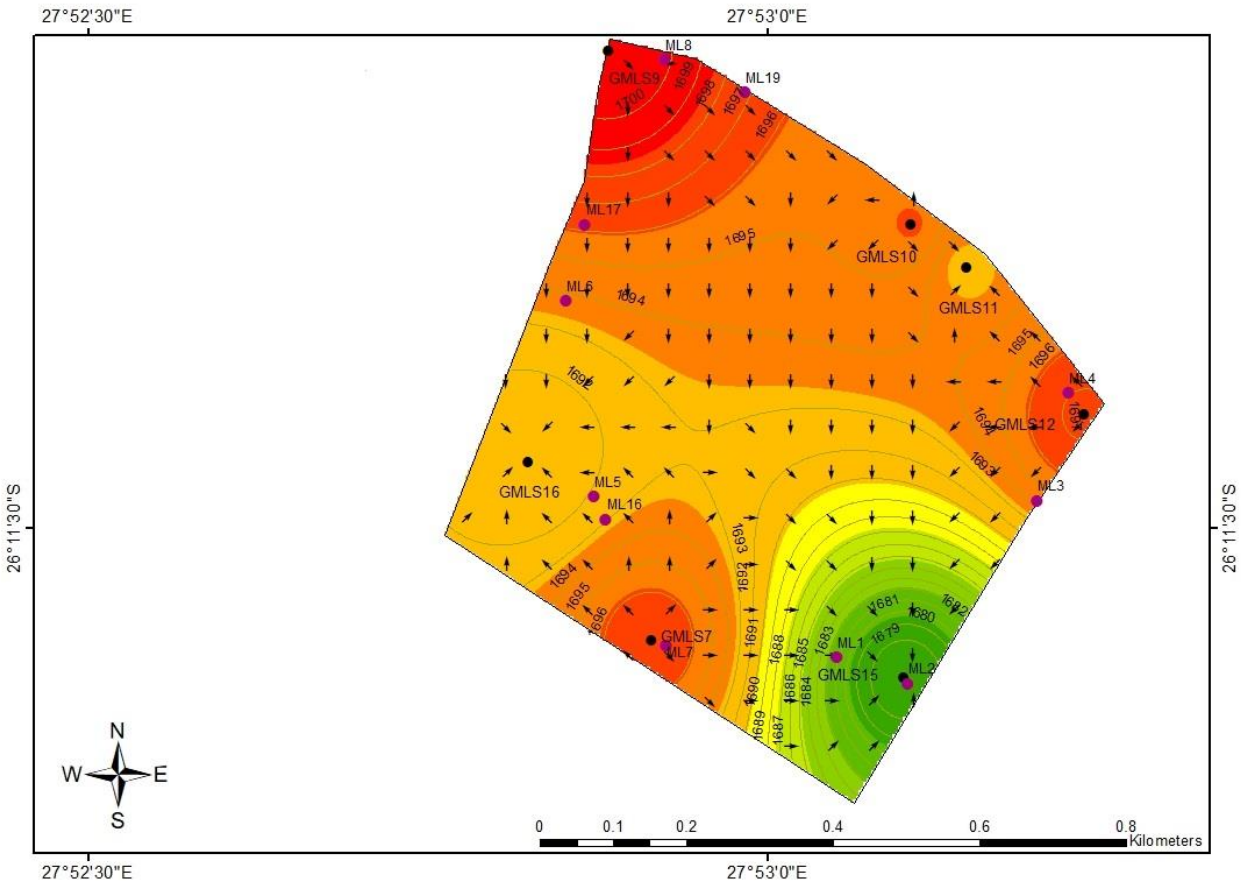

Figure 5-37: Groundwater flow direction at Marie Louise

5.3.2 Robinson landfill

5.3.2.1 Field Parameters

As demonstrated in Table 5.9, the electrical conductivity measured at the groundwater, surface water, and leachate at the Robinson landfill site varies between 34 mS/m and 694 mS/m, whereas TDS varies between 275 mg/l and 4590 mg/l. The highest EC and TDS is from the leachate pond, where salinity is high. Hydrogeological processes such as mineral dissolution from rocks, evaporation, and leaching from soil affect TDS. TDS is therefore influenced by the aquifer's geological and mineralogical characteristics. The relatively high TDS in GR14 (1165 mg/l) is likely from the soil, considering its shallow groundwater depth (Figure 5.39). The high TDS in borehole GR8 (2738 mg/l) is likely from mineral dissolution from rocks, given the deep groundwater depth of this borehole. TDS is increasing with groundwater flow direction in the case of boreholes GR9, GR12, GR14, and GRS01 (Figure 5.46). The increase in TDS can be attributed to rock-water interaction. The pH in the area varies between 5.9 to 7.6 with the pH of borehole GR12 falling below the recommended pH range of 6.5-9.2 by WHO (2008) and 6.0-9.2 by DWA (1996). Borehole GR9 complies with the recommended TDS concentration by WHO (2003) of 100-500 mg/l whilst the other samples have TDS concentrations above the permissible concentrations. Given that the Robinson landfill site is situated in an area where the hydrogeological characteristics of the underlying environment make the aquifer moderately vulnerable to pollution, if the leachate seeps into the sub-surface, groundwater will likely be contaminated as the soil has little attenuation properties, whilst the vadose zone is permeable, and the aquifer is fractured with high hydraulic conductivity.

Table 5.9: Physicochemical parameters of samples collected at Robinson landfill

Description	Sample Name	Electrical Conductivity (mS/m)	pH	TDS (mg/l)
Groundwater	GR 8	334	6.2	2738
Groundwater	GR 12	142	5.9	1260
Groundwater	GRS_01	205	6.5	1344
Groundwater	GR9	34	6.2	275
Groundwater	GR14	254	7.5	1165
Leachate dam	DR1	694	7.6	4590
Surface water	SR1	178	6.9	1225

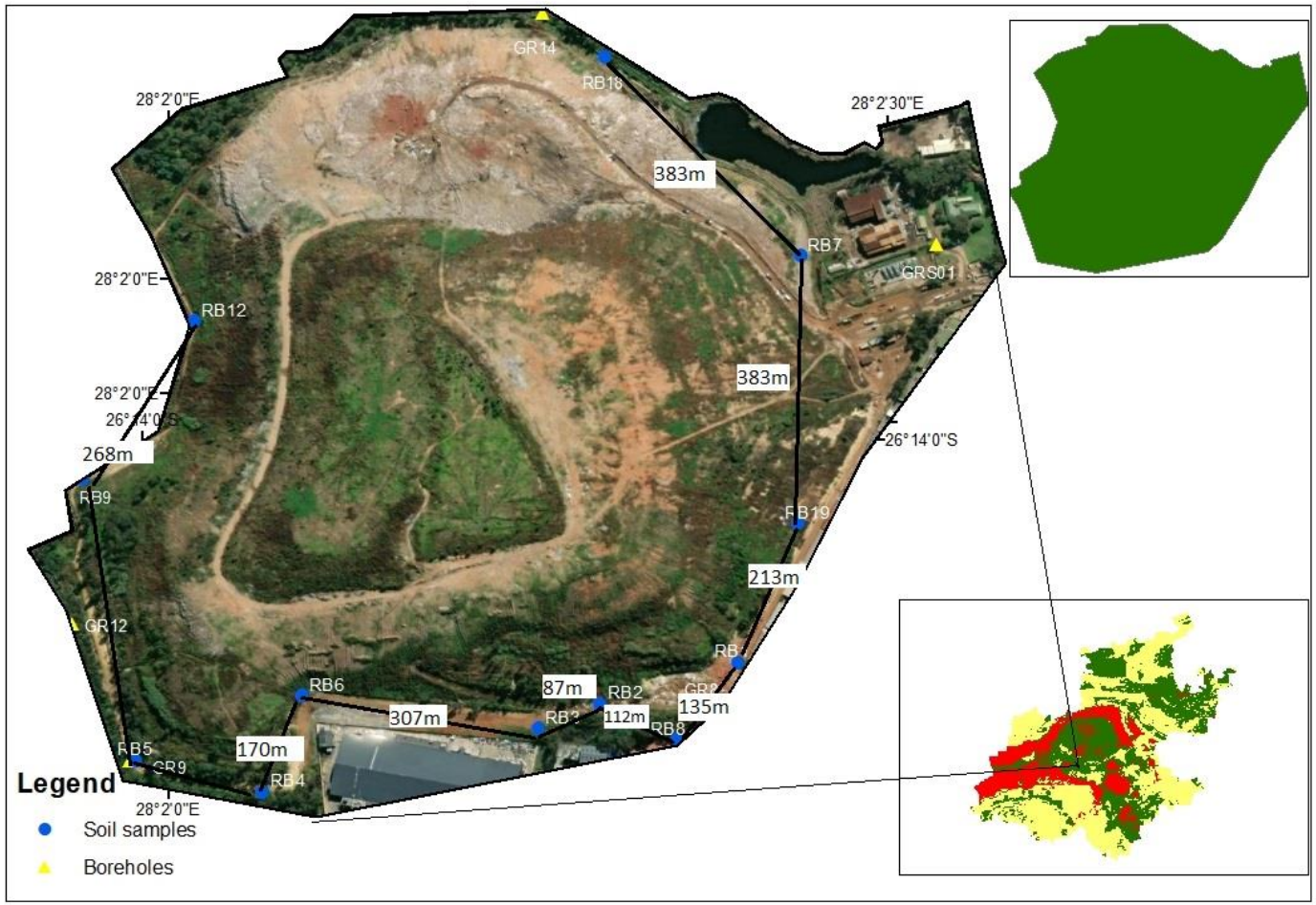

Figure 5-38: Sampling locations and distance between soil samples collected at Robinson landfill

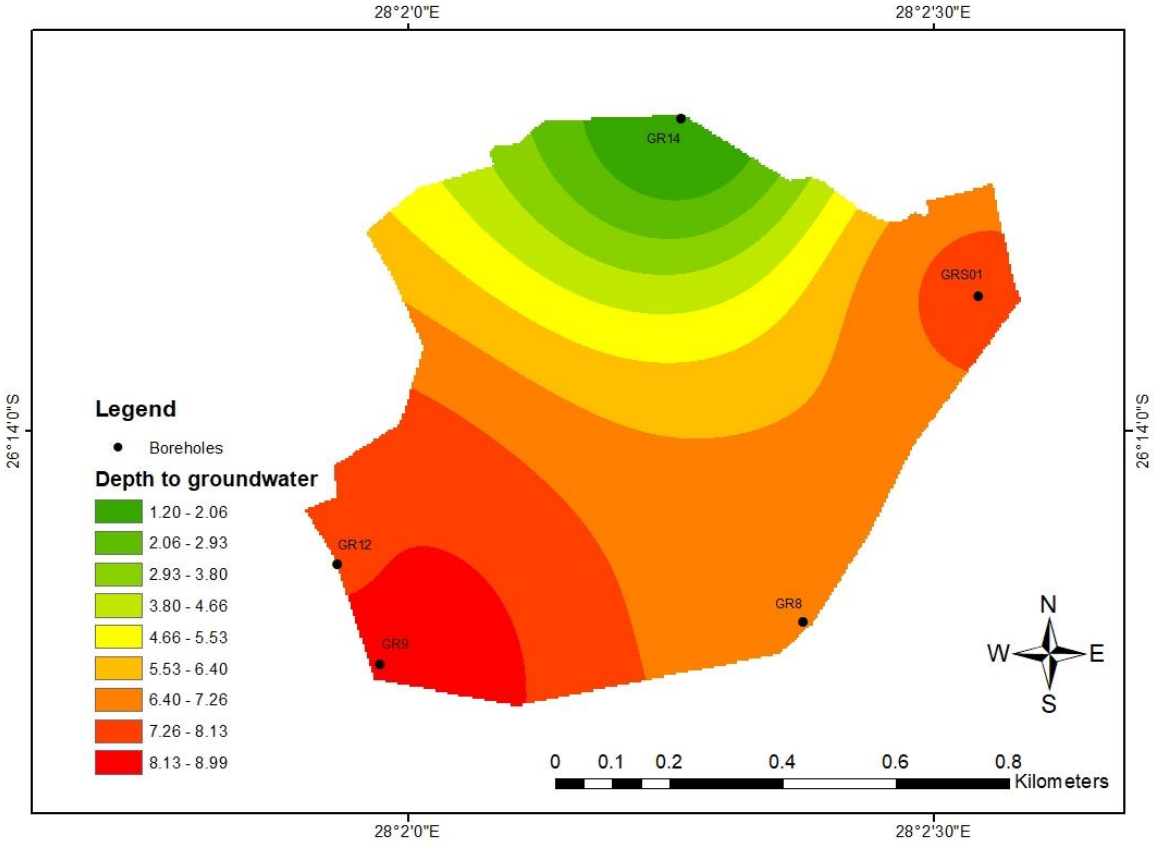

Figure 5-39: Depth to groundwater at Robinson landfill site

5.3.2.2 Stable isotopes of water

The isotopic signature of rainfall is affected by factors such as altitude, latitude, distance to moisture, humidity, amount of rainfall, and temperature (Clark and Fritz, 1997). The isotopic signature of water reservoirs is, therefore, a reflection of the aforementioned factors that affected the rainfall that recharged that water reservoir. As depicted in Table 5.10 and Figure 5.40, Robinson rainwater has enriched isotopic signatures, demonstrating isotopic signatures of 26.2‰ (δ^2H) and 1.53‰ ($\delta^{18}O$) which suggests recharge from low altitude during high temperature seasons, whereas the rest of the samples have depleted isotopic signatures. According to (Clark and Fritz 1997), highly depleted isotopic signatures are attributed to rainfall that occurred at high altitudes and during low-temperature seasons. Borehole GR9 has highly depleted isotopic

signatures with -32.1‰ for $\delta^{2}H$ and -4.96‰ for $\delta^{18}O$. Concerning the temperature and altitude effect, this sample was recharged by water at high altitude and low temperature. Surface water has -14.9 ‰ ($\delta^{2}H$) and -3.01‰ ($\delta^{18}O$) isotopic signatures, which shows less depletion as compared to other samples. Leketa *et al.* (2018) also showed the relationship between temperature effect, amount, and altitude effect in isotopic signatures in the Johannesburg rainfall, confirming that highly depleted isotopes relate to recharge that occurred during colder climates. All the samples have different isotopic signatures. The variation in isotopic signatures of these samples is, therefore, a representation of variation in recharge events and not the spatial distribution of the recharge mechanism.

Table 5.10: Stable isotope results from samples collected at Robinson landfill

Sample Name	**δ 2H (‰)**	**±‰**	**δ 18O (‰)**	**±‰**	**D-EXCESS**
GR8	-17.0	0.7	-4.16	0.1	10.84
GR9	-32.1	1.1	-4.96	0.1	1.17
Rain	26.2	7.4	1.53	0.5	15.95
GR12	-16.0	1.3	-3.75	0.2	9.16
Surface water (SR1)	-14.9	0.4	-3.01	0.1	5.30

According to Fritz *et al.* (1976), polluted samples have heavy isotopic compositions (less depleted). Borehole GR12 has isotopic compositions that are less depleted which attribute to pollution. The pollution in borehole GR12 is supported by the high TDS concentration and an 8.9 TU which is higher than the rainfall tritium and the Johannesburg tritium unit. The moderately-vulnerable environment in which the landfill is located encourages the pollution of groundwater.

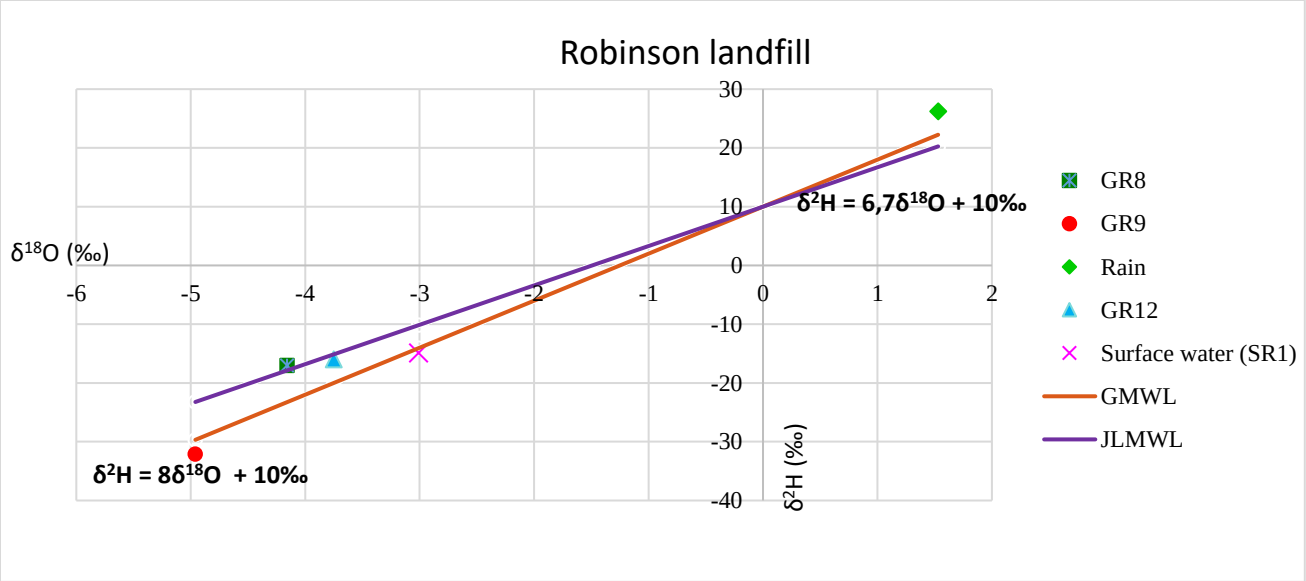

Figure 5-40: Stable isotopes of surface water, groundwater and rain samples collected at Robinson landfill

5.3.2.3 Tritium

In the Robinson landfill site, tritium was used to identify and trace pollution by leachate in the surface and groundwater and to determine ancient and recent recharge. As demonstrated by Table 5.11, the tritium in the borehole GR8, GR9, GR12, and GRS01 varies between 0.7 - 8.9 TU.

Sample GR8, GR9, and GR12 have tritium units of 0.8, 1.0, and 0.7 TU, respectively, whilst rainfall recorded 1.7 TU. The low tritium in GR8, GR9, and GR12 suggest that the groundwater underlying these boreholes has no artificial tritium as they have tritium units below 5.6 TU of the Johannesburg rainfall recorded by Abiye *et al.* (2015). The low tritium also suggests that the aquifer system of these boreholes is less permeable with slow recharge and groundwater circulation. Sample GRS01 has an 8.9 TU, which exceeds the 5.6 TU of the Johannesburg rainfall (Abiye *et al.,* 2015) and that of rainfall at the Robinson landfill (1.7 TU). The high tritium unit indicates artificial tritium. Since the tritium in GRS01 is above 5.6 TU, it can be assumed that the groundwater of borehole GRS01 is to some degree contaminated. As expected, the leachate dam has relatively high tritium (380.2 TU). The elevated tritium unit in the groundwater of borehole GR01 (8.9 TU), which represents pollution by landfill leachate in the Robinson landfill site is evidence that the hydrogeological factors such as the permeable vadose zone, permeable soil with little clay content increase the chances of groundwater pollution by enabling the movement of contaminants.

Table 5.11: Tritium results from Robinson water samples

Laboratory Number	**Sample Identification**	**Tritium**	
		(T.U.)	**±**
WITS 1535	GR 08	0.8	0.3
WITS 1536	GR 09	1.0	0.3
WITS 1537	GR 12	0.7	0.3
WITS 1538	GRS 01	8.9	0.5
WITS 1539	Robinson Leachate	380.2	61.3
WITS 1540	Robinson Rain	1.7	0.3

5.3.2.4 Hydrochemical facies

The major ions presented in Table 5.12 were used to plot the Piper diagram in Figure 5.42. As depicted in Table 5.12, borehole GR8 has elevated sulphate, calcium and sodium concentrations that exceed the recommended limit for drinking water by WHO (2011). The elevated SO_4 concentration is possibly from gypsum, anhydrite, and magnesium sulphate, given that the Robinson landfill site is in a mine-tailing dump, as these minerals are found mostly in a mine-tailing dump. The elevated calcium concentration is likely from the soil. According to the aquifer vulnerability map depicted in Figure 5.23, the Robinson landfill resides in a moderately vulnerable region. Similar to Marie Louise landfill, the fractured quartzite and shale make the aquifer beneath this landfill moderately vulnerable to contamination. All the samples have relatively major ion concentrations that are below the recommended limit for drinking water by WHO (2011), with the exception of GR8 and the leachate dam. Furthermore, sample GR8, GR9, GR12, and SR1 have ammonia concentrations of 0.4 mg/l, 0.3 mg/l, 0.1 mg/l, and 2.1 mg/l, respectively. Ammonia concentration above 2.1 mg/l is present in surface water (SR1) which indicates pollution. The high ammonia concentration of 458 mg/l in sample DR1 also suggests pollution from waste.

Table 5.12: The Robinson landfill major ion results (mg/L)

Parameter	GR8	GR9	GR12	SR1	DR1
Total Alkalinity ($CaCO_3$)	40	184	48	120	2460
P-alkalinity ($CaCO_3$)	<5	<5	<5	<5	<5
Bicarbonate (HCO_3)	49	224	59	146	2999
Carbonate (CO_3)	<5	<5	<5	<5	<5
Chloride as (Cl)	423	18	105	73	3972
Sulphate as (SO_4)	1250	7	142	83	575
Ammonia (N)	0.4	0.3	0.1	2.1	458
Sodium (Na)	409	18	80	42	1584
Potassium (K)	7.6	43	3.7	22	981
Calcium (Ca)	122	28	27	40	314
Magnesium (Mg)	186	6	22	18	232

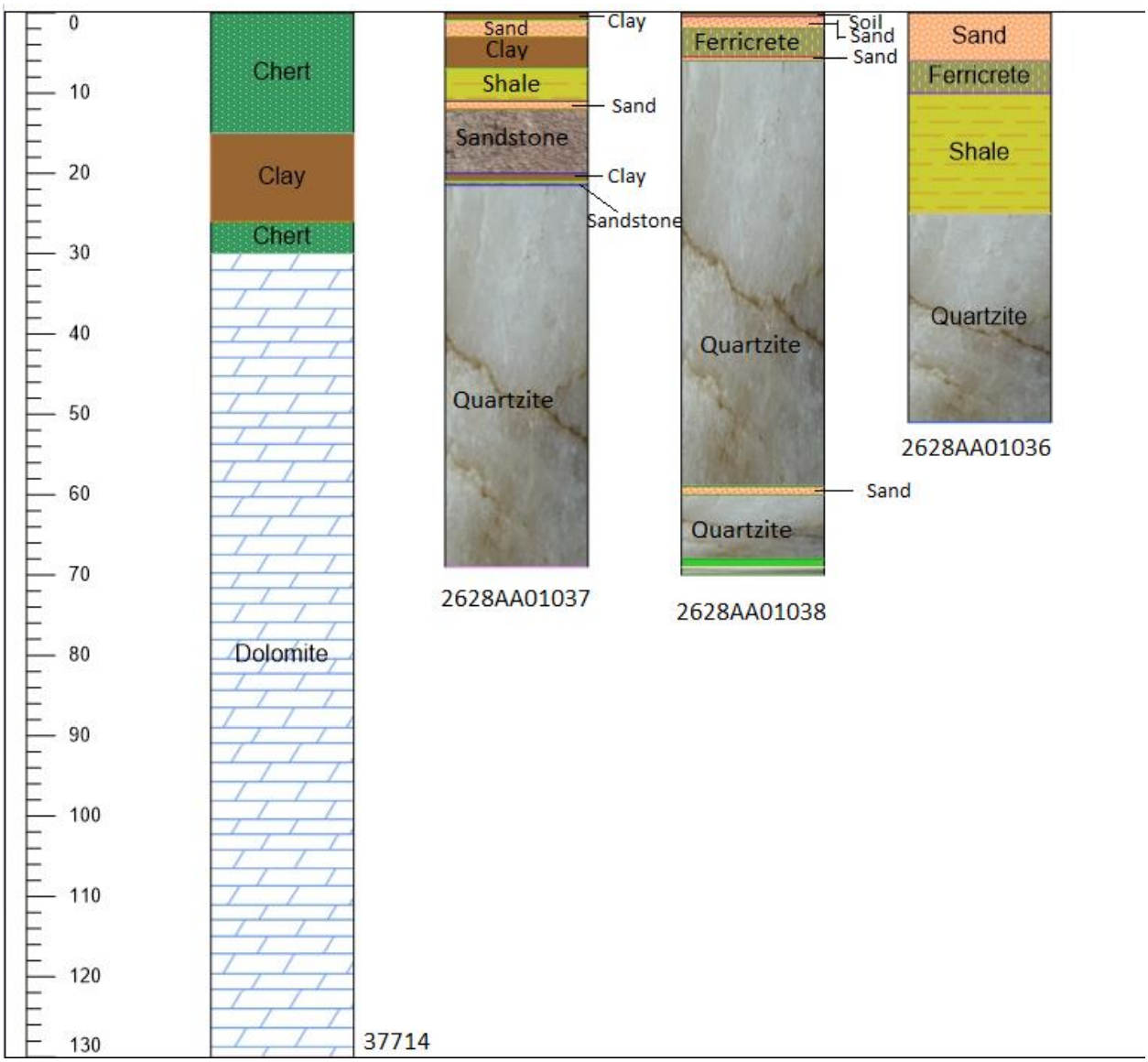

Figure 5-41: Robinson landfill site lithology (source: DWS National Groundwater Archive)

The Piper diagram in Figure 5.42 depicts the different water types from the surface and groundwater samples collected at the Robinson landfill site. Four water type exists: Na-SO_4, Ca-HCO_3, Na-Cl, and Ca-Cl. Sample GR8 belongs to the Na-SO_4 water type, and according to the Piper diagram, it plots along the intrusion region. The groundwater of sample GR9 belongs to the Ca-HCO_3 water type and plots along the refreshing region. The presence of bicarbonate in sample GR9 is likely from bicarbonate that existed in the soil, which leached to the aquifer. GR12 and DR1 belong to the Na-Cl water type. The high sodium and chloride concentration in GR12 and DR1 is likely from leachate.

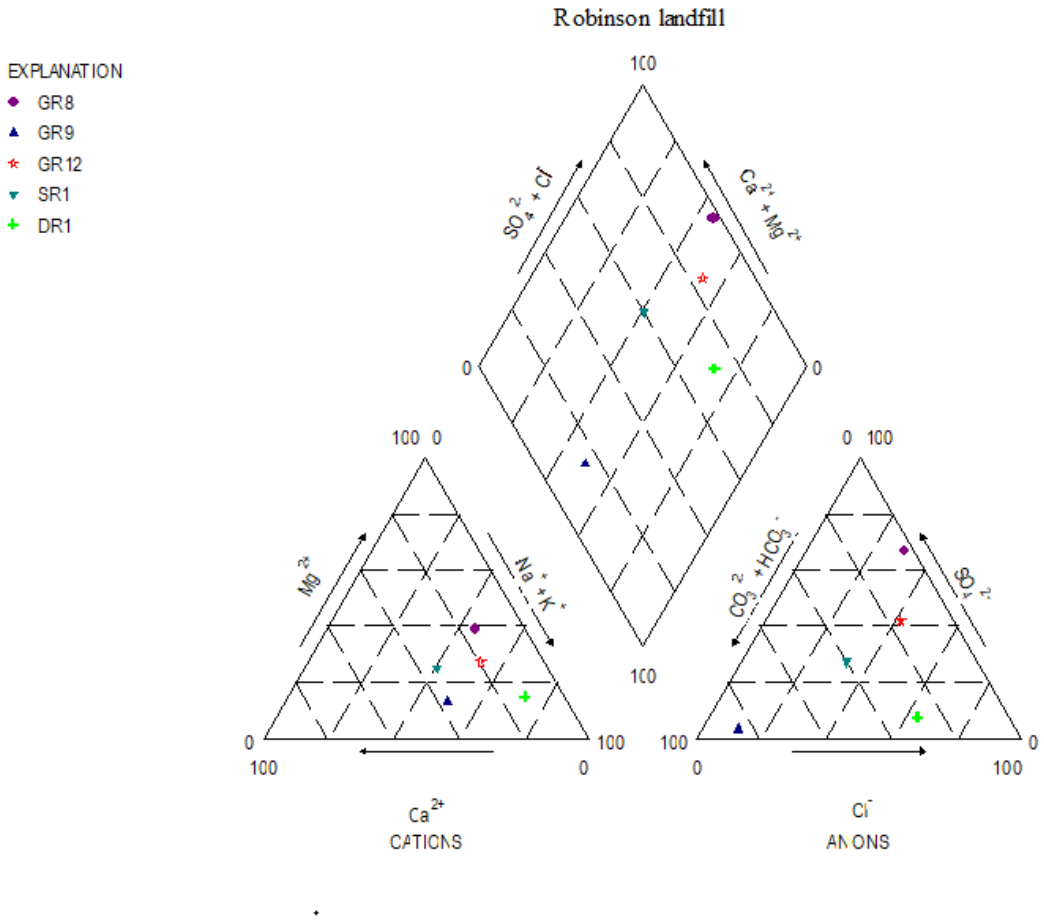

Figure 5-42: Piper diagram (Robinson landfill site)

Table 5.13: Hydrochemical facies of groundwater and leachate in Robinson landfill

Sample name	Water chemistry
GR8	$Na^+ - SO_4^{2+}$
GR9	$Ca^{2+} - HCO_3^-$
GR12	$Na^+ - Cl^-$
SR1	$Ca^{2+} - Cl^-$

Figure 5.43 shows a high correlation between Na-Cl, Ca-HCO_3, and Ca-Cl. This suggests that Na derives from the same source as Cl, Ca derives from the same source as HCO_3, and Ca and Cl derives from the same source. The source of the chemical component of Na-Cl and Ca-Cl could be landfill leachate. Nevertheless, Na-SO_4 has a weak correlation, suggesting that the two ions are from different sources.

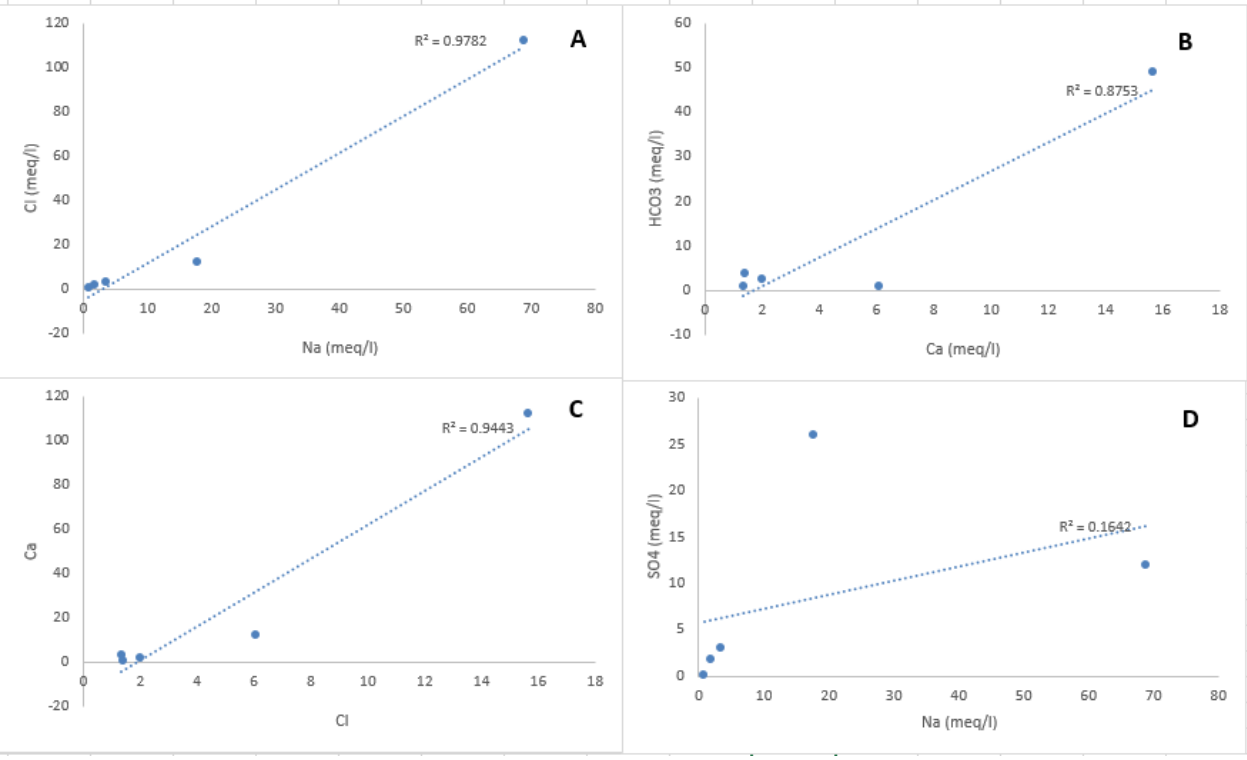

Figure 5-43: The Robinson landfill bivariate correlation

As depicted in Figure 5.44, the main mechanism controlling groundwater chemistry is evaporation and rock weathering. Evaporation can potentially increase ion concentrations produced by chemical weathering, resulting in high salinity (Jalali, 2006). Since the Robinson landfill area experiences a semi-arid climate, evaporation is ultimately favored, therefore encouraging evaporation dominance (Figure 5.44). Sample GR9 plots in the rock dominance area, making rock weathering the main factor controlling this sample's chemical component whereas sample GR8, GR12, SR1, and DR1 plots in the evaporation dominant area. The effect of evaporation in sample SR1 is supported by the stable isotope, as this sample plots in the evaporation line (Figure 5.40).

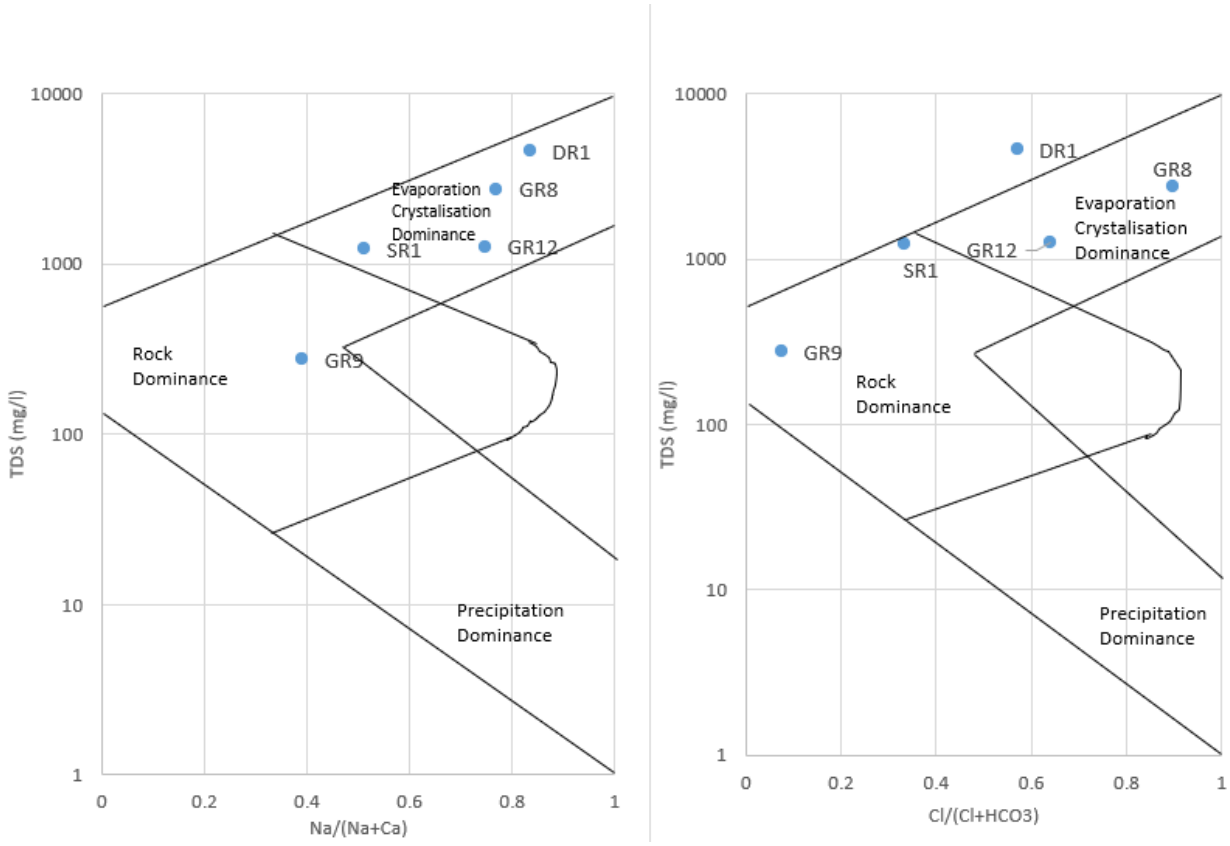

Figure 5-44: Gibbs diagram in the Robinson landfill site

5.3.2.5 Metals

The metal concentrations of soil samples collected at the Robinson landfill site are presented in Table 5.14, Table 5.15, and Figure 5.45. Cr, Zr, and Ba concentrations are high in all the samples collected in the Robinson landfill site, with mean concentrations of 232.60 ppm, 161.11 ppm, and 272.72 ppm, respectively. Sample RB18, sampled close to the leachate dam, has elevated concentrations of Cr and Ba (Figure 5.38). The elevated concentrations of Cr and Ba in sample RB18 can be attributed to leachate since this soil sample was collected close to the leachate dam. This sampling point with high concentrations of Cr and Ba is also within close range of borehole GR14 which has a TDS value of 1165 mg/l. Soil sample RB7 also depicts high Cr (248.68 ppm) and Ba (337.53 ppm) concentrations. This sample was collected in close range with borehole GRS_01, which depicts high TDS concentrations of 1344 mg/l. Considering the groundwater flow direction shown in Figure 5.46, if the toxic metal concentrations of Cr and Ba infiltrate into the aquifer, GRS_01 is most likely to be contaminated by these metals, given the shallow groundwater depth of the borehole. If the high concentrations of metals persist over the years as a result of leaking leachate, the quality of groundwater in boreholes GR14 and GRS_01 will be heavily impacted. Furthermore, sample RB4 has elevated concentrations of Zn (187.19 ppm), whilst Pb is elevated in sample RB7 (117.41 ppm). The top soils in waste disposal sites experience a lot of accumulation of toxic metal as a result of leachate that is generated from the deposited waste on site. Therefore, the monitoring of metal concentration distribution is significant, especially in soils where the soil properties have little clay and slit content that may filter contaminants. In addition, an aquifer's first line of defence from contamination is the soil media, therefore, proper knowledge of the soil composition, vadose zone properties, and thickness is significant.

Table 5.14: Metal concentrations of soils collected in Robinson landfill site (ppm)

(ppm)	RB1	RB2	RB3	RB4	RB5	RB6	RB7	RB8	RB9	RB12	RB18	RB19
Sc	3.92	5.94	13.5	7.1	5.31	13.26	15.74	6.84	9.87	6.29	8.43	10.71
V	50.62	55.6	105.72	46.81	38.6	74.08	78.91	54.1	52.18	53.82	79.02	80.18
Cr	189.2	187.77	228.56	234.86	172.36	256.29	248.68	216.96	181.58	201.16	443.62	230.15
Co	6.06	12.45	17.94	18.41	12.25	17.31	26.07	3.39	2.9	8.67	18.55	14.82
Ni	27.8	52.14	57.56	24.58	32.3	57.43	63.72	23.28	31.69	19.48	46.97	51.1
Cu	35.94	156.95	50.07	123.86	37.33	49.99	302.95	36.21	37.92	45.73	58.99	41.67
Zn	30.79	94.57	42.23	187.19	45.17	87.22	187.48	31.3	31.85	28.81	93.54	97.69
Ga	7.62	8.1	14.69	9.85	7.66	12.69	14.09	8.59	7.71	7.7	11	10.92
Rb	33.91	34.93	69.77	72.66	40.92	64.04	101.84	40.45	26.23	35.24	94.93	37.06
Sr	35.18	138.61	37.04	32.22	25.02	123.37	97.58	42.18	26.4	25.39	121.61	128.02
Y	9.83	14.39	17.84	14.1	13.97	19.32	17.84	10.22	10.45	10.5	17.16	14.91
Zr	134.25	160.89	189.88	173.43	176.34	171.62	132.84	129.81	168.02	171.09	168.15	157.03
Nb	4.61	6.11	10.24	7.95	6.38	9.4	9.13	5.04	6.24	6.3	10.3	7.63
Mo	0.24	1.88	1.79	0.89	0.58	1.38	0.78	0.78	1.09	1.15	1.52	1.25
Ba	270.62	286.75	195.23	204.63	172.01	343.61	337.53	302.6	202.89	243.87	362.71	350.22
Pb	41.61	74.04	28.99	90.97	50.28	36.7	117.41	71.22	29.53	35.63	45.97	80.14
Th	7.31	10.83	7.38	5.69	5.14	9.6	8.17	5.91	7.01	6.12	8.6	9.32
U	dl	3.49	dl	4.2	1.49	1.63	1.63	2.74	1.53	12.01	dl	dl

Robinson landfill site lies on a moderately vulnerable area where the soil in the sub-surface has little clay content; and where the vadose zone is permeable. The likeliness of the elevated Cr, Zr, and Ba concentrations in the soil polluting the underlying groundwater of this region would be a result of the movement of metals to the permeable vadose zone and the groundwater, carried by the recharging water. The presence of elevated Cr, Zr, and Ba metal concentrations is proof that the soil is permeable with little clay and silt that can immobilize the movement of metals, which also correlates with the aquifer vulnerability map in Figure 5.23 which depicts that the underlying environment below Robinson landfill site is moderately-vulnerable to pollution.

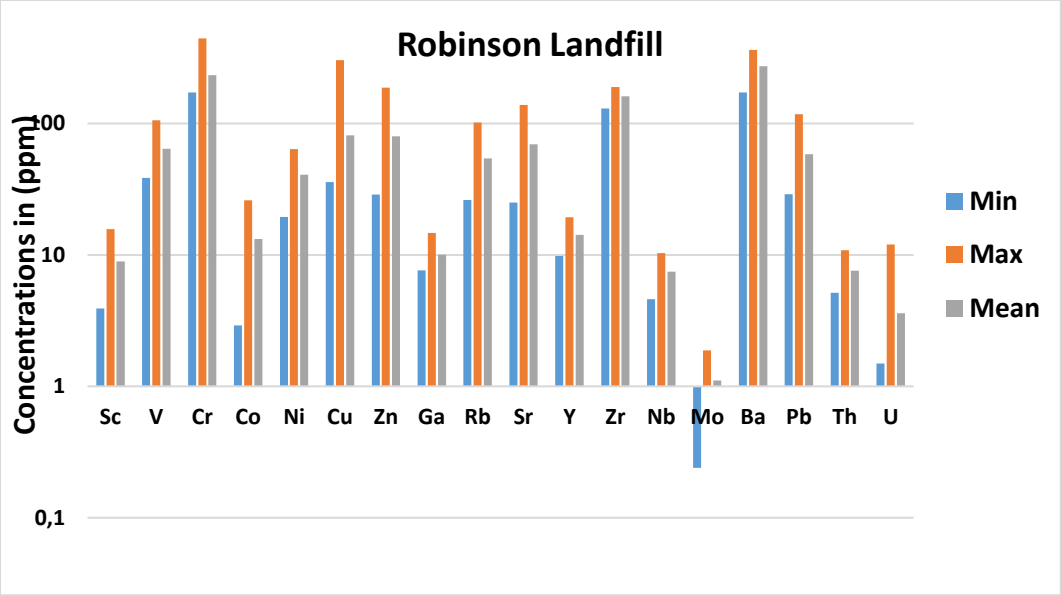

Figure 5-45: Metal concentration of soil samples collected at Robinson landfill site

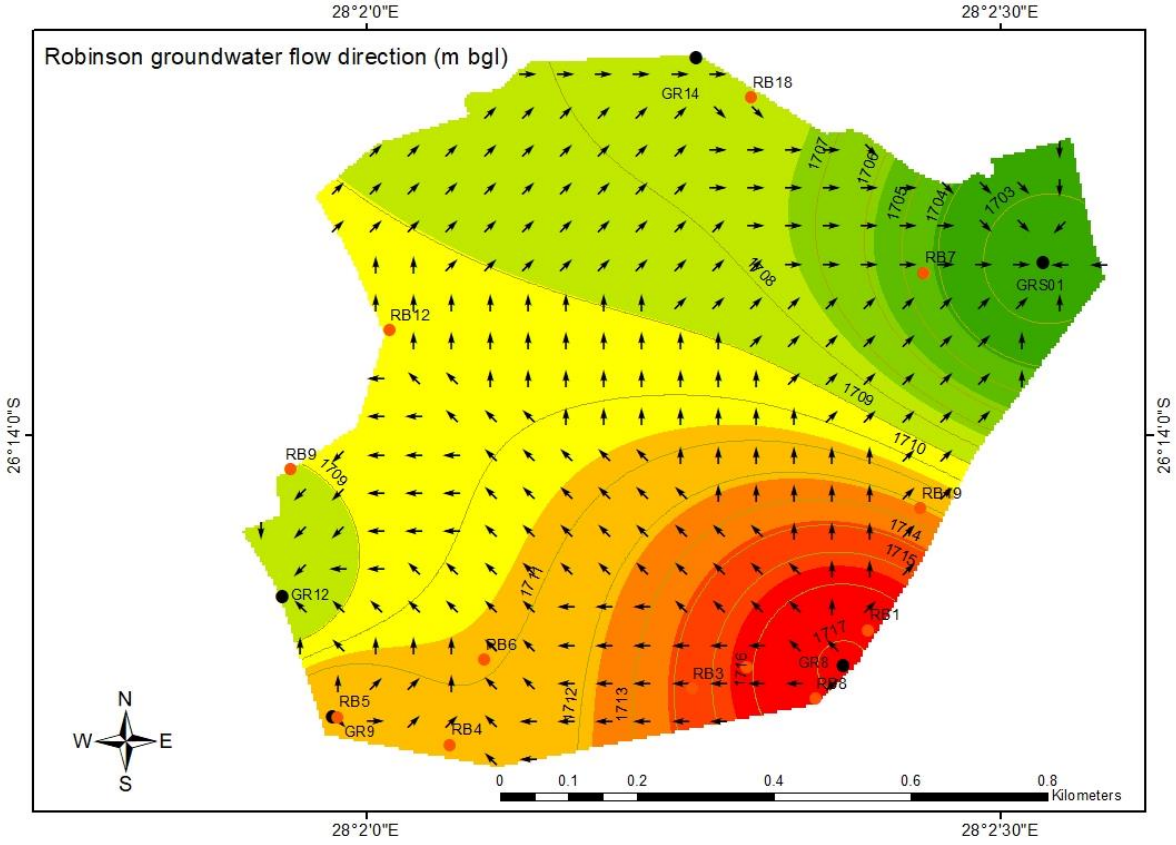

Figure 5-46: Groundwater flow direction (Robinson landfill site)

Table 5.15: Minimum, Maximum, and mean results of metals (Robinson landfill)

Metal (ppm)	Min	Max	Mean
Sc	3.92	15.74	8.91
V	38.6	105.72	64.14
Cr	172.36	443.62	232.60
Co	2.9	26.07	13.24
Ni	19.48	63.72	40.67
Cu	35.94	302.95	81.47
Zn	28.81	187.48	79.82
Ga	7.62	14.69	10.05
Rb	26.23	101.84	54.33
Sr	25.02	138.61	69.39
Y	9.83	19.32	14.21
Zr	129.81	189.88	161.11
Nb	4.61	10.3	7.44
Mo	0.24	1.88	1.11
Ba	172.01	362.71	272.72
Pb	28.99	117.41	58.54
Th	5.14	10.83	7.59
U	1.49	12.01	3.59

CHAPTER 6: CONCLUSION

Applying the DRASTIC method in the Gauteng Province, where pollution by landfill leachate is a concern, and where groundwater is used for various purposes, showed effective results in identifying low, moderate, and highly vulnerable areas based on the hydrogeochemical characteristics of the aquifer system. To achieve the aim and objectives of this study, intrinsic and specific vulnerability maps that indicated the degree of vulnerability of groundwater to pollution were generated using the seven DRASTIC parameters. Both the intrinsic and specific vulnerability maps showed that areas with high vulnerability are associated with the permeable vadose zone, loamy sand, high hydraulic conductivity, karst aquifers of dolomite, and gentle topography. Although the NO_3+NO_2-N data provided by the Department of Water and Sanitation was inadequate for mapping the entire Province, high nitrate concentrations were concentrated within the highly-vulnerable areas. The field investigation conducted in the Marie Louise and Robinson landfill sites enabled a detailed study of the groundwater quality of the underlying aquifers, which were used to validate the vulnerability maps. The use of environmental isotopes, physicochemical parameters, and chemical analyses showed the state of groundwater and surface water quality and the degree of pollution in the Robinson and Marie Louise landfill sites, which were used to validate the DRASTIC index. The tritium results from boreholes GMLS11 and GMLS10 showed relatively high tritium units, which exceed that of Johannesburg rainfall (5.6 TU). The high tritium unit supported by the high TDS and ammonia concentration in GMLS11 confirms that this borehole is polluted by landfill leachate. In the Robinson landfill site, pollution from landfill leachate was detected from borehole GRS01, as the tritium unit found in this borehole exceeded the natural tritium unit. As shown by the Gibbs diagram, the main factors controlling the groundwater and surface water in Marie Louise and Robinson landfill are rock dominance and evaporation dominance. The metal concentration results in the two landfill sites showed elevated concentrations of Cr, Ba, and Zr. The validation of the groundwater vulnerability maps using stable isotopes, physicochemical parameters, tritium, and metal results from the soil samples showed the presence of groundwater pollution possibly by landfill leachate which may have likely been encouraged by the fractured aquifer media, moderate hydraulic conductivity, permeable vadose zone, and loamy sand with little clay content. The presence of pollution in some of the boreholes in the Marie Louise and Robinson landfill site is a result of the aforementioned hydrogeochemical

parameters that make the underlying groundwater moderately vulnerable to pollution by landfill leachate, as proven by the intrinsic and specific vulnerability maps. The findings in this study are relevant in the management of groundwater resources in the Gauteng Province, whilst the shortcomings addressed in this study can be used to improve future research conducted in this Province.

CHAPTER 7: LIMITATIONS

- The DRASTIC method is subjective, and the precision of the groundwater vulnerability map produced depends on the quality of data used and the user's knowledge of the hydrogeological characteristics of the aquifer system.
- The NO_3+NO_2-N data provided by the Department of Water and Sanitation was inadequate and not spatially distributed
- The water level data provided by the Department of Water and Sanitation was not spatially distributed.

CHAPTER 8: RECOMMENDATIONS

DRASTIC method

- There is a need for efficient hydrogeological data management and more studies of DRASTIC regionally in waste disposal areas in South Africa.
- Adequate hydrogeological, geological, and hydrology data (spatial water level, hydraulic conductivity, and nitrate) of good quality needs to be available. The availability of this data will enhance the accuracy of the DRASTIC index results
- Groundwater flow models should be integrated with the DRASTIC method to validate the accuracy of the DRASTIC method and to map the movement of pollution within fractures and faults.

Landfill sites

- The stormwater system should be constructed in the landfill sites to regulate runoff with leachate flowing downstream.
- Lithological data should be made available at all the landfill sites to help understand the underlying geology
- Pumping test data should be made available by the landfill managers for future research that may apply the DRASTIC method at landfill sites.

- Stable isotopes and radioactive isotopes (tritium) should be included in the monitoring of the water quality as they are significant in identifying the residence time of water and tracing artificial tritium in groundwater.

REFERENCES

Aller L., Bennett T., Lehr J.H., Petty R.J., Hackett, G. (1987). DRASTIC: a standardized system for evaluating ground water pollution potential using hydrogeologic settings. EPA-600/2-87-035, EPA, Washington, DC.

Abiye, T.A. (2011). Provenance of groundwater in crystalline aquifer of Johannesburg area, South Africa. *International Journal of Physical Sciences*, 6(1), 98-111

Abiye, T. A., Mengistu, H., & Demlie, M. B. (2011). Groundwater resource in the crystalline rocks of the Johannesburg area, South Africa. *Journal of Water Resource and Protection*, *03*(04), 199–212. https://doi.org/10.4236/jwarp.2011.34026

Abiye, T.A. (2013). The use of isotope hydrology to characterize and assess water resources in South(ern) Africa. WRC Report No. TT570/13, Pretoria. 211pp.

Abiye, T. A., Mengistu, H., Masindi, K., & Demlie, M. (2015). Surface water and groundwater interaction in the Upper Crocodile River Basin, Johannesburg, South Africa: Environmental isotope approach. *South African Journal of Geology*, *118*(2), 109–118. https://doi.org/10.2113/gssajg.118.2.109

Babiker, I.S., Mohamed, M.A.A., Hiyama, T., Kato, K. (2015).A GIS-based DRASTIC model for assessing aquifer vulnerability in Kakamigahara Heights, Gifu Prefecture, central Japan. Science of the Total Environment, 345 (2005) 127 – 140. https://doi.org/10.1016/j.scitotenv.2004.11.005.

Barnard H.C (1999). Hydrogeological map of Johannesburg 2526. 1:500,000. Department of Water Affairs and Forestry, Pretoria, Johannesburg, RSA.

Barnard H.C (2000). An explanation for the 1:500,000 hydrogeological map of Johannesburg 2526, Department of Water Affairs and Forestry, Pretoria, Johannesburg, RSA.

Basu, A., Saha, D., Saha, R., Ghosh, T., & Saha, B. (2014). Cheminform Abstract: A review on sources, toxicity and remediation technologies for removing arsenic from drinking water. *ChemInform*, *45*(11). https://doi.org/10.1002/chin.201411276

Beavon K.S.O (2004) Johannesburg: The Making and Shaping of the City. UNISA Press, Pretoria. 373 pp.

Blight, G. (2011). Chapter 30 – Landfills – Yesterday, Today and Tomorrow. A handbook for Management. Waste. 2011, p 469-485. https://doi.org/10.1016/B978-0-12-381475-3.10030-0.

Braune, E., & Xu, Y. (2008). Groundwater management issues in southern Africa – an IWRM perspective. Water SA, 34(6), 699. https://doi.org/10.4314/wsa.v34i6.183672

Catuneanu, O., Wopfner, H., Eriksson, P. G., Cairncross, B., Rubidge, B. S., Smith, R. M. H., & Hancox, P. J. (2005). The Karoo basins of south-Central Africa. *Journal of African Earth Sciences*, *43*(1-3), 211–253. https://doi.org/10.1016/j.jafrearsci.2005.07.007

CIWM & WasteAid UK (2018). From the land to the sea. Northampton. UK. Cole, C., (2018). Plastic crisis: divert foreign aid to dumpsites in developing countries. Available at: https://theconversation.com/plastic-crisis-divert-foreign-aid-todumpsites-in-developing-countries-94341 (accessed 22 April 2019).

Clark, I.D., & Fritz, P. (1997). Environmental isotopes in Hydrogeology. CRC Press LLC. Boca Raton, Florida, 328pp

Corniello A., Ducci D., Napolitano P. (1997). Comparison between parametric methods to evaluate aquifer pollution vulnerability using GIS: an example in the Piana Campana, southern Italy. In: Marinos PG, Koukis GC, Tsiambaos GC, and Stournaras GC (eds) Engineering geology and the environment. Balkema, Rotterdam, pp 1721–1726.

de Vries, J. J., & Simmers, I. (2002). Groundwater recharge: An overview of processes and challenges. *Hydrogeology Journal*, *10*(1), 5–17. https://doi.org/10.1007/s10040-001-0171-7.

Department of Water Affairs and Forestry (DWAF). (1996). South African Water Quality Guidelines (Second Edition). Volume 1: Domestic Use, edited by Holmes, S., Council for Scientific and Industrial Research, Pretoria. – 214 pp.

Department of Environmental Affairs. (2018). South Africa State of Waste. A report on the state of the environment. First draft report. Department of Environmental Affairs, Pretoria. htpps://www.environment.gov.za [Assessed 23 October 2021]

Dyson, L. L. (2009). Heavy daily-rainfall characteristics over the Gauteng Province. *Water SA*, *35*(5). https://doi.org/10.4314/wsa.v35i5.49188.

El Naqa, A. (2004). Aquifer vulnerability assessment using the drastic model at Russeifa landfill, Northeast Jordan. *Environmental Geology*, *47*(1), 51–62. https://doi.org/10.1007/s00254-004-1126-9.

Eriksson, PG., & Clendenin CW (1990). A review of the Transvaal Sequence, South Africa. J. Afr. Earth Sci., 10(1/2): 101-116.

Eriksson, P.G., Altermann, W., Hartzer, F.J (2006). The Transvaal Supergroup and its precursors. In "The Geology of South Africa". Johnson, M.R Anhaeusser C.R, and Thoms, R.J eds., pp. 237-260.

Evans, B.M, Myers, W.L. (1990). A GIS-based approach to evaluating regional groundwater pollution potential with DRASTIC. J Soil Water Conservation 45(2):242-245.

Foster SSD (1987) Fundamental concepts in aquifer vulnerability, pollution risk and protection strategy. In: Duijvenbooden W van, Waegeningh HG van (eds) TNO Committee on Hydrological Research, The Hague. Vulnerability of soil and groundwater to pollutants, Proceedings and Information. 38 : 69–86

Fritz, P., Matthess, G., & Brown, R.M. (1976). Deuterium and Oxygen-If as Indicators of Leachwater Movement from a Sanitary Landfill. In: Interpretation of Environmental Isotope and Hydrochemical Data in Groundwater Hydrology. Panel Proc. Series, IAEA, Vienna, pp 131-142.

Fritch, T. G., McKnight, C. L., Yelderman Jr., J. C., & Arnold, J. G. (2000). An aquifer vulnerability assessment of the paluxy aquifer, Central Texas, USA, using GIS and a modified drastic approach. *Environmental Management*, *25*(3), 337–345. https://doi.org/10.1007/s002679910026

GAUTENG DEPARTMENT OF HOUSING (2006) Gauteng Housing Annual Report 2006. Gauteng Department of Housing, Marshalltown.

Gintamo, T.T. (2021). GIS and remote sensing-based integrated modelling of climate and land use change impacts on groundwater quality: Cape Flats Aquifer, South Africa. PhD dissertation, Department of Earth Sciences, University of the Western Cape, Cape Town, South Africa

Gogu, R.C., Pandele, A., Ionita, A., Ionescu, C. (1996). Groundwater vulnerability analysis using a low-cost Geographical Information System. MIS/UDMS Conference WELL-GIS WORKSHOP's Environmental Information Systems for Regional and Municipal Planning, Prague, pp 35-49.

Gogu, R. C., & Dassargues, A. (2000). Current trends and future challenges in groundwater vulnerability assessment using overlay and Index Methods. *Environmental Geology*, *39*(6), 549–559. https://doi.org/10.1007/s002540050466

Gupta, N. (2014). Groundwater vulnerability assessment using DRASTIC method in Jabalpur District of Madhya Pradesh. International Journal of Recent Technology and Engineering. Vol. 3. Iss. 3 p. 36–43.

Hasiniaina F , Zhou J, Guoyi L. (2010). Regional assessment of groundwater vulnerability in Tamtsag basin, Mongolia using drastic model. Journal of American Science, 2010;6(11)

Hasan, M., Islam, M. A., Aziz Hasan, M., Alam, M. J., & Peas, M. H. (2019). Groundwater vulnerability assessment in savar upazila of Dhaka District, Bangladesh — a GIS-based drastic modeling. Groundwater for Sustainable Development, 9, 100220. https://doi.org/10.1016/j.gsd.2019.100220

Heath R.C. (1983). *Basic ground-water hydrology*. U.S. Geological Survey Water-Supply Paper 2220 pp. 86

He, X., Li, P., Wu, J., Wei, M., Ren, X., & Wang, D. (2020). Poor groundwater quality and high potential health risks in the Datong Basin, Northern China: Research from published data. *Environmental Geochemistry and Health*, *43*(2), 791–812. https://doi.org/10.1007/s10653-020-00520-7

Hosseini, M., & Saremi, A. (2018). Assessment and estimating groundwater vulnerability to pollution using a modified drastic and gods models (case study: Malayer plain of Iran). *Civil Engineering Journal*, *4*(2), 433. https://doi.org/10.28991/cej-0309103

Hoyos, I.C., Krakauer N.Y., Khanbilvardi, R., Armstrong, R. (2016). A Review of Advances in the Identification and Characterization of Groundwater Dependent Ecosystems Using Geospatial Technologies

Huan, H., Wang, J., & Teng, Y. (2012). Assessment and validation of groundwater vulnerability to nitrate based on a modified drastic model: A case study in Jilin City of Northeast China. Science of The Total Environment, 440, 14–23. https://doi.org/10.1016/j.scitotenv.2012.08.037

Idowu, I. A., Atherton, W., Hashim, K., Kot, P., Alkhaddar, R., Alo, B. I., & Shaw, A. (2019). An analyses of the status of landfill classification systems in developing countries: Sub Saharan Africa Landfill Experiences. *Waste Management*, *87*, 761–771. https://doi.org/10.1016/j.wasman.2019.03.011

Jahan, C. S., Rahaman, M. F., Arefin, R., Ali, M. S., & Mazumder, Q. H. (2018). Delineation of groundwater potential zones of Atrai–Sib River basin in north-west Bangladesh using remote sensing and GIS techniques. Sustainable Water Resources Management, 5(2), 689–702. https://doi.org/10.1007/s40899-018-0240-x

Jalali, M. (2006). Salinization of groundwater in arid and semi-arid zones: An example from Tajarak, western Iran. Environmental Geology, 52(6), 1133–1149. https://doi.org/10.1007/s00254-006-0551-3

Jaseela, C., Prabhakar, K., & Harikumar, P. S. (2016). Application of GIS and drastic modeling for evaluation of groundwater vulnerability near a solid waste disposal site. International Journal of Geosciences, 07(04), 558–571. https://doi.org/10.4236/ijg.2016.74043

Jovanovic, N. Z., Adams, S., Thomas, A., Fey, M., Beekman, H. E., Campbell, R., Saayman, I., & Conrad, J. (2006). Improved drastic method for assessment of groundwater vulnerability to generic aqueous-phase contaminants. *Waste Management and the Environment III*. https://doi.org/10.2495/wm060421

Kalinski, R. J., Kelly, W. E., Bogardi, I., Ehrman, R. L., & Yaniamoto, P. D. (1994). Correlation between DRASTIC vulnerabilities and incidents of VOC contamination of municipal wells in Nebraska. *Ground Water*, *32*(1), 31–34. https://doi.org/10.1111/j.1745-6584.1994.tb00607.x

Khosravi, K., Sartaj, M., Tsai, F. T.-C., Singh, V. P., Kazakis, N., Melesse, A. M., Prakash, I., Tien Bui, D., & Pham, B. T. (2018). A comparison study of drastic methods with various objective methods for groundwater vulnerability assessment. Science of The Total Environment, 642, 1032–1049. https://doi.org/10.1016/j.scitotenv.2018.06.130

Kruger, A.C., & Mbatha, S. (2021). Regional Weather and Climate of South Africa: Gauteng. South African Weather Service. WCS-CLS-REGIONAL_CLIMATE_GAUTENG.001.

Kumar, M., Kumari, K., Singh, U. K., & Ramanathan, A. L. (2009). Hydrogeochemical processes in the groundwater environment of Muktsar, Punjab: Conventional graphical and multivariate statistical approach. *Environmental Geology*, *57*(4), 873–884. https://doi.org/10.1007/s00254-008-1367-0

Kumar, S., Thirumalaivasan, D., & Radhakrishnan, N. (2014). GIS based assessment of groundwater vulnerability using drastic model. *Arabian Journal for Science and Engineering*, *39*(1), 207–216. https://doi.org/10.1007/s13369-013-0843-3

Kwesi, E. A. A., Asamoah, K. N., Arthur, F. A. & Kwofie, J. A. (2020). Mapping of Ground Water Vulnerability for Landfill Site Selection Assessment at the District Level – A Case Study at the Tarkwa Nsuaem Municipality of Ghana, Ghana Journal of Technology, Vol. 4, No. 2, pp. 57 - 65.

Leketa, K., Abiye, T., & Butler, M. (2018). Characterisation of groundwater recharge conditions and flow mechanisms in bedrock aquifers of the Johannesburg area, South Africa. *Environmental Earth Sciences*, *77*(21). https://doi.org/10.1007/s12665-018-7911-7

Leketa, K., Abiye, T., Zondi, S., & Butler, M. (2019). Assessing groundwater recharge in crystalline and karstic aquifers of the Upper Crocodile River Basin, Johannesburg, South Africa. *Groundwater for Sustainable Development*, *8*, 31–40. https://doi.org/10.1016/j.gsd.2018.08.002

Levin, M and Verhagen B, Th. (1997). The use of environmental isotopes in pollution studies. SAIEG Conference, Geology for Engineering, Urban Planning and the Environment. Eskom Conference Centre, Midrand, Gauteng, 12 – 14 November 1997

Luo, W., Gao, X., & Zhang, X. (2018). Geochemical processes controlling the groundwater chemistry and fluoride contamination in the Yuncheng basin, China—an area with complex hydrogeochemical conditions. *PLOS ONE*, *13*(7). https://doi.org/10.1371/journal.pone.0199082

Lynch, S.D., Reynders, A.G., Schulze, R.E. (1994). Preparing input data for a national-scale groundwater vulnerability map of southern Africa. Water SA. Vol. 20 Iss. 3 p. 239-246.

Masindi, K., & Abiye, T. (2018). Assessment of natural and anthropogenic influences on regional groundwater chemistry in a highly industrialized and urbanized region: A case study of the

vaal river basin, South Africa. Environmental Earth Sciences, 77(20). https://doi.org/10.1007/s12665-018-7907-3

McCarthy, T., & Rubidge, B., 2005. The story of Earth and Life A southern African perspective on a 4.6-billion year journey. published by Struik, Cape Town, pp. 333

McCarthy TS (2006). The Witwatersrand Supergroup. In "The Geology of South Africa". Johnson, M.R Anhaeusser C.R, and Thoms, R.J eds., pp. 155-186

McLay, C. D. A., Dragten, R., Sparling, G., & Selvarajah, N. (2001). Predicting groundwater nitrate concentrations in a region of mixed agricultural land use: A comparison of three approaches. *Environmental Pollution*, *115*(2), 191–204. https://doi.org/10.1016/s0269-7491(01)00111-7

Mepaiyeda, S., Baiyegunhi, C., Madi, K., & Gwavava, O. (2019). A geophysical and hydro physico-chemical study of the contaminant impact of a solid waste landfill (SWL) in king Williams' town, Eastern Cape, South Africa. *Open Geosciences*, *11*(1), 549–557. https://doi.org/10.1515/geo-2019-0045

Merchant JW (1994) GIS-based groundwater pollution hazard assessment: A critical review of the DRASTIC model. Photogramm Eng Remote Sensing 60(9):1117–1127

Meyers, R.E., McCarthy, T.S., Stanistreet, I.G. (1990). A tectono-sedimentary reconstruction of the development and evolution of the Witwatersrand Basin, with particular emphasis on the Central rand Group, S. Afr. J. Geol., 93: 180-201.

Moges, S.S., Dinka, M.O. (2021). Assessment of groundwater vulnerability using the DRASTIC model: A case study of Quaternary catchment A21C, Limpopo River Basin, South Africa. Journal of Water and Land Development. No. 49 (IV– VI) p. 35–46.

Mohuba, S.K. (2020). Hydrogeological characterization and groundwater vulnerability to pollution mapping of the Thyspunt nuclear site, Eastern Cape. MSc research report, Faculty of Science, School of Geosciences, University of Witwatersrand, South Africa.

Moolla, R., Valsamakis, S. K., Curtis, C. J., & Piketh, S. J. (2013). Occupational health risk assessment of benzene and toluene at a landfill site in Johannesburg, South Africa. Safety and Security Engineering V. https://doi.org/10.2495/safe130631

Morris, J.W.F. (2001). Effects of waste composition on landfill processes under semi-arid climatic conditions, Unpublished Ph.D. thesis, University of the Witwatersrand, Johannesburg, South Africa.

Morris, B.L., Lawrence, A.R., Chilton, P.J., Adams, B., Calow, R.C., Klinck, B.A. (2003). Groundwater and its susceptibility to degradation, a global assessment of the problem and options for management. United Nations Environment Programme, Nairobi (unpublished).

Mostert, J.S. (2014). A GIS-based DRASTIC approach to assessing aquifer vulnerability adapted for intrinsic risks posed by differing land uses (Rustenburg Municipality). Unpublished MSc dissertation, Faculty of Natural Sciences and Agricultural Sciences, University of Pretoria, South Africa.

Musekiwa, C., Majola, K. (2013). Groundwater vulnerability map for South Africa. S Afr J Geomat 2(2):152–162.

Muzenda, E. (2012). Gauteng's Waste Outlook: A Reflection. International Journal of Environmental, Chemical, Ecological, Geological and Geophysical Engineering Vol:6, No:8, 2012.

Napolitano, P., Fabbri, A.G. (1996). Single-parameter sensitivity analysis for aquifer vulnerability assessment using DRASTIC and SINTACS. HydroGIS 96: Application of Geographic Information Systems in Hydrology and Water Resources Management (Proceedings of the Vienna Conference, April 1996). IAHS Publ. No. 235, 559–566.

Naqa, A.E. (2004). Aquifer vulnerability assessment using the DRASTIC model at Russeifa landfill, northeast Jordan. Environmental Geology (2004) 47:51–62.

Ntanganedzeni, B., Elumalai, V., & Rajmohan, N. (2018). Coastal aquifer contamination and geochemical processes evaluation in tugela catchment, South Africa—geochemical and Statistical Approaches. *Water, 10*(6), 687. https://doi.org/10.3390/w10060687

Oke, S. A. (2020). Regional aquifer vulnerability and pollution sensitivity analysis of drastic application to Dahomey Basin of nigeria. International Journal of Environmental Research and Public Health, 17(7), 2609. https://doi.org/10.3390/ijerph17072609

Panagopoulos, G.P., Antonakos, A.K., Lambrakis, N.J. (2004). Optimization of the DRASTIC method for groundwater vulnerability assessment via the use of simple statistical methods and GIS. Hydrogeology Journal (2006) 14: 894–911.

Panagopoulos, G. P., Antonakos, A. K., & Lambrakis, N. J. (2006). Optimization of the drastic method for groundwater vulnerability assessment via the use of simple statistical methods and GIS. Hydrogeology Journal, 14(6), 894–911. https://doi.org/10.1007/s10040-005-0008-x

Pandey, H. K., Duggal, S. K., & Jamatia, A. (2016). Fluoride contamination of groundwater and it's hydrogeological evolution in district sonbhadra (U.P.) India. *Proceedings of the National Academy of Sciences, India Section A: Physical Sciences*, *86*(1), 81–93. https://doi.org/10.1007/s40010-015-0228-y

Pérez Hoyos, I., Krakauer, N., Khanbilvardi, R., & Armstrong, R. (2016). A review of advances in the identification and characterization of groundwater dependent ecosystems using geospatial technologies. Geosciences, 6(2), 17. https://doi.org/10.3390/geosciences6020017

Piscopo, G. (2001). Groundwater vulnerability map, explanatory notes, Castlereagh Catchment, NSW. Department of Land and Water Conservation, Australia.

Press, J. (2020). Assessment of groundwater vulnerability to pollution in the Upper Crocodile River basin: A GIS based DRASTIC model approach. Unpublished MSc research Report, School of Geosciences, University of the Witwatersrand, Johannesburg, South Africa, p96.

Rajesh, R., Brindha, K., Murugan, R., & Elango, L. (2012). Influence of hydrogeochemical processes on temporal changes in groundwater quality in a part of Nalgonda district, Andhra Pradesh, India. *Environmental Earth Sciences*, *65*(4), 1203–1213. https://doi.org/10.1007/s12665-011-1368-2

Ramaroson, V., Rakotomalala, C. U., Rajaobelison, J., Fareze, L. P., Razafitsalama, F. A., & Rasolofonirina, M. (2018). Tritium as tracer of groundwater pollution extension: Case study of andralanitra landfill site, antananarivo–madagascar. *Applied Water Science*, *8*(2). https://doi.org/10.1007/s13201-018-0695-9

Rasmeni, Z. Z., & Madyira, D. M. (2019). A review of the current municipal solid waste management practices in Johannesburg City Townships. *Procedia Manufacturing*, *35*, 1025–1031. https://doi.org/10.1016/j.promfg.2019.06.052

Reyes-López, J. A., Ramírez-Hernández, J., Lázaro-Mancilla, O., Carreón-Diazconti, C., & Garrido, M. M.-L. (2008). Assessment of groundwater contamination by landfill leachate: A case in México. Waste Management, 28. https://doi.org/10.1016/j.wasman.2008.03.024

Robb, L. J., & Meyer, F. M. (1995). The Witwatersrand Basin, South Africa: Geological Framework and mineralization processes. *Ore Geology Reviews*, *10*(2), 67–94. https://doi.org/10.1016/0169-1368(95)00011-9

Rosen, L. (1994). A study of the drastic methodology with emphasis on Swedish conditions. Ground Water, 32(2), 278–285. https://doi.org/10.1111/j.1745-6584.1994.tb00642.x

Rupert, M. G. (1999). Improvements to the drastic ground-water vulnerability mapping method. *Fact Sheet*. https://doi.org/10.3133/fs06699

Sakala, E., Fourie, F., Gomo, M., & Coetzee, H. (2018). GIS-based groundwater vulnerability modelling: A case study of the witbank, Ermelo and Highveld Coalfields in South Africa.

Journal of African Earth Sciences, *137*, 46–60. https://doi.org/10.1016/j.jafrearsci.2017.09.012

Sakala, E., Fourie, F., Gomo, M., & Coetzee, H. (2019). Groundwater vulnerability mapping of witbank coalfield in South Africa using Deep Learning Artificial Neural Networks. *South African Journal of Geomatics*, *8*(2), 282–293. https://doi.org/10.4314/sajg.v8i2.12

Santhosh, L. G., & Sivakumar Babu, G. L. (2018). Landfill site selection based on reliability concepts using the drastic method and AHP integrated with GIS – A case study of Bengaluru city, India. *Georisk: Assessment and Management of Risk for Engineered Systems and Geohazards*, *12*(3), 234–252. https://doi.org/10.1080/17499518.2018.1434548

Secunda, S., Collin, M. L., & Melloul, A. J. (1998). Groundwater vulnerability assessment using a composite model combining drastic with extensive agricultural land use in Israel's Sharon Region. *Journal of Environmental Management*, *54*(1), 39–57. https://doi.org/10.1006/jema.1998.0221

Senthilkumar, M., & Elango, L. (2013). Geochemical processes controlling the groundwater quality in Lower Palar River basin, southern India. *Journal of Earth System Science*, *122*(2), 419–432. https://doi.org/10.1007/s12040-013-0284-0

Sheikhy Narany, T., Ramli, M. F., Aris, A. Z., Sulaiman, W. N., Juahir, H., & Fakharian, K. (2014). Identification of the hydrogeochemical processes in groundwater using classic integrated geochemical methods and geostatistical techniques, in Amol-Babol Plain, Iran. *The Scientific World Journal*, *2014*, 1–15. https://doi.org/10.1155/2014/419058

Shirazi, S. M., Imran, H. M., & Akib, S. (2012). GIS-based drastic method for Groundwater Vulnerability Assessment: A Review. *Journal of Risk Research*, *15*(8), 991–1011. https://doi.org/10.1080/13669877.2012.686053

Sibiya, I. V., Olukunle, O. I., & Okonkwo, O. J. (2017). Seasonal variations and the influence of geomembrane liners on the levels of PBDEs in landfill leachates, sediment and groundwater

in Gauteng Province, South Africa. *Emerging Contaminants*, *3*(2), 76–84. https://doi.org/10.1016/j.emcon.2017.05.002

Subba Rao, N., Ravindra, B., & Wu, J. (2020). Geochemical and Health Risk Evaluation of fluoride rich groundwater in Sattenapalle region, Guntur district, Andhra Pradesh, India. *Human and Ecological Risk Assessment: An International Journal*, *26*(9), 2316–2348. https://doi.org/10.1080/10807039.2020.1741338

Swain, S., Taloor, A. K., Dhal, L., Sahoo, S., & Al-Ansari, N. (2022). Impact of climate change on Groundwater Hydrology: A comprehensive review and current status of the Indian hydrogeology. Applied Water Science, 12(6). https://doi.org/10.1007/s13201-022-01652-0

Tahoora, S.N., Mohammad, F.R., Ahmad, Z.A., Wan, N.A.S, Hafizan, J., and Kazem., F. (2014). Identification of the hydrogeochemical processes in groundwater using classic integrated geochemical methods and geostatistical techniques, in Amol-Babol Plain, Iran. The Scientific World Journal, 2014, 15.

Tilahun, K., & Merkel, B. J. (2009). Assessment of groundwater vulnerability to pollution in Dire Dawa, Ethiopia using drastic. *Environmental Earth Sciences*, *59*(7), 1485–1496. https://doi.org/10.1007/s12665-009-0134-1

Vaccari, M., Tudor, T., & Vinti, G. (2019). Characteristics of leachate from landfills and dumpsites in Asia, Africa and Latin America: An overview. *Waste Management*, *95*, 416–431. https://doi.org/10.1016/j.wasman.2019.06.032

Verhagen, B.Th., Geyh, M.A., Frohlich, K. and Wirth, K. (1991). Isotope Hydrological Methods/or the Quantitative Evaluation of Ground Water Resources in Arid and Semi-arid Areas. Development of a Methodology. Research Reports for the Federal Ministry for Economic Cooperation (BMZ), Weltforum Verlag, p 164.

Verhagen, B Th, Levin, M., Walton, D.G., and Butler, M.J. (1996). Investigation of groundwater pollution associated with waste disposal: Development of an environmental isotope approach. WRC Project No 311/1/01, January 1996.

Voudouris, K., Kazakis, N., Polemio, M., Kareklas, K. (2010). Assessment of intrinsic vulnerability using DRASTIC model and GIS in the Kiti aquifer, Cyprus. European water 30: 13-24, 2010.

Wang, J., He, J., & Chen, H. (2012). Assessment of groundwater contamination risk using hazard quantification, a modified drastic model and groundwater value, Beijing Plain, China. *Science of The Total Environment*, *432*, 216–226. https://doi.org/10.1016/j.scitotenv.2012.06.005

WHO (2003). Uranium in drinking water. Background document for preparation of WHO Guidelines for drinking-water quality. Geneva, World Health Organization (WHO/SDE/WSH/03.04/118).

Witkowski, A.J., Kowalczyk, A., Vrba, J. (2004). Groundwater Vulnerability Assessment and Mapping. INTERNATIONAL ASSOCIATION OF HYDROGEOLOGISTS

Witkowski, A.J., Kowalczyk, A., and Vrba, J. (2007). Groundwater Vulnerability Assessment and Mapping: selected papers from the Groundwater Vulnerability Assessment and Mapping International Conference : Ustron, Poland, 2004. Taylor & Francis eLibrary, pp. 105.

Wong, M. H., Wu, S. C., Deng, W. J., Yu, X. Z., Luo, Q., Leung, A. O. W., Wong, C. S. C., Luksemburg, W. J., & Wong, A. S. (2007). Export of Toxic Chemicals – a review of the case of uncontrolled electronic-waste recycling. *Environmental Pollution*, *149*(2), 131–140. https://doi.org/10.1016/j.envpol.2007.01.044

World Health Organization. (2008). Guidelines for Drinking-water Quality [electronic resource]: incorporating 1st and 2nd addenda, Vol. 1, Recommendations.

World Health Organization (WHO). (2011). Guidelines for drinking-water quality (4th ed.). WHO Library Cataloguing-in-Publication Data, pp. 564.

Wronkiewicz, D. J., & Condie, K. C. (1987). Geochemistry of Archean shales from the Witwatersrand Supergroup, South Africa: Source-area weathering and provenance.

Geochimica Et Cosmochimica Acta, 51(9), 2401–2416. https://doi.org/10.1016/0016-7037(87)90293-6

Younger P.L. (2009). Groundwater in the environment: An introduction. London. John Wiley & Sons. ISBN 9781444309041 pp. 336.

Zeh, A., Ovtcharova, M., Wilson, A. H., & Schaltegger, U. (2015). The Bushveld complex was emplaced and cooled in less than one million years – results of zirconology, and geotectonic implications. Earth and Planetary Science Letters, 418, 103–114. https://doi.org/10.1016/j.epsl.2015.02.035